DEPARTMENT OF PATHOLOGY
UNIVERSITY OF HELSINKI
HELSINKI UNIVERSITY HOSPITAL
FINLAND

# NEUROENDOCRINE TUMORS: THE QUALITY OF PROGNOSTIC AND PREDICTIVE MARKERS

**Satu Maria Remes**

ACADEMIC DISSERTATION

To be publicly discussed,
with the permission of the Faculty of Medicine of the University of Helsinki,
in Auditorium 2 at the Haartman Institute, Haartmaninkatu 3, Helsinki,
on 16th of October 2020, at 12 noon

Helsinki, 2020

**Supervised by**
Professor Johanna Arola, MD, PhD
Department of Pathology, University of Helsinki and
Helsinki University Hospital, Helsinki, Finland

Professor Caj Haglund, MD, PhD
Department of Surgery, University of Helsinki and
Helsinki University Hospital, Helsinki, Finland
Translational Cancer Medicine Research Program
Faculty of Medicine, University of Helsinki, Finland

**Reviewed by**
Docent Anita Naukkarinen, PhD
Department of Pathology, University of Eastern Finland and
Kuopio University Hospital, Kuopio, Finland

Docent Teemu Tolonen, MD, PhD
Department of Pathology, University of Tampere and
Tampere University Hospital, Tampere, Finland

**Opposed by**
Docent Raija Ristamäki, MD, PhD
Department of Oncology, University of Turku and
Turku University Hospital, Turku, Finland

ISBN 978-951-51-5983-0 (paper pack)
ISBN 978-951-51-5984-7 (PDF)

http://ethesis.helsinki.fi/

The Faculty of Medicine uses the Urgund system (plagiarism recognition)
to examine all doctoral dissertations.

# CONTENTS

# LIST OF ORIGINAL PUBLICATIONS

This thesis is based on the following publications.

I Pulkkinen V, Ezer S, Sundman L, Hagström J, Remes S, Söderhäll C, Greco D, Haglund C, Kere J, and Arola J: Neuropeptide S receptor 1 (NPSR1) activates cancer-related pathways and is widely expressed in neuroendocrine tumors. *Virchows Arch.* (2014) 465:173–183. Erratum in: *Virchows Arch.* (2014) 465:251.

II Remes SM, Leijon H, Vesterinen T, Louhimo J, Pulkkinen V, Ezer S, Kere J, Haglund C*, and Arola J*: PCSK2 expression in neuroendocrine tumors points to a midgut, pulmonary or pheochromocytomas-paraganglioma origin. *APMIS.* (2020) Aug 14. doi: 10.1111/apm.13071. Online ahead of print.

III Remes SM, Leijon HL, Vesterinen TJ, Arola JT*, and Haglund CH*: Immunohistochemical Expression of Somatostatin Receptor Subtypes in a Panel of Neuroendocrine Neoplasias. *J Histochem Cytochem.* (2019) 67:735–743.

IV Remes SM, Tuominen VJ, Helin H, Isola J, and Arola J: Grading of neuroendocrine tumors with Ki-67 requires high-quality assessment practices. *Am J Surg Pathol.* (2012) 36:1359–1363.

* indicates an equal contribution.

The publications are referred to in the text by their roman numerals.

# ABBREVIATIONS

| | |
|---|---|
| 5-HIAA | 5-hydroxyindole-5-acetic acid |
| ACTH | Adrenocorticotropic hormone |
| AI | Artificial intelligence |
| AJCC | American Joint Committee on Cancer |
| ANN | Artificial neural network |
| AP | Alkaline phosphate |
| AR | Antigen retrieval |
| CDX2 | Caudal-type homeobox 2 |
| CGA | Chromogranin A |
| CNS | Central nervous system |
| CT | Computed tomography |
| DAB | 3,3'-diaminobenzidine |
| DHFR | Dihydrofolate reductase |
| DLL3 | Delta-like 3 |
| DMEM | Dulbecco's modified Eagle's medium |
| DOTA | 1,4,7,10-tetraazacyclodecane-1,4,7,10-tetraacetic acid |
| ENETS | European Neuroendochrine Tumor Society |
| FBS | Fetal bovine serum |
| FDG | Fluorodeoxyglucose |
| FNA | Fine-needle aspiration |
| GEP–NEN | Gastroenteropancreatic neuroendocrine neoplasias |
| GI | Gastrointestinal |
| GST | Glutatheione S transferase |
| GUI | Graphical user interface |
| HE | Hematoxylin-eosin |
| HER2 | Human epidermal growth factor receptor 2 |
| HIER | Heat-induced epitope retrieval |
| HPF | High-power field |
| HRP | Horseradish peroxidase |
| HUSLAB | Department of Pathology, Helsinki University Hospital |
| IHC | Immunohistochemistry or immunohistochemical |
| IMP3 | Insulin-like growth factor II mRNA-binding protein 3 |
| INSM1 | Insulinoma-associated protein 1 |
| ISH | *In situ* hybridization |
| ISL1 | Insulin gene enhancer-binding protein islet 1 |
| LCNEC | Large-cell neuroendocrine carcinoma |

| | |
|---|---|
| MEN1 | Multiple endocrine neoplasias type 1 |
| MEN2 | Multiple endocrine neoplasias type 2 |
| MRI | Magnetic resonance imaging |
| NE | Neuroendocrine |
| NEC | Neuroendocrine carcinoma |
| NEN | Neuroendocrine neoplasias |
| NET | Neuroendocrine tumor |
| NGS | Next-generation sequencing |
| ngTMA | Next-generation tissue microarray |
| NPSR1 | Neuropeptide S receptor 1 |
| NPS | Neuropeptide S |
| NSE | Neuro-specific enolase |
| OS | Overall survival |
| PAX8 | Paired-box 8 |
| PC | Prohormone convertase |
| PCSK2 | Proprotein convertase subtilisin/kexin type 2 |
| PET | Positron emission tomography |
| PGL | Paraganglioma |
| PHEO | Pheochromocytoma |
| PI | Proliferation index |
| ROI | Region of interest |
| SCLC | Smal- cell lung cancer |
| SEER | Surveillance, Epidemiology, and End Results registry |
| SSA | Somatostatin analog |
| SSTR | Somatostatin receptor |
| SYP | Synaptophysin |
| TMA | Tissue microarray |
| TNM | Tumor, node and metastasis |
| TTF1 | Thyroid transcription factor 1 |
| UICC | Union for Internation Cancer Control |
| VHL | von Hippel-Lindau |
| WHO | World Health Organization |
| WSI | Whole-slide imaging |

# ABSTRACT

Neuroendocrine tumors (NETs) are derived from neuroendocrine (NE) cells. NETs can appear in a variety of organs because of the disseminated nature of NE cells. NETs show histomorphological similarities independent of the tumor origin, with prognoses varying between different NETs depending upon the primary tumor location and tumor grade.

The diagnosis of an NET is confirmed by the immunohistochemical (IHC) expression of common NE markers including chromogranin A (CGA) and synaptophysin (SYP). The proliferation marker Ki-67 plays a central role in tumor grading in NETs. In practice, all of these markers are determined using IHC, whereby the reliable assessment of staining is crucial. High-quality diagnostics require careful technical verification of protocols and a full understanding of the target antigen.

This thesis aims to identify new diagnostic IHC markers for NETs and to improve the interpretation of staining. Particular focus in this study lies on validating IHC for these new NE markers and verifying the ability of image analysis to reproduce quantitative scores.

The primary study cohort consisted of 91 neuroendocrine neoplasias (NENs) from 12 different primary sites including primary tumor - metastatic pairs. Additional cohorts of tumors from a specific site of origin were used for further study. A multi-NET tissue microarray (TMA) was constructed using TMA technology. The specificity of the primary antibodies was first confirmed using known positive control tissues. Proper staining protocols were used for the IHC staining of multi-NET TMAs. In addition, image analysis using the ImmunoRatio software was used to assess the proliferation labeling index for grading purposes.

All NETs except the pheochromocytomas (PHEOs) expressed neuropeptide S receptor 1 (NPSR1) and its ligand neuropeptide S (NPS). The expression of proprotein convertase subtilisin/kexin type 2 (PCSK2) was found primarily in the small intestine and appendicular NETs, PHEOs, and paragangliomas (PGLs), and half of the typical and atypical pulmonary carcinoids. NETs from other primary locations were negative. In metastases, the expressions of NPSR1 and PCSK2 were comparable to those of the primary tumor.

Different primary antibody clones for somatostatin receptors (SSTRs) varied in terms of staining results. Not all clones could localize in the correct cell components in positive control tissues. The UMB clones exhibited a good staining pattern in the cell membranes. Five SSTRs showed individual and varying profiles in NENs of different origins.

The assessment of Ki-67 using conventional human scoring showed interobserver variation resulting in different gradings. Thus, grading using image analysis proved more reproducible and, thus, more reliable than traditional human analysis.

**In conclusion,** most NENs express NPSR1 widely. Instead, only midgut NENs, PHEOs, PGLs, and some of the lung carcinoids expressed PCSK2. These antibodies can be used in the panel of NE markers and for screening metastatic NENs from an unknown primary tumor. Expression analysis of SSTRs in formalin-fixed paraffin embedded sections, detected using validated IHC methods, may guide therapeutic planning with different somatostatin analogs (SSAs). Image analysis of the proliferation index (PI) is a preferable method for the high-quality grading of NENs.

# 1 INTRODUCTION

Neuroendocrine neoplasias (NENs) represent a heterogeneous group of rare tumors arising from neuroendocrine (NE) cells (Andrew et al. 1998, Rosai 2011) distributed across the human body (Rekhtman 2008). The endocrine system comprises the endocrine organs (pituitary and parathyroid), single disseminated NE cells (gastrointestinal tract) as well as clustered NE cells (islet of Langerhans). The NE cells produce and secrete a variety of hormones that participate in normal physiological functions (de Herder 2007).

The incidence of NENs has increased markedly in recent decades (Dasari et al. 2017). Clinical symptoms can be absent or nonspecific leading to delayed diagnosis with metastatic disease. Thus, NENs are quite frequently diagnosed from small biopsies of a metastatic tumor with an unknown primary.

Immunohistochemical (IHC) markers are used to verify the NE nature of a tumor. Chromogranin A (CGA) and synaptophysin (SYP) represent the most commonly used NE-specific biomarkers in the diagnosis of NENs (Perren et al. 2017). However, knowledge of the primary tumor location is also needed for the management of disease (Oronsky et al. 2017, Milione et al. 2018). In this situation, location-specific IHC markers can be helpful. Tumor grade, which relates to the proliferation activity of the tumor, carries a major prognostic significance, while also guiding treatment options (Cavalcanti et al. 2016). Thus, the grading of NENs is based on the quantitative analysis of Ki-67-positive nuclei on IHC slides or counting the mitotic figures on hematoxylin-eosin (HE) stained slides (Klöppel et al. 2017a).

The growing incidence of NENs (Dasari et al. 2017) has driven attempts to find new potential markers that could serve as crucial diagnostic tools indicative of the treatment response as well as disease prognosis. Discovery of new reliable NE markers is needed since no single primary antibody used today is fully specific (Agaimy et al. 2013, Zimmermann et al. 2016). Markers pointing towards the primary tumor location from a tissue specimen are remarkably valuable, since the primary tumor can be small and, thus, undetectable during imaging (Oronsky et al. 2017). In addition, accurate grading of NENs affects the prognosis, requiring further quality development (Klöppel et al. 2017a, Cavalcanti et al. 2016). The treatment and management of NENs using somatostatin analogs (SSAs) has proved efficient (Qian et al. 2016). The efficacy of SSAs is based on the existence of somatostatin receptors (SSTRs) on the tumor cell membrane, further stressing the importance of the analysis of the SSTR profile in different NENs. Therefore, technical verification and validation of prognostic and predictive markers are needed for the management of NE tumor patients.

# 2 REVIEW OF THE LITERATURE

## 2.1 NORMAL ENDOCRINE SYSTEM

The endocrine system comprises a complex of neuroendocrine (NE) cells with the ability to produce hormones. Most of these hormones are peptides, which are synthetized from precursors via post-translational modification along the secretory pathway. These prohormones are transported into the rough endoplasmic reticulum, where they undergo cleavage and modification mediated by various enzymes (Montuenga et al. 2003). Then, the peptide precursors move into the Golgi apparatus, where they are further processed and eventually packed and stored as secretory granules (Montuenga et al. 2003). Hormones coordinate diverse physiological and behavioral functions such as growth, development, and biorhythms. For example, the parathyroid hormone and calcitonin regulate blood calcium levels; insulin and glucagon regulate blood sugar by lowering or raising blood glucose levels. The NE cell of the adrenal medulla releases adrenaline and noradrenaline as a response to stress. Hormonal actions follow exocytosis to the vascular system.

The word *neuroendocrine* implies that NE cells possess two different elements, components similar to neurons and classic endocrine cells (Rekhtman 2008). The small vesicles found in the cytoplasm of an NE cell (Klöppel 2007) refer to "neuro", while the "endocrine" refers to the NE cell's ability to secrete and release different hormones in response to stimulation (Montuenga et al. 2003, Rekhtman 2008). Despite the ultrastructural similarity of neurons and NE cells, they differ in terms of cell structure (no processes) and the signaling mode (Rekhtman 2008). Highly condensed cytoplasmic vesicles represent the characteristic feature of NE cells at the electron microscopic level (Klöppel 2007).

Disseminated, single or clustered NE cells are found in almost every anatomic site, as illustrated in Figure 1. Scattered NE cells are usually found within the epithelial linings, and are widespread and diverse in the gastrointestinal (GI) tract, which comprises the stomach, small intestine, appendix, colon, and rectum (Montuenga et al. 2003, Klöppel et al. 2007). In the respiratory system, NE cells are found in the bronchi (Montuenga et al. 2003). NE cells are also present although in lower numbers, for example, in the thymus, thyroid gland (calcitonin-producing cells), skin (Merkel cells), and urogenital and biliary tract (Montuenga et al. 2003, Klöppel 2007). The pancreas contains clusters of endocrine cells, referred to as the so-called islets of Langerhans (Klöppel 2007). Classic endocrine glands are formed by groups of endocrine cells, such as the pituitary, pineal, parathyroid, and adrenal gland, namely, the adrenal medulla (Klöppel 2007).

In addition, NE cells have different embryological origins according to their location. They are derived either from the neural crest (chromaffin cells of the adrenal medulla and extra-adrenal paraganglia, and thyroid C cells) or from an endodermal origin (the GI track and the pancreas) (Andrew et al. 1998, Rosai 2011). Table 1 summarizes the terminology associated with a NE system.

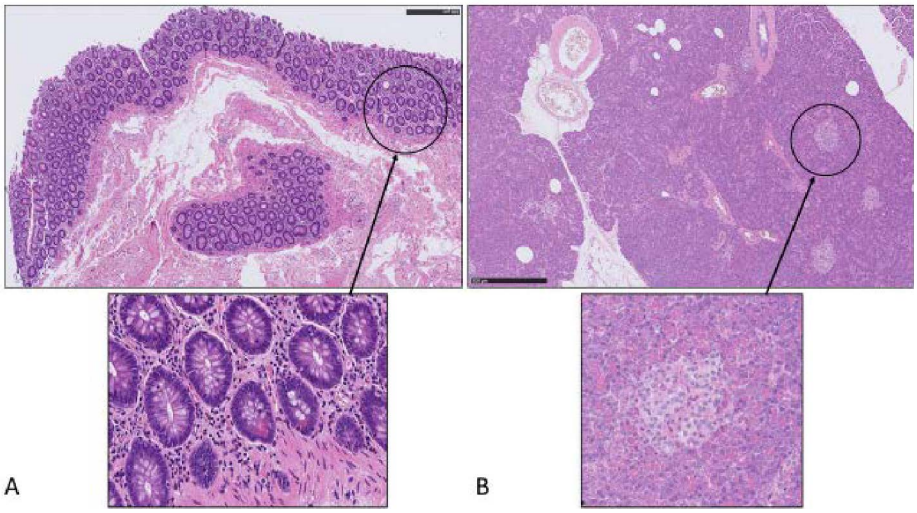


**Figure 1.** Neuroendocrine (NE) cells are widespread in the human body. Single NE cells (A) are found in the epithelium of the small intestine and aggregates of NE cells (B) appear in the pancreatic islet of Langerhans. Scale bar = 500 µm.

**Table 1.** Terminology associated with the neuroendocrine (NE) system. Modified from Montuenga et al. (2003).

| TERMINOLOGY | DEFINITION |
|---|---|
| Clear cell, Kultschitzky, Chromaffin, Enterochromaffin | Synonyms for NE |
| Acidophilic, Argentaffin, Argyrophil | Descriptive name by staining |
| Endocrine cells | Functional term |
| Neuroendocrine cells | A cell having a neuroendocrine phenotype |
| Neuroendocrine phenotype | NE granules, secretory vesicle proteins, hormones, peptides |
| Endocrine secretory granules | Electron dense, small vesicles containing peptides |
| Diffuse neuroendocrine system | Refers to the widespread location of the neuroendocrine cells |

## 2.2 NEUROENDOCRINE NEOPLASIAS

Neuroendocrine neoplasias (NENs) comprise a large, diverse group of NE tumors. NENs are characterized as well-differentiated or poorly differentiated tumors (Rindi et al. 2018). Well-differentiated NENs feature the morphological hallmarks of NE differentiation, including monotonous nuclei with finely speckled chromatin, and typically strongly express NE markers (Rekhtman 2008). Poorly differentiated carcinomas, subdivided into small- and large-cell neuroendocrine carcinomas (NECs) according to the nuclear size, are highly aggressive tumors often with barely detectable NE features (Rekhtman 2008, Klöppel et al. 2017a, Washington 2019).

The diagnostic challenge of NENs lies in the heterogeneity of these tumors. The morphological and behavioral features depend on the location of the primary NEN. In addition, NEN incidence rates vary depending upon the primary tumor location. NENs occur frequently in the GI tract (62-67%) and in the bronchopulmonary system (22–27%) (Oronsky et al. 2017). In the GI, NENs are mostly found in the small intestine (30%) (Frilling et al. 2012). In the lung, the majority of NENs are high-grade, poorly differentiated tumors, comprising small-cell lung cancer (SCLC) (79%), large-cell neuroendocrine carcinoma (LCNEC) (16%), typical carcinoids (5%), and atypical carcinoids (0.5%) (Rindi et al. 2018). Thymic NENs are rare, constituting about 2% to 5% of thymic epithelial tumors (Ströbel et al. 2015). Genitourinary, male and female genital organ NENs, and breast NENs are extremely rare (Oronky et al.2017, Rindi et al. 2018). Some NEN types have specific names. These include Merkel cell carcinoma of the skin, a high-grade, poorly differentiated tumor as well as medullary carcinoma of the thyroid, pheochromocytoma (PHEO) of the adrenal gland, and extra adrenal paraganglioma (PGL) (Rekhtman 2008, Delellis et al. 2017, Busam et al. 2018). PHEOs and PGLs are distinct from other NENs because they are not epithelial. Figure 2 illustrates the anatomical distribution of different NENs (Frilling et al. 2012, Oronsky et al. 2017). Table 2 lists the World Health Organization (WHO) classification of NENs with different primary origins (E. Brambilla 2015, Klöppel et al. 2017b, Busam et al. 2018, Washington 2019).

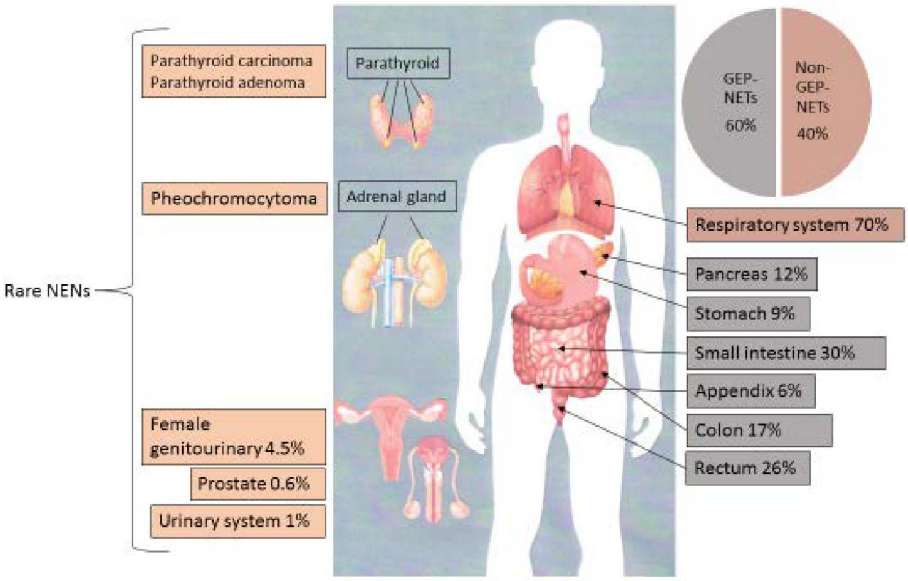


**Figure 2.** Distribution of neuroendocrine neoplasms (NENs). NENs primarily stem from a gastroenteropancreatic (GEP–NEN) origin (top-left). Non-GEP–NENs are primarily located in the respiratory system. NENs metastasize frequently in the liver. Modified from Frilling et al. (2012) and Oronsky et al. (2017).

.

**Table 2.** World Health Organization (WHO) classification of neuroendocrine neoplasias (NENs). Modified from E. Brambilla (2015), Klöppel et al. (2017b), Busam et al. (2018), and Washington (2019).

| ORGAN | WHO CLASSIFICATION | | | WHO |
|---|---|---|---|---|
| LUNG<br>THYMUS | Carcinoid tumors | | Typical carcinoids | 2015 |
| | | | Atypical carcinoids | |
| | Large-cell carcinoma | | | |
| | Small-cell carcinoma | | | |
| STOMACH | Neuroendocrine tumor (NET) | G1 NET | | 2019 |
| | | G2 NET | | |
| | | G3 NET | | |
| | Neuroendocrine carcinoma (NEC) | Large-cell NEC | | |
| | | Small-cell NEC | | |
| | Mixed neuroendocrine–non-neuroendocrine neoplasm | | | |
| | Hormone producing neuroendocrine neoplasms: histamine-producing enterochromaffin-like-cell NET (Type 1-3), somatostatin-producing D-cell NET, gastrin-producing G-cell NET, and serotonin-producing enterochromaffin NET | | | |
| PANCREAS | Well-differentiated pancreatic neuroendocrine tumors (NET) | | PanNET G1 | 2017 |
| | | | PanNET G2 | |
| | | | PanNET G3 | |
| | Poorly differentiated pancreatic neuroendocrine carcinoma (NEC) | | Large-cell NEC | |
| | | | Small-cell NEC | |
| | Mixed neuroendocrine–non-neuroendocrine neoplasm | | | |
| | Hormone producing neuroendocrine neoplasms: insulinoma, glucagonoma, somastostatinoma, gastrinoma, VIPoma, serotonin-producing tumor, and ACTH-producing tumor | | | |
| SMALL INTESTINE | Neuroendocrine tumor (NET) | NET G1 | | 2019 |
| | | NET G2 | | |
| | | NET G3 | | |
| | Neuroendocrine carcinoma (NEC) | Large-cell NEC | | |
| | | Small-cell NEC | | |
| | Mixed neuroendocrine–non-neuroendocrine neoplasm | | | |
| | Hormone producing neuroendocrine neoplasms: gastrinoma, somatostatinoma, enterochromaffin-cell carcinoid | | | |
| APPENDIX | Neuroendocrine tumor (NET) | NET G1 | | |
| | | NET G2 | | |
| | | NET G3 | | |
| | Neuroendocrine carcinoma (NEC) | Large-cell NEC | | |
| | | Small-cell NEC | | |
| | Mixed neuroendocrine–non-neuroendocrine neoplasm | | | |
| | Hormone producing neuroendocrine neoplasms: L-cell tumor, glucagon-like peptide-producing tumor, PP/PYY-producing tumor, enterochromaffin-cell carcinoid, and serotonin-producing carcinoid | | | |
| COLON AND RECTUM | Neuroendocrine tumor (NET) | NET G1 | | |
| | | NET G2 | | |
| | | NET G3 | | |
| | Neuroendocrine carcinoma (NEC) | Large-cell NEC | | |
| | | Small-cell NEC | | |
| | Mixed neuroendocrine–non-neuroendocrine neoplasm | | | |
| | Hormone producing neuroendocrine neoplasms: L-cell tumor, glucagon-like peptide-producing tumor, PP/PYY-producing tumor, enterochromaffin-cell carcinoid, and serotonin-producing tumor | | | |
| THYROID | Medullary thyroid carcinoma | | | 2017 |

| | | | |
|---|---|---|---|
| PARATHYROID | Adenoma | | 2017 |
| | Carcinoma | | |
| ADRENAL MEDULLA | Pheochromocytoma | | 2017 |
| EXTRA-ADRENAL PARAGANGLIOMA | Head and neck paragangliomas | Carotid body paraganglioma | 2017 |
| | | Jugulotympatic paraganglioma | |
| | | Vagal paraganglioma | |
| | | Laryngeal paraganglioma | |
| | Sympathetic paragangliomas | | |
| SKIN | Merkel cell carcinoma | | 2018 |

### 2.2.1 INCIDENCE

The incidence of NENs represents about 0.5% of all newly diagnosed malignant neoplasms (Oronsky et al. 2017). The incidence of NENs (Figure 3) for most anatomical sites, stages, and grades is increasing. The rate of NENs increased 6.4-fold from 1973 to 2012 (1.09 to 6.98 per 100 000) in the Surveillance, Epidemiology and End-Results (SEER) 18 registry (Dasari et al. 2017). The highest incidence rates were found in the lung (1.49 per 100 000) and gastroenteropancreatic (GEP) sites (3.56 per 100 000) (Dasari et al. 2017). The incidence rate of neuroendocrine tumors (NETs) with an unknown primary site is 0.84 per 100 000 individuals (Dasari et al. 2017). There is no apparent explanation, but most likely owing to the detection of early-stage disease through more sophisticated diagnostic methods. A comparison of the incidence rates between genders follows a similar distribution (Dasari et al. 2017). Yet, little is known about the environmental, ethnic, genetic or other predisposing risk factors influencing the development of NENs (Leoncini et al. 2017).

NENs can develop sporadically or in association with hereditary syndromes. Most NENs are sporadic, including 80% of GEP–NENs, 95% of pulmonary NENs, 65% of PHEOs and PGLs, and 75% of medullary thyroid carcinomas (Crona and Skogseid 2016). In hereditary syndromes, tumors occur at a younger age and often arise multifocally in multiple organs. A genetic syndrome is behind approximately 20% of all NENs (Crona and Skogseid 2016). At least ten hereditary syndromes (Table 3) including NEN are recognized (Klöppel and Lloyd 2017). The classic syndromes consist of multiple endocrine neoplasias type 1 and 2 (MEN1 and MEN2) and von Hippel-Lindau (VHL).

MEN1 is an autosomal dominantly inherited syndrome in which the *MEN1* gene mutates (Wermer 1954). Over 1000 mutations have been recognized, often leading to the truncation of the menin protein (Crona and Skogseid 2016). Carriers of *MEN1* experience tumors of the parathyroid (95%), pituitary gland (20–40%), and pancreatic/duodenum NENs (40–80%) (Crona and Skogseid 2016). MEN2, in comparison, features subtypes A and B, from which subtype A accounts for 80% of all cases. A mutation of the proto-oncogene *RET* (Mulligan et al. 1993) results in the activation of the RAS/MAPK and PI3K/AKT signalling pathways leading to medullary thyroid carcinoma (90–100%) and tumors of the adrenal medulla (20–80%) (Crona and Skogseid 2016). VHL increases the risk of various tumors, including PGLs and pancreatic NETs (Klöppel and Lloyd 2017). This syndrome is caused by the inactivation of the *VHL* tumor-suppressor gene resulting in the truncation of the VHL protein and the disregulation of hypoxia-inducible factors (Nordstrom-O'Brien et al. 2010).

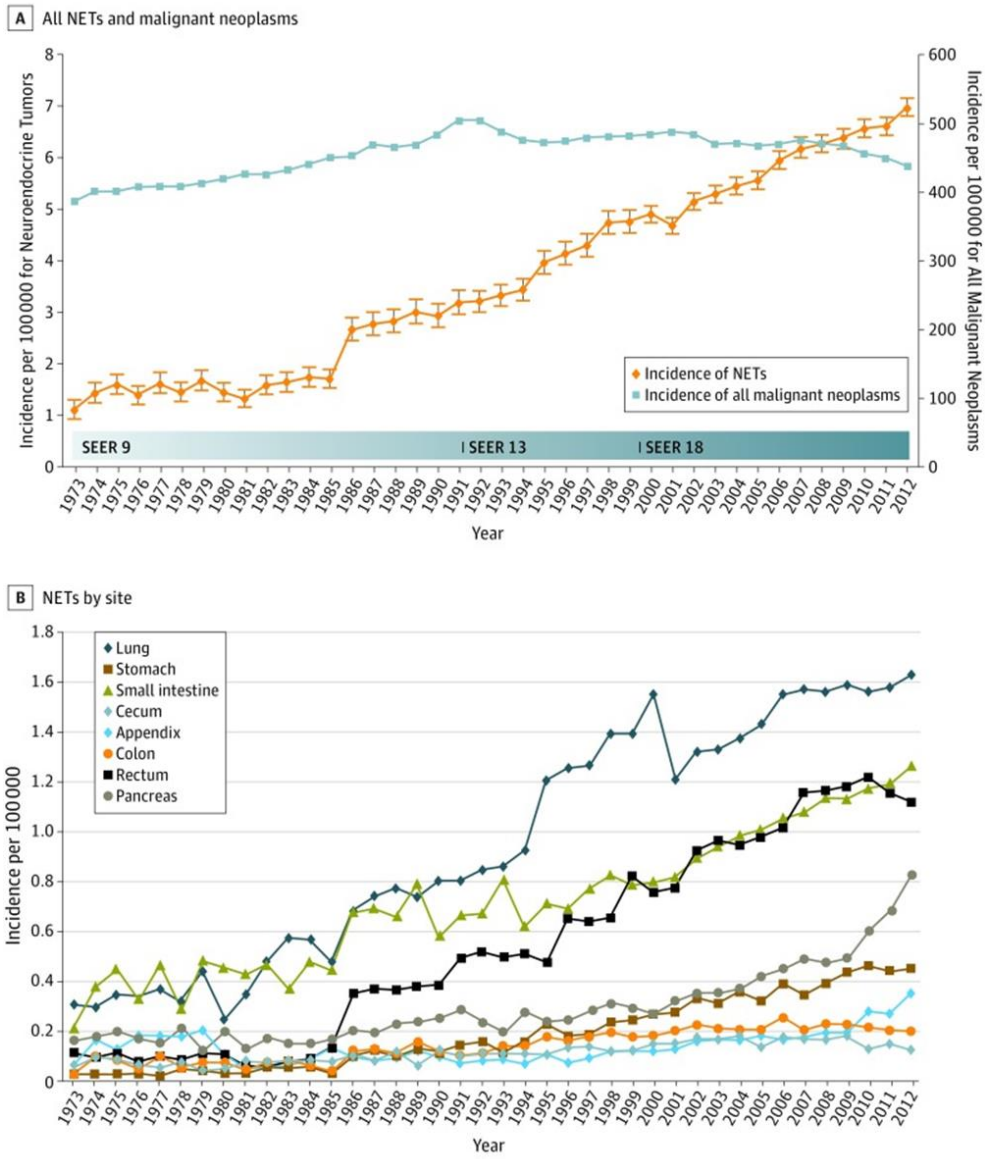


**Figure 3.** Incidence rates for neuroendocrine tumors (NETs) compared to all malignancies (A) and by NET origin (B) from 1973 to 2012. Figure adapted from Dasari et al. (2017) in accordance with the terms and conditions stipulated by Elsevier and the Copyright Clearance Center.

**Table 3.** Hereditary syndromes associated with neuroendocrine neoplasias (NENs). Modified from Klöppel and Lloyd (2017).

| INHERITED SYNDROM | GENE MUTATION | NENs | OTHER LESIONS |
|---|---|---|---|
| Multiple endocrine neoplasias type 1 | MEN1 | ✓ Parathyroid adenomas<br>✓ Pituitary tumors<br>✓ Duodenal tumors<br>✓ Pancreatic tumors | Adrenal cortical lesions, cutaneous lesion, central nervous system (CNS), soft tissue and breast lesions |
| Multiple endocrine neoplasias type 2 | RET | ✓ Medullary thyroid carcinoma<br>✓ Pheochromocytoma<br>✓ Paraganglioma<br>✓ Parathyroid adenomas | Hirschsprung disease, cutaneous lichen amyloidosis |
| Multiple endocrine neoplasias type 4 | CDKN1B | ✓ Parathyroid adenomas<br>✓ Pituitary tumors<br>✓ Pancreatic tumors<br>✓ Cervix tumors<br>✓ Bronchial tumors<br>✓ Stomach tumors | |
| Hyperparathyroidism-jaw tumor syndrome | CDC73 | ✓ Parathyroid carcinoma<br>✓ Parathyroid adenoma | Fibro-osseous lesions of the mandible and maxilla |
| von Hippel-Lindau syndrome | VHL | ✓ Pheochromocytoma<br>✓ Paraganglioma<br>✓ Pancreatic tumors | Hemangioblastomas of CNS and retinas, clear-cell renal carcinoma and cysts |
| Familial paraganglioma-pheochromocytoma syndromes | SDHB<br>SDHC<br>SDHD | ✓ Pheochromocytoma<br>✓ Paraganglioma | |
| Neurofibromatosis type 1 | NF1 | ✓ Pheochromocytoma<br>✓ Paraganglioma<br>✓ Pancreatic tumors<br>✓ Duodenal tumors | Multiple neurofibromas, café-au-lait spots, freckling of the axilla and/or groin, bone dysplasia, gliomas, gastrointestinal stromal tumors |
| Carney complex | PRKA-R1A | ✓ Pituitary tumors<br>✓ Thyroid tumors | Adrenal cortical lesions, lentiginosis, myxomas |
| McCune–Albright syndrome | GNAS | ✓ Parathyroid adenomas<br>✓ Hyperfunctioning syndromes | Café-au-lait spots, fibrous dysplasia |
| DICER1 syndrome | DICER1 | ✓ Thyroid tumors<br>✓ Pituitary blastoma<br>✓ Ovarian sertoli cell tumors | Cystic nephroma, pleuropulmonary blastoma |
| Glucagon cell hyperplasia and neoplasias | GCGR | ✓ Pancreatic tumors; glucagon cell | |

### 2.2.2 CLINICAL PRESENTATION

The clinical presentation of NENs varies depending upon the stage and site of the tumor, as well as the tumor's hormonal activity. Patients may be asymptomatic or symptoms can be nonspecific. Thus, NENs are typically found incidentally.

#### *2.2.2.1 Functioning neuroendocrine neoplasms*

If tumor cells release hormones, patients may suffer from symptoms related to the secreted hormone (de Herder 2007). These tumors are syndromic or functioning NENs (Klöppel et al. 2017b). Functioning NENs are named according to the hormone produced, such as insulinomas, glucagonomas, gastrinomas, somatostatinomas, VIPomas, and serotonin or adrenocorticotrophin (ACTH) -producing NENs (Klöppel et al. 2017b, Washington 2019). For example, the autonomic secretion of insulin causes the hypoglycemic syndrome and the overexpression of gastrin causes the Zollinger–Ellison syndrome. The production of serotonin causes the classical carcinoid syndrome with flushing, sweating, and diarrhea. Carcinoid syndrome usually requires the presence of liver metastases to manifest. Table 2 summarizes the terms and locations of the functioning NENs, while Table 4 provides examples of hormone-producing cell types.

#### *2.2.2.2 Nonfunctioning neuroendocrine neoplasms*

Most NENs, however, are asymptomatic. These NENs can be clinically silent for years until late presentation due to the tumor load or symptoms related to metastasis. These tumors are called non-syndromic or nonfunctioning NENs (Klöppel et al. 2017b, Washington 2019). Clinical presentations due to the tumor load or location include pain, weight loss, GI bleeding or obstruction. On average, the diagnosis of a nonfunctioning NEN is more often delayed and misdiagnosed leading to the development of local invasion and metastases.

### 2.2.3 BIOCHEMICAL MARKERS

Preliminary diagnosis of NENs is usually based on elevated levels of NE differentiation–specific and hormone-specific biochemical markers. These tumor markers can be analyzed from different body fluids, such as urine and serum. Biochemical markers can be divided into general NE markers and tumor type–specific markers (Oberg et al. 2017). The most commonly used markers

are serum chromogranin A (CGA) and urinary 5-hydroxyindole-5-acetic acid (5-HIAA), a metabolite of serotonin (Aluri and Dillon 2017). Circulating CGA is quite nonspecific, with a sensitivity and specificity of around 60% to 90% (Oberg et al. 2017, Hofland et al. 2018). Serotonin and 5-HIAA are markers of serotonin secretion, typically suggesting a primary tumor location of the small intestine (Frilling et al. 2012, Aluri and Dillon 2017). Neuro-specific enolase (NSE) is a relevant biochemical marker to diagnose high-grade NENs (Oberg et al. 2017). Biochemical markers are used not only in diagnosis, but also in the follow-up of tumor patients. Elevated levels of markers may indicate disease recurrence.

**Table 4.** Hormone-producing neuroendocrine neoplasias (NENs), specific hormones with the hormone-producing cell type and anatomic location. Modified from Klöppel et al. (2017b).

| NEN TYPE | HORMONE | CELL TYPE | ORGAN |
|---|---|---|---|
| ACTH-producing NENs | ACTH | Basophils | ✓ Pituitary gland, anterior pituitary |
| Medullary carcinoma | Calcitonin | C cells | ✓ Thyroid |
| Gastrinoma | Gastrin | Gastrin cells | ✓ Pancreas<br>✓ Stomach pyloric antrum<br>✓ Small intestine Duodenum |
| Insulinoma | Insulin | Beta cells | ✓ Pancreas, islet of Langerhans |
| Glucagonoma | Glucagon | Alpha cells | ✓ Pancreas, islet of Langerhans |
| Serotonin-producing NENs | Serotonin | Enterochromaffin cells Kulchitsky cells | ✓ GI tract<br>✓ Lung |
| Somatostatinoma | Somatostatin | Delta cells | ✓ Pancreas<br>✓ Stomach pyloric antrum<br>✓ Small intestine Duodenum |
| VIPoma | Vasointestinal polypeptide | Nerves | ✓ GI tract<br>✓ Pancreas |

### 2.2.4 IMAGING

Various imaging methods form the basis of NEN diagnostics (Maxwell and Howe 2015). The detection sensitivity and specificity of imaging varies depending upon the anatomical location and NEN type. Nuclear imaging techniques play an additional role in selecting treatment options and during follow-up to detect recurrent disease (Sundin et al. 2017).

#### 2.2.4.1 Radiological examination

Computed tomography (CT) and magnetic resonance imaging (MRI) are methods which yield detailed information from tissue structures. Contrast-enhanced CT of the neck-thorax-abdomen and pelvis is the primary imaging method for patients with signs and symptoms of a NET (Sundin et al. 2017).

In CT, the mean sensitivity and specificity to detecting NETs are 82% and 86%, respectively, with the lesion-based sensitivity and specificity standing at 77% to 85% and 71% to 85%, respectively (Gabriel et al. 2007, Ruf et al. 2011, Veit-Haibach et al. 2011, Sundin et al. 2017). CT is useful in the context of an unknown primary tumor (Maxwell and Howe 2015). MRI with contrast enhancement is the preferred method for the visualization of the liver, metastases and primary pancreatic NETs (Maxwell and Howe 2015, Sundin et al. 2017). The mean MRI sensitivity and specificity in the diagnosis of pancreatic NENs stand at 70% to 75% and 98% to 100%, respectively (Brenner et al. 2012, Mayerhoefer et al. 2013, Schmid-Tannwald et al. 2013, Sundin et al. 2017).

#### 2.2.4.2 Nuclear imaging

Nuclear imaging utilizes short-lived radioactive substances linked to different molecules (Pauwels et al. 2018). Combining CT and nuclear imaging procedures carries a complementary role to NEN imaging (Maxwell and Howe 2015, Sundin et al. 2017).

Somatostatin receptor (SSTR) scintigraphy benefits the isotope-labeled somatostatin analogs (SSAs) which bind to SSTRs. OctreoScan™ imaging of SSTRs is based on the use of the $^{111}$Indium-labelled conjugate of octreotide, which binds especially to SSTR subtype 2. Upon binding and internalization, the bound radioisotope ligand allows for the imaging of tumors expressing SSTRs (Frilling et al. 2012, Pauwels et al. 2018). Positron emission topography (PET) is an isotope imaging method that observes the metabolic processes in organs and possible tumors. PET utilizes common radioligands, fluoride-18 and gallium-68, linked to different chelators, including 1,4,7,10-tetraazacyclodecane-1,4,7,10-tetraacetic acid (DOTA) and fluorodeoxyglucose (FDG) (Pauwels et al. 2018). Combining PET/CT with 68Ga-labeled SSAs is optional for the OctreoScan, providing a higher sensitivity (Maxwell and Howe 2015).

The choice of imaging method depends on the differentiation of the tumor. The expression of SSTRs is lower in high-grade NENs (Schmid et al. 2012). Therefore, these tumors have a lower uptake isotope-labeled ligand and are less visible in imaging (Maxwell and Howe 2015, Olsen et al. 2016). PET/CT with 18F-FDG is more suitable for poorly differentiated NECs than well-differentiated NETs

because NECs grow more actively (Frilling et al. 2012). Slow-growing, well-differentiated NETs have a lower metabolic rate and do not uptake metabolic 18F-FDG so readily (Frilling et al. 2012). Positivity in 18F-FDG-PET/CT predicts poor survival (Binderup et al. 2010, Johnbeck et al. 2016, Majala et al. 2019).

While a variety of imaging techniques have improved the visualization of NEN lesions, some GEP–NENs can remain undetected (Schott et al. 2011, Frilling et al. 2012). A study of the imaging sensitivity of small micrometastases in the liver by Elias et al. (2010) found an MRI detection rate of 33%, a CT detection rate of 21%, and an ultrasonography detection rate of 22% (Elias et al. 2010), highlighting the limitations of current imaging techniques. SSTR scintigraphy carries a detection sensitivity of 60% to 80% and PET carries a mean sensitivity of 88% to 93% (Sundin et al. 2017). If lesions fall under the limits of resolution, as very small tumors, they may remain undetected during imaging (Frilling et al. 2012). The histological or hormonal type of NEN (gastrinomas and insulinomas) may also influence the imaging sensitivity (Frilling et al. 2012, Sundin et al. 2017).

### 2.2.5 PATHOLOGY

The cornerstone of diagnosing NEN is the histopathological analysis of a tumor specimen (Perren et al. 2017). Specimens are mainly formalin-fixed and paraffin-embedded tissue. Gross examination and histopathology data provide information on the tumor size, invasiveness, resection margins, and the possible presence of local metastases, thus the criteria for the tumor, node, and metastasis (TNM) classification (Klöppel et al. 2009).

#### *2.2.5.1 Cytology*

Fine-needle aspiration (FNA) is used for the microscopic examination of cells from a suspicious tissue structure. The reliability of FNA depends on the representativeness of the tumor cells in the sample. In cytological preparation, NENs have a plasmacytoid appearance characterized by an eccentrically placed nucleus and a typical NE-type chromatin (Klöppel et al. 2017b). Cytological samples are commonly taken from organs where histological biopsies prove difficult to collect (the pancreas and thyroid gland) (Klöppel et al. 2017b). Diagnosis relying on FNA is less reliable compared to diagnosis based on a core-needle biopsy. For example, the tumor grade cannot be determined from a cytological sample and, in general, immunohistochemistry (IHC) does not work as well as when analyzing formalin-fixed tissues (Vinayek et al. 2014).

#### *2.2.5.2 Histopathology*

NEN diagnosis can be made from a histological tissue specimen of the primary tumor or from a metastatic lesion (Perren et al. 2017). The specimen can be a core-needle biopsy, endoscopic biopsy or surgical specimen.

Common nuclear features are characteristic for NENs. Tumor cells are usually monotonic, while the nuclei are uniform and round with smooth nuclear membranes. Chromatin is evenly dispersed showing a characteristic "salt-and-pepper" appearance without prominent nucleoli. The cytoplasm is finely granular corresponding to dense-core granules (Rekhtman 2008, Schmitt et al. 2016). The cellular features of NENs are better distinguished in well-differentiated NENs than in poorly differentiated NECs.

Depending upon the primary site, NENs feature different histological growth patterns (Rekhtman 2008, Schmitt et al. 2016). Classic patterns (Figure 4) characteristic of well-differentiated tumors include 1) a trabecular pattern which forms long nests and cords of cells separated by fibrous septa; 2) a glandular pattern which forms gland structures with lumens; 3) a solid pattern featuring a non-organoid growth pattern; and 4) a pseudorosette or rosette-forming pattern, whereby tumor cells grow around vessels (Schmitt et al. 2016). In a poorly differentiated NEC, the architecture of the growth pattern is often diffuse (Rekhtman 2008).

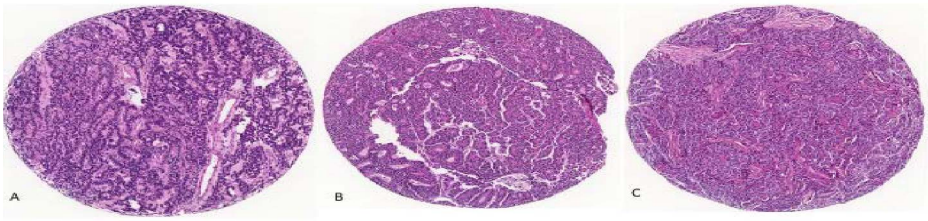


**Figure 4.** Neuroendocrine neoplasias feature various histological growth patterns: A) trabecular, B) glandular, and C) solid-growth patterns.

#### *2.2.5.3 Neuroendocrine phenotype*

The neuroendocrine phenotype is confirmed through IHC (Rekhtman et al. 2008, Perren et al. 2017). Most NENs, except PHEOs and PGLs, are positive for pan-cytokeratin, indicating an epithelial origin for the tumor. Common NE markers (Figures 5 and 6) are CGA and synaptophysin (SYP) (Schmitt et al. 2016). Chromogranins are a family of glycoproteins including types A, B, and C, comprising the majority of soluble proteins in the neurosecretory granules of NE cells (Doblinger et al. 2003, Klöppel 2007). SYP is a glycoprotein, part of the synaptic vesicles of neurons and NE cells (Klöppel 2007). SYP is a broad-spectrum NE marker with a high sensitivity for identifying the NE nature of a tumor, but possessing a lower specificity than CGA (Gut et al. 2016, Perren et al. 2017).

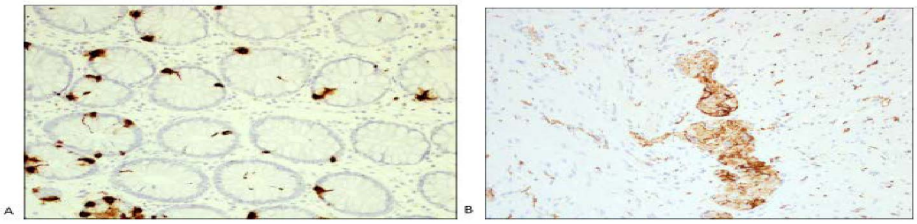


**Figure 5.** Chromogranin A (A) and synaptophysin (B) are expressed in normal neuroendocrine cells and nerves.

The specificity of NE markers varies. The histological differentiation of NENs influences the expression levels of CGA and SYP; well-differentiated NETs unlike poorly differentiated NECs express NE markers abundantly. Well-differentiated NENs are commonly diffusely positive for SYP, although the expression of CGA is often heterogeneous (Perren et al. 2017) since the expression level of CGA correlates with the number of secretory granules (Gut et al. 2016). In poorly differentiated NECs, the staining intensities of the NE markers typically decrease (Schmitt et al. 2016). The application of less-specific NE markers, such as CD56 and neuro-spesific enolase (NSE), is not recommended, because CD56 is often expressed in non-NENs and NSE is a typical neural marker (Perren et al. 2017). However, recently identified insulinoma-associated protein 1 (INSM1) is a good NE marker for NECs (Fujino et al. 2017). Table 5 summarizes the typical markers expressed in NENs.

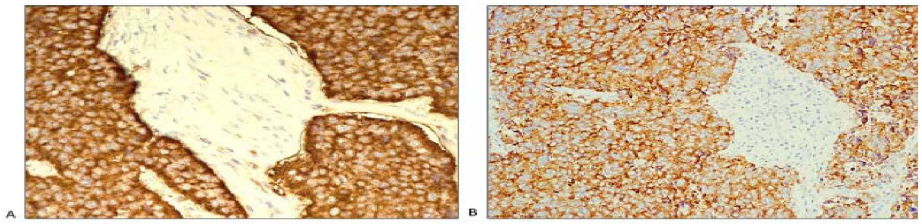

**Figure 6.** Neuroendocrine neoplasias express A) chromogranin A and (B) synaptophysin.

### *Proprotein convertase subtilisin/kexin type 2*

Proprotein convertases (PCs) are a large family of nine enzymes responsible for the activation of different peptides, proteins, and growth factors (Seidah and Prat 2012). Within the PC family, proprotein convertase subtilisin/kexin type 2 (PCSK2) takes part in the hormonal processing of the regulated secretory pathway of NE cells (Li et al. 2003). PCSK2 is stored in the dense core secretory granules of a normal NE cell (Portela-Gomes et al. 2004, Seidah and Prat 2012). Hormones such as somatostatin, glucagon, and insulin as well as CGA are processed by PCSK2 (Doblinger et al. 2003, Portela-Gomes et al. 2008). PCSK2 was discovered two decades ago, and many NENs from different origins have exhibited PCSK2 positivity (Scopsi et al. 1995, Kajiwara et al. 1999, Kimura et al. 2000, Tomita 2001).

**Table 5.** Neuroendocrine markers localized in the secretory granules, cytoplasm, cell membrane or nuclei of the neuroendocrine cell. Modified from Portela-Gomes et al. (2004).

| **I Secretory granule proteins** |
|---|
| a) Core-related proteins<br>Hormones: insulin, glucagon, serotonin, vasoactive intestinal polypeptide<br>Chromogranin A<br>Proprotein convertase subtilisin/kexin type 2 |
| b) Membrane-related proteins<br>Synaptophysin |
| **II Cytosolic proteins** |
| Neuro-specific enolase |
| Protein Gene Product 9.5 |
| **III Cell membrane** |
| Somatostatin receptors |
| **IV Nuclei** |
| Insulinoma-associated protein 1 |

#### *2.2.5.4 Tumor differentiation and grading*

According to the WHO classification, NENs fall into the categories of well-differentiated NETs and poorly differentiated NECs (Klöppel et al. 2017a, Washington 2019). NEN grading is based on the proliferation activity of the tumor cells. The proliferation index (PI), assessed using Ki-67 IHC, is the most important marker for tumor grading together with the mitotic index of the tumor cells. The Ki-67 PI is evaluated from the areas of highest nuclear labeling, referred to as hotspots, including 500 to 2000 tumor cells (Rindi et al. 2006, Rindi et al. 2007, Klimstra et al. 2010, Klöppel et al. 2017a, Klimstra et al. 2019). The nuclear expression of Ki-67 is observed during the active phases of the cell cycle, but not during the resting phase (van Dierendonck et al. 1989). For NEN grading, any level of positivity should be considered a positive finding (Brown and Gatter 1990, Lopez et al. 1991). Grades 1 and 2 in GI and pancreatic NENs are well-differentiated NETs with low mitotic and proliferation activity (Klöppel et al. 2017b, Washington 2019). Grade 3 can be a well-differentiated tumor or a poorly differentiated carcinoma (Klöppel et al. 2017b, Washington 2019). Different NEN types have organ-specific criteria for grading, as summarized in Table 6 (E. Brambilla 2015, Busam et al. 2018, Rindi et al. 2018).

**Table 6.** WHO tumor grading for specific neuroendocrine neoplasm (NENs) according the proliferation index (PI) and mitotic count. Modified from E. Brambilla (2015), Klöppel et al. (2017b), and Washington (2019). *Indicates the normative classification. High-power field (HPF)

| WHO | NENs | | PI Ki-67 | MITOTIC COUNT |
|---|---|---|---|---|
| 2019 | Gastrointestinal NENs | NET, G1 well-differentiated | <3% | <2 per 10 HPF |
| | | NET, G2 well-differentiated | 3–20% | 2–20 per 10 HPF |
| | | NET, G3 well-differentiated | >20% | >20 per 10 HPF |
| | | NEC, small-cell type<br>NEC, large-cell type | >20% | >20 per 10 HPF |
| 2015 | Pulmonary NENs | Small-cell carcinoma | 50–100%* | >10 per 2 $mm^2$ |
| | | Large-cell carcinoma | 40–80%* | >10 per 2 $mm^2$ |
| | | Typical carcinoids | ≥5%* | <2 per 2 $mm^2$ |
| | | Atypical carcinoids | ≥20%* | 2–10 per 2 $mm^2$ |
| 2017 | Pancreatic NENs | PanNET, G1 well-differentiated | <3% | <2 per 10 HPF |
| | | PanNET, G2 well-differentiated | 3–20% | 2–20 per 10 HPF |
| | | PanNET, G3 well-differentiated | >20% | >20 per 10 HPF |
| | | PanNEC G3, small-cell type<br>PanNEC G3, large-cell type | >20% | >20 per 10 HPF |
| | Endocrine organs | Parathyroid adenoma | ≤4%* | <1 per 10 HPF* |
| | | Parathyroid carcinoma | 6–8%* | >5 per 50 HPF* |

### 2.2.6 CLASSIFICATION

Classifying tumors forms the basis of determining prognosis, disease management, and follow-up of patients. The classification of NENs relies on WHO guidelines and TNM staging proposed by the European Neuroendocrine Tumor Society (ENETS) (Rindi et al. 2006, Rindi et al. 2007, Pavel and de Herder 2017), the American Joint Committee on Cancer (AJCC), and the Union for International Cancer Control (UICC) (Brierley et al. 2017).

#### *2.2.6.1 World Health Organization*

In 1963, Williams and Sandler separated NETs according to embryological tumor origin into the foregut, midgut, and hindgut types (Williams and Sandler 1963), while WHO classifications began in the 1980s (Williams et al. 1980). In 1995, Capella and co-workers proposed the first unified classification model for lung, pancreatic, and GI NETs taking into consideration the potential malignancy of the tumor based on histological criteria (Capella et al. 1995). The WHO classifications continue to aim towards predicting clinical outcomes; the proliferation activity of a tumor seems to carry prognostic significance in NENs (Capella et al. 1995, Solcia et al. 2000, Klöppel et al. 2017a, Klimstra et al. 2019).

#### *2.2.6.2 Tumor-Node-Metastasis*

TNM staging relies on the size of the tumor, the status of the regional lymph nodes, and the absence or presence of metastases. AJCC/UICC staging applies to well-differentiated NENs of the GI tract (G1 and G2 of the gastric, small intestine, appendix, and colorectum), including the pancreas (Brierley et al. 2017). High-grade (G3) NECs follow the same criteria as adenocarcinomas of the respective tumor location (Brierley et al. 2017). The AJCC/UICC staging of Merkel cell carcinoma relies on its own separate classification criteria (Brierley et al. 2017). TNM classification of pulmonary carcinoids complies with the rules governing lung tumors (Brierley et al. 2017).

### 2.2.7 MANAGEMENT

As a heterogeneous tumor type, NENs require multidisciplinary medical teams (Figure 7) for management with the goals of slowing down tumor growth, controlling hormonal symptoms, and improving the quality of life (Oronsky et al. 2017).

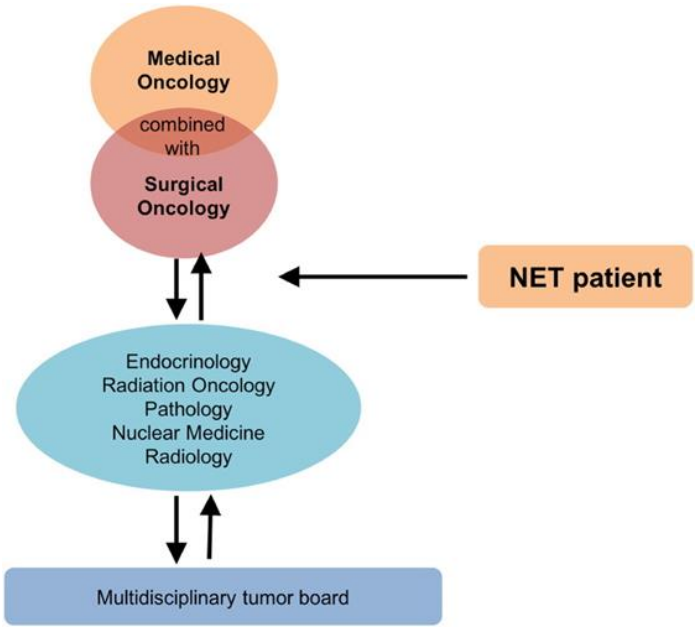


**Figure 7.** Neuroendocrine tumors (NETs) require a multidisciplinary healthcare team. Image from Oronsky et al. (2017), reproduced here in accordance with Elsevier Inc., Creative Commons Attribution-NonCommercial-No Derivatives License (CC BY NC ND).

#### *2.2.7.1 Surgery*

The tumor location and extent of disease play crucial roles in therapeutic planning. Surgery represents first-line treatment for NENs. Indications for surgery depend upon the tumor size, location, histological grade, metastases, and the patient's clinical symptoms. In general, radical resection is preferred, although patients with advanced or nonresectable disease may receive palliative surgery to decrease the tumor burden and to help control hormonal symptoms (Oronsky et al. 2017)

#### *2.2.7.2 Medical therapy*

Medical management aims to relieve clinical symptoms and suppress tumor growth and progression given the late diagnostic status of most NETs (Oronsky et al. 2017). Therapy for NENs includes treatment with SSAs and alpha interferons, primarily indicating treatment of functioning NENs causing clinical and hormone-related syndromes (Zandee and de Herder 2018).

##### *Somatostatin analogs*

Somatostatin is a hormone with a broad range of inhibitory actions, including regulating hormone secretion and cell proliferation (Theodoropoulou and Stalla 2013). Somatostatin binds SSTRs, G-protein-linked receptors, with a single polypeptide chain that passes through the cell membrane seven times.

SSAs are structurally similar to biological somatostatins. Octreotide (Sandostatin) and lanreotide (Somatuline) are synthetic long-acting SSAs, which inhibit growth and the progression of an SSTR-positive tumor (Figure 8). SSAs also reduce clinical symptoms (carcinoid syndrome), thereby improving the quality of life of patients with well-differentiated NENs (Frilling et al. 2012). By comparison, SSAs are ineffective in poorly differentiated NECs due to the lower expression of SSTRs (Schmid et al. 2012).

Octreotide and lanreotide have a high affinity to SSTR2, SSTR3, and SSTR5 (Theodoropoulou and Stalla 2013). More recent analog pasireotide (Signifor), a multi-receptor SSA, binds with a higher affinity to SSTR5 and SSTR1-3 (Vitale et al. 2018). In disseminated disease, analog therapy represents the first-line medical treatment (Rinke et al. 2009, Oronsky et al. 2017).

##### *Interferon*

Interferon alpha treatment is recommended as second-line medical therapy after disease progression during treatment on SSAs (Zandee and de Herder 2018). Cytokine, interferone alpha provides palliative effects in functional NENs with a low PI, by stabilizing the disease in 50% of patients (Oronsky et al. 2017). Interferon alpha also carries potential side effects, thereby limiting its use in practice (Mirvis et al. 2014).

### *Other medical treatments*

Other oncological medical treatments include anti-proliferative agent everolimus and vascular endothelial growth factor receptor inhibitor sunitinib. The RADIANT 1–4 trials studied the effects of everolimus in NETs revealing their safety and efficacy in well-differentiated NETs (Pusceddu et al. 2016). Sunitinib was studied in pancreatic NETs by Raymond et al. (2011). In a study of 171 patients with advanced, well-differentiated pancreatic NETs, sunitinib increased progression-free survival from 5.5 to 11.4 months (Raymond et al. 2011). These target therapy agents are registered for progressive, metastatic, pancreatic and small intestine NETs (Zandee and de Herder 2018).

For the treatment of poorly differentiated NECs, chemotherapy remains the first-line treatment (Eriksson et al. 2009, Oronsky et al. 2017). High-grade tumors respond better to cytotoxic chemotherapy compared to low-grade tumors, since the tumor cells divide more aggressively. Chemotherapy for NECs includes treatment with combinations of streptozotocin plus doxorubicin and/or 5-fluorouracil, cisplatin plus etoposide, and dacarbazine (Garcia-Carbonero et al. 2017).

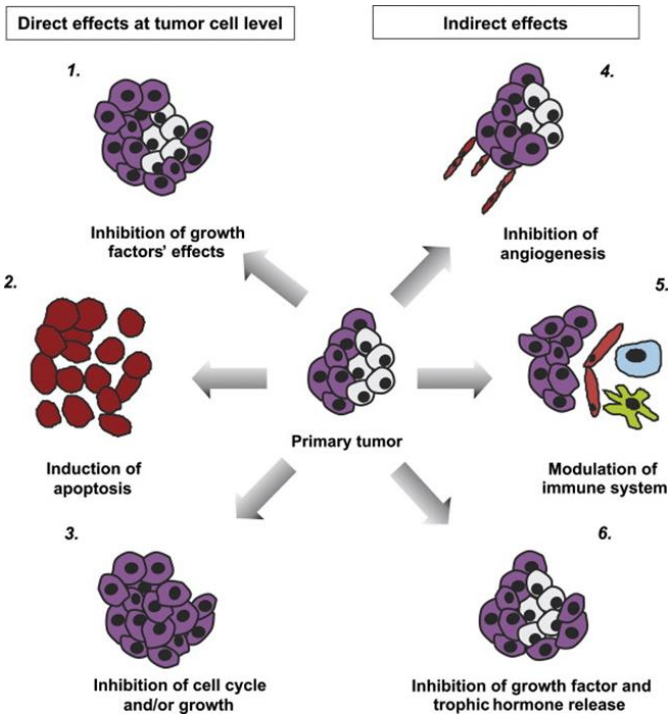


**Figure 8.** Somatostatin analog therapy has antiproliferative effects on tumor cells. The direct mechanisms (1–3) associate with the inhibition of the cell cycle and the induction of apoptosis. The indirect mechanisms (4–6) include inhibition of the vascularization, the secretion of tumor-promoting signals, and the production of growth factors. Image from Theodoropoulou and Stalla (2013) in accordance with the terms and conditions provided by Elsevier and Copyright Clearance Center.

#### *2.2.7.3 Peptide receptor radionuclide therapy*

Peptide receptor radionuclide therapy (PRRT) utilizes radio-labelled (lutetium-177 and yttrium-90) synthetic SSAs for systemic radiotherapy (Theodoropoulou and Stalla 2013). PRRT provides a safe and effective treatment option for disseminated GEP–NETs, where adequate densities of specific SSTRs are found (Hicks et al. 2017). Other potential NENs for PRRT include lung NETs, PHEOs, and PGLs (Werner et al. 2018). The NETTER-1 trial involved 229 patients with metastatic small intestine NETs (Strosberg et al. 2017). Treatment with $^{177}$Lu-DOTATATE improved progression-free survival and a 60% lower risk of death compared to the octreotide long-acting repeatable group (Hicks et al. 2017, Strosberg et al. 2017). Figure 9 summarizes the steps for NEN diagnosis and management.

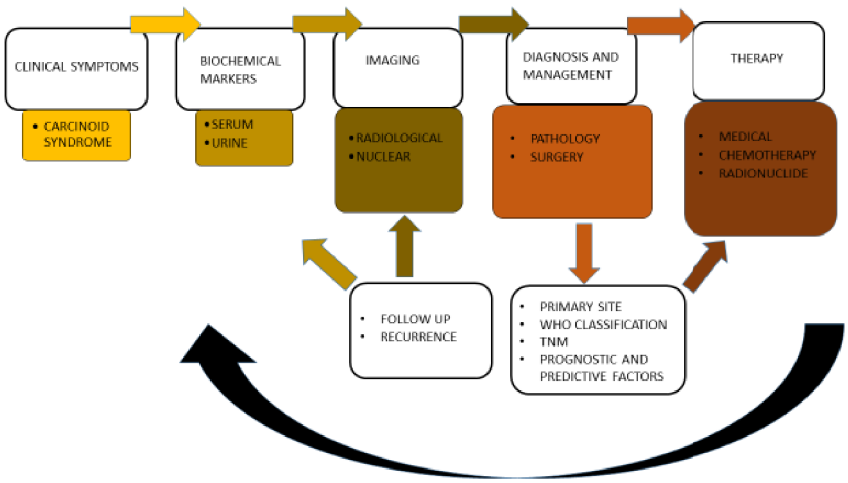


**Figure 9.** Overview of the clinical investigations, diagnostics, and treatment steps in the management of neuroendocrine neoplasms.

### 2.2.8 PROGNOSIS

The overall survival (OS) for all types of NENs has improved over time, with a current median OS for all NEN patients of 9.3 years (Dasari et al. 2017). Tumor stage, grade, and primary tumor site all affect OS. Localized NETs accompany a better OS than distant NETs ranging from >30 years to 12 months, and G1 NETs have the highest median OS, while G3 and G4 NETs have the poorest OS irrespective of tumor site (Dasari et al. 2017). When survival is evaluated according to tumor site, appendiceal and rectal NETs feature the best median OS (>30 and 24.6 years, respectively) and NETs from the lung and pancreas (5.5 and 3.6 years, respectively) have the worst median OS (Dasari et al. 2017).

## 2.3 NEUROENDOCRINE TUMOR RESEARCH

In recent decades, the diagnosis and management of NENs have experienced impressive improvements. Tissue microarray (TMA) technology enables the examination of a large number of tissue samples on one slide. The simultaneous study of multiple histological samples began with the "sausage technique" in 1986 (Battifora 1986). Juha Kononen developed the first version of the modern TMA technique in 1998 by introducing a punch instrument that allowed for the rigorous placement and relocalization of individual tissue cores (Kononen et al. 1998). Currently, computer-assisted TMA technology allows for a more detailed orientation of punches through the annotation of digital images to navigate the punching sites (Zlobec et al. 2014). The TMA platform remains the method of choice when novel NE markers are studied in large tumor cohorts (Schmid et al. 2012, Qian et al. 2016, Bellizzi 2020).

### 2.3.1 TISSUE MICROARRAY

The type of TMA varies depending upon the study focus. TMA can be constructed using normal tissues with or without tumor material. Tumor tissue TMAs are further classified as 1) multitumor arrays used to screen for a large number of tumors of different origins and subtypes; 2) progression arrays to assess various diagnostic stages of a particular tumor type; or 3) prognostic arrays for patients with a known clinical outcome (Ramya et al. 2018). Normal tissue TMAs commonly serve as the control material or the verification array (Packeisen et al. 2003).

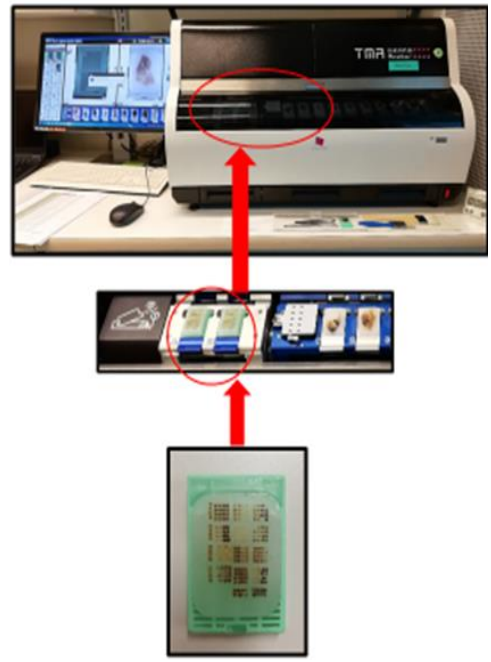

**Figure 10.** An automated array includes a computer and a connection to a scanner. The tissue microarray instrument holds the donor and receipt blocks.

#### *2.3.1.1 Tissue microarray technique*

The construction of a TMA begins with the selection of a tissue cohort (normal tissue, tumor tissue or both). After reviewing the original material, the area of interest is marked on the slide (hematoxylin and eosin, HE) and defined on the corresponding region of the paraffin block (Kononen et al. 1998, Zlobec et al. 2014). The construction of an array can be manual, semi-manual or automatic. Core needles are available in varying diameters, ranging from 0.6 mm to 2.0 mm (Ramya et al. 2018). The appropriate areas from the donor block are punched and relocalized into the ready-made holes on the recipient block. The resulting array block needs warming in an incubator to seal the tissue core holes, after which the block is ready. Tissue data with the coordinates are documented (Kononen et al. 1998, Zlobec et al. 2014).

#### *2.3.1.2 Next-generation tissue microarray*

Next-generation TMA (ngTMA) represents a new approach to constructing TMAs, relying on digitalization, and automated arraying (Zlobec et al. 2013). The digitalization of slides allows for a more accurate annotation of the desired tissue area for punching compared to conventional arraying, while slides can be viewed from a computer screen rather than via a microscope, factors rendering ngTMA advantageous (Zlobec et al. 2014).

Digitalization allows for the accurate selection of the region of interest (ROI) for TMA (Zlobec et al. 2013). For example, this may include the selection of areas covering various distances from the tumor border, the areas of tumor-infiltrating lymphocytes, vascularization or tumor budding or the neural and vascular invasion. Selected areas are annotated digitally allowing for notes and for the differentiation of various annotations and to record the information provided into a logbook (Zlobec et al. 2014).

In automated arraying (Figure 10), recipient blocks are placed into the TMA instrument together with empty donor blocks. A camera takes a picture of the recipient blocks, and objective slides are scanned for viewing and annotations. Pictures from these two images are overlapped allowing for the precise drilling of the tissue cores. The instrument prepares the donor block according to the instructions provided by the user, including the size, number, and place of the tissue cores in the block, and the total number of prepared TMA blocks.

### 2.3.2 NEUROENDOCRINE TUMOR MARKERS

The morphological examination of tumor cells is supported by the IHC expression of specific markers, as illustrated in Table 7. Differential diagnoses include the primary diagnostic categories following the subclassification of a neoplasm (Bellizzi 2013, Conner and Hornick 2015).

#### *2.3.2.1 Markers for the primary location*

NETs from various anatomical sites share similar histomorphological features. Predicting the tumor origin is not always possible from an HE slide. Moreover, identifying the primary tumor site from metastatic tissues is important for managing and choosing medical treatment. For example, the primary site of gastric and colon tumors carries a worse OS when disease disseminates (Chan et al. 2017, Dasari et al. 2017). Drug trials have indicated that different NETs, particularly pancreatic NENs, respond differently to chemotherapeutic agents compared to other GI NETs (Kulke et al. 2011, Chan et al. 2017). Primary site-specific IHC markers can be helpful in clinical settings characterized by unknown primary tumors (Schmitt et al. 2016).

**Table 7.** First-line classification of tumors supported by cell line–specific IHC markers addressing tumor origin. Modified from Jackson and Blythe (2008), Koo et al. (2012), Li et al. (2015), Schmitt et al. (2016), and Zhao et al. (2019).

| CARCINOMA – EPITHELIAL ORIGIN | SARCOMA – MESENCHYMAL ORIGIN | LYMPHOMA – HEMATOPOIETIC ORIGIN | | MELANOMA – MELANOSYTIC ORIGIN | NEUROENDOCRINE – NEUROENDOCRINE ORIGIN |
|---|---|---|---|---|---|
| MAJOR DIAGNOSTIC CATEGORIES | | | | | |
| Cytokeratin | Vimentin | CD45 | CD3 | S100<br>HMB-45<br>Melan A | Chromogranin A<br>Synaptophysin |
| | | | CD20 | | |
| CLASSIFICATION BY CELL ORIGIN | | | | | |
| **Lung:** Thyroid transcription factor 1, napsin, serotonin | | | | | |
| **Thyroid and parathyroid:** Calsitonin, thyroid transcription factor 1, thyroglobulin, parathyroid hormone | | | | | |
| **Gastrointestinal tract and pancreas:** Caudal-type homeobox 2, serotonin, villin, insulin gene enhancer-binding protein islet 1, paired-box 8 | | | | | |
| **Adrenal gland, cortex, and medulla:** Melan A, inhibin alpha, calretinin | | | | | |
| **Liver:** Hepatocyte specific antigen | | | | | |
| **Kidney and urinary tract:** Renal cell carcinoma, uroplakin III | | | | | |
| **Breast and prostate:** Gross cystic disease fluid protein-15, mammaglobin, estrogen receptor, prostata specific antigen, prostata specific membrane antigen | | | | | |

### *Caudal-type homeobox 2*

Caudal-type homeobox 2 (CDX2) is a transcription factor that influences the development of the small and large intestines and differentiates the epithelial cells of the intestine and pancreas (James and Kazenwadel 1991). CDX2 is expressed in the small intestine and colorectum as well in the pancreatic ducts (Moskaluk et al. 2003), and is used as a diagnostic marker for intestinal origin in adenocarcinomas and NENs. In NENs, CDX2 has exhibited a specificity for a midgut origin (Moskaluk et al. 2003, Koo et al. 2012) among both primary and metastatic tumors with a sensitivity of 87% to 89% and a specificity of 94% to 100% (Koo et al. 2012). While NENs from the midgut exhibit intense IHC staining for CDX2, its expression in foregut and hindgut NENs remains weaker and patchy (Bellizzi 2013).

### *Thyroid transcription factor 1*

Thyroid transcription factor 1 (TTF1) plays a role in the morphogenesis of the lung and thyroid gland (Lazzaro et al. 1991). TTF1, a homeodomain-containing transcription factor, is expressed by lung type II pneumocytes and thyroid follicular and C cells (Lazzaro et al. 1991). Thyroid neoplasms and C cell–derived medullary carcinomas are positive for TTF1 (Katoh et al. 2000). Pulmonary adenocarcinomas and NENs widely express TTF1 (Bellizzi 2013). NENs of other anatomical localizations are mostly TTF1 negative. Small-cell carcinomas of the prostate and lung are morphologically similar. In a study of 95 prostatic small-cell NECs, Wang et al. (2008) observed TTF1 positivity in 52.3% of cases (Wang and Epstein 2008). Agoff et al. (2000) reported similar results, identifying TTF1 positivity in extrapulmonary small cell carcinomas (Agoff et al. 2000). In comparison, Ordonez et al. (2000) reported TTF1 negativity for all studied small-cell NECs from the prostate (Ordonez 2000). Conflicting reports regarding TTF1 positivity indicate that TTF1 is not only specific to lung origin (Ordonez 2000, Wang and Epstein 2008).

### *Insulin gene enhancer–binding protein islet 1 and paired-box 8*

Transcription factor insulin gene enhancer-binding protein islet 1 (ISL1) mediates the development of islet cells in the pancreas (Gierl et al. 2006). ISL1 detects pancreatic primary and metastatic NENs with an overall sensitivity of 88% (Graham et al. 2013). While ISL1 is sensitive to a pancreatic tumor origin, it is not specific. Furthermore, according to Graham et al., 89% of duodenal and 100% of rectal NENs are also positive for ISL1 (Graham et al. 2013). Interestingly, 25/25 of Merkel cell carcinoma expressed ISL1 in a study including a total of 124 NENs from different origins (Agaimy et al. 2013). Yet, ISL1 positivity has not been identified in gastric NENs (Bellizzi 2013, Graham et al. 2013). Pulmonary atypical carcinoids and SCLC, however, have demonstrated a variable positivity for ISL1 (Koo et al. 2012, Agaimy et al. 2013). The broad spectrum of possible NENs expressing ISL1 has remained a disappointment when trying to clarify the unknown primary location.

In addition, paired-box 8 (PAX8) positivity has been demonstrated in NENs. Like ISL1, PAX8 is positive in primary NENs of the pancreas (74–88%) and the rectum (9–79%) (Sangoi et al. 2011, Koo et al. 2013). PAX8 positivity in pulmonary NENs and gastric NENs is neglible (10–23%), while ileal NENs show PAX8 negativity (Sangoi et al. 2011, Koo et al. 2012).

#### 2.3.2.2 Prognostic and predictive markers

##### Ki-67

Ki-67 represents the most essential prognostic marker for NENs. As such, together with the mitotic count, Ki-67 defines the grade of NENs (Klöppel et al. 2017a, Klimstra et al. 2019), and Ki-67 expression in tumor cells correlates with the clinical behavior of NENs (McCall et al. 2013, Warth et al. 2013, van Velthuysen et al. 2014).

The gene *MK167,* localized in chromosome 10, encodes the Ki-67 protein (Fonatsch et al. 1991). Ki-67 is present only in actively proliferating cells (Gerdes et al. 1983), constantly present in the S, G2, M, and G1 phases, but absent in the G0 phase of the cell cycle (Gerdes et al. 1984). Ki-67 is a nonhistone protein (Gerdes et al. 1991) associated with the chromosomes and nucleolar structures leading to a special, intranuclear staining pattern throughout the cell cycle (van Dierendonck et al. 1989, Verheijen et al. 1989, Isola et al. 1990).

##### Somatostatin receptors

Five SSTRs have been characterized in humans. The SSTR1–5 genes are located on chromosomes 14q13, 17q24, 22q13.1, 20p11.2, and 16p13.3, respectively (Theodoropoulou and Stalla 2013). SSTR1, 2, 3, and 4 are closely related in size and structure, unlike SSTR5 which also exists as truncated isoforms with four to five transmembrane domains (Duran-Prado et al. 2009). Patel et al. (1993) identified two distinct splicing variants of SSTR2 in humans, named SSTR2A and SSTR2B (Patel et al. 1993). SSTR1, 2, 3, and 4 selectively bind to somatostatin-14, while SSTR5 prefers somatostatin-28 (Theodoropoulou and Stalla 2013), derived from pro-somatostatin precursor (Schally et al. 1980). The expression of SSTRs predicts the response to SSA therapy (Gatto et al. 2013, Pokuri et al. 2016). Different NENs are known to express SSTRs. The majority of NENs co-express multiple SSTR subtypes with SSTR2 representing the dominant subtype (Schmid et al. 2012, Hankus and Tomaszewska 2016). A study of 151 PHEOs and PGLs demonstrated that SSTR2 and SSTR3 were the most abundant subtypes, whereas subtypes SSTR1, SSTR4, and SSTR5 were often negative (Leijon et al. 2019). In a study of parathyroid neoplasms by Storvall et al. (2019), receptors 1 through 5 expressed in parathyroid NENs, with the lowest expression accompanying adenomas and the strongest found in carcinomas (Strorvall et al. 2019).

SSTR expression also associates with clinical outcome. Qian et al. (2016) indicated that a high SSTR2 expression associates with a better OS, especially

in ileal NENs (Qian et al. 2016). Vesterinen et al. (2019) studied a cohort of 178 pulmonary carcinoids and found that negativity for SSTR1 and SSTR2 and positivity for SSTR3 and SSTR4 associated with a shorter disease-specific survival (Vesterinen et al. 2019). In addition, poorly differentiated NENs express lower amounts of SSTRs compared to well-differentiated NENs (Schmid et al. 2012).

#### *2.3.2.3 Recent novel markers*

##### *Insulinoma-associated protein 1*

Insulinoma-associated protein 1 (INSM1), expressed by various NENs, is a key regulator of NE cell development in the pancreas and GI tract (Gierl et al. 2006). Studies by Fujino et al. (2017) and Abe et al. (2019) indicated that INSM1 is a stable NE marker for poorly differentiated NECs. Rectal NENs and SCLC, which often lack CGA positivity (Klöppel et al. 2009), express INSM1 (Fujino et al. 2017). In addition, INSM1 is a useful marker in cytological samples of SCLC (Abe et al. 2019).

##### *Insulin-like growth factor II mRNA-binding protein 3*

Insulin-like growth factor II mRNA-binding protein 3 (IMP3) overexpresses in the lung, colon, and gastric adenocarcinomas and associates with tumor progression (Beljan Perak et al. 2012, Okada et al. 2012). Er et al. (2017) studied IMP3 expression in GEP–NENs. IMP3 expression correlated positively with the tumor size, grade, and stage, increasing in poorly differentiated NENs (Er et al. 2017).

##### *Delta-like 3*

Molecular profiling of tumors is becoming increasingly common. George et al. (2018) and Hermans et al. (2019) indicated that delta-like 3 (DLL3) expression is related to the mutational status of STK11/KEAP1 in pulmonary LCNECs (George et al. 2018, Hermans et al. 2019). In addition, Hermans et al. (2019) observed a DLL3 protein-level expression in 74% of LCNEC samples (Hermans et al. 2019). DLL3 falls within the Notch family, an intensively studied pathway candidate for a therapeutic target. The high prevalence of positivity at the protein level in LCNECs and the low level of DLL3 in healthy tissue may predict the potential of DLL3-targeted therapy (Hermans et al. 2019).

### *Neuropeptide S receptor 1*

Neuropeptide S receptor 1 (NPSR1) is a G protein–coupled receptor that associates with inflammatory conditions in the intestine (D'Amato et al. 2007, Sundman et al. 2010). NPSR1 is expressd as two different splice variants (Vendelin et al. 2005) inducing signaling upon ligand neuropeptide S (NPS) stimulation. The ligand NPS appears to regulate the production of a range of NE cell hormones (Sundman et al. 2010). Furthermore, NPS appears to play a regulatory role in cell growth in cultured human colon cancer cells (Reinscheid et al. 2005). In 2010, Sundman et al. (2010) showed that the NE cells of the small intestine expressed both the receptor NPSR1 and its ligand NPS at the protein level, indicating their possible role in intestinal functions (Sundman et al. 2010).

## 2.4 QUALITY REQUIREMENTS OF IMMUNOHISTOCHEMISTRY

The strength of IHC lies in the possibility of visually analyzing target proteins and their cellular distribution. Classification, phenotyping, the assessment of prognostic and predictive markers all rely on IHC. As new biomarkers are identified and their role in predicting prognosis and treatment becomes increasingly essential, understanding the quality of the IHC methodology becomes crucial (Matos et al. 2010, Kim et al. 2016).

### 2.4.1 PRIMARY ANTIBODY

The primary antibody (Figure 11) defines the recognition of the target protein. Antibodies are glycoproteins produced by the plasma cells in the immune system. In IHC, the most common subtypes of immunoglobulins consist of IgG and IgM (Lipman et al. 2005, Saper 2009). The Fab fragment of an antibody represents the unique structure of the immunoglobulin, which recognizes the antigen. Antibodies are either polyclonal or monoclonal depending upon the type of antigen recognition and production (Schacht and Kern 2015).

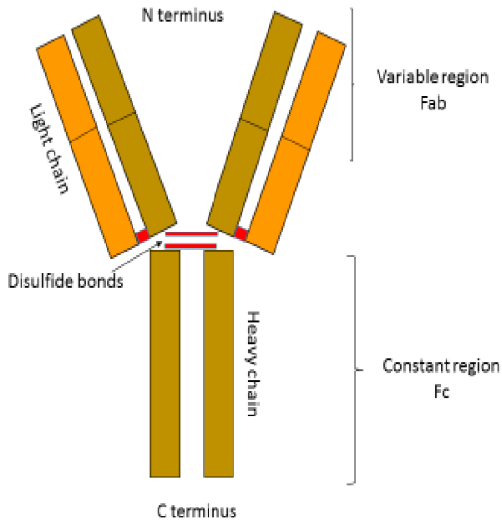


**Figure 11.** The structure of the antibody molecule. The immunoglobulin molecule has two light chains (orange) and two heavy chains (brown) joined by sulfur bridges. The variable region (Fab fragment) is involved in antigen binding comprising one light chain and one heavy chain segment on the N-terminal side. Modified from Buchwalow and Böcker (2010).

#### *2.4.1.1 Polyclonal and monoclonal antibodies*

The clone of an antibody impacts the staining outcome. Hybridoma technology generates stable cell lines (Kohler and Milstein 1975, Margulies 2005) that secrete defined primary antibody clone with a specificity to a unique part of the target molecule epitopes (Kohler and Milstein 1975, Spieker-Polet et al. 1995, Weber et al. 2017). A polyclonal antibody comprises multiple immunoglobulins that recognize the same antigen with different epitopes. Thus, polyclonal antibodies have a higher affinity and better sensitivity, but are less specific (Lipman et al. 2005, Saper 2009). For example, polyclonal PAX8 is used for staining well-differentiated pancreatic NENs (Haynes et al. 2011, Sangoi et al. 2011). Based on gene expression studies, human islet cells do not contain detectable levels of the PAX8 transcript (Lorenzo et al. 2011). Instead, another member of the PAX family, PAX6, seems to serve as the key regulator of pancreatic islet development (Sander et al. 1997). The polyclonal PAX8 antibody is raised against the N-terminal peptide which contains the DNA binding domain conserved in all members of the family (Lang et al. 2007), consequently recognizing a part of the endogenous PAX6 (Lorenzo et al. 2011). Instead, the monoclonal antibody of PAX8 recognizes the C-terminal region of the protein and and staining pancreatic NENs with

monoclonal PAX8 leads to negative staining results (Lorenzo et al. 2011, Tacha et al. 2013).

#### *2.4.1.2 Rabbit and mouse monoclonal antibodies*

Depending upon the animal in which the antibody is produced, different clones have demonstrated a variable sensitivity. Antibodies produced in a rabbit have a higher affinity to antigens than antibodies raised in a mouse (Weber et al. 2017, Huang et al. 2006). TTF1 is an important marker for lung origin in NENs (Lin et al. 2007, Zhao et al. 2019). In pulmonary NENs, the rabbit monoclonal antibody SPT24 demonstrated a stronger IHC reactivity than the mouse monoclonal antibody 8G7G3/1 (La Rosa et al. 2010). Findings from Roge et al. (2019) indicated that rabbit monoclonal clones yielded higher PI values compared to mouse monoclonal clones of Ki-67. Buonocore et al. (2019) also reported similar results with cytological samples from SCLS (Buonocore et al. 2019). However, some studies have demonstrated an unexpected antigen reactivity and coincidental positivity with rabbit monoclonal antibodies in tumors traditionally considered as negative (Comperat et al. 2005, Galloway and Sim 2007, Matoso et al. 2010). According to Ibrahim et al.'s (2008) findings, rabbit monoclonal SP2 yielded a false-positive progesterone receptor staining of a breast tumor, lymphocytes, and endothelial cells compared to other clones of the same antigen (Ibrahim et al. 2008).

The cut-off points of the PI separate the G1 through G3 groups in NENs (Table 6), underscoring the challenge and importance of selecting the primary antibody clone. The preferred clone for PI assessment in NENs is MIB-1 (Klöppel et al. 2017a), which recognizes a highly conserved amino acid sequence from the antigen (Gerdes et al. 1991). Furthermore a comparison of different SSTR2 clones indicated that cell membrane positivity is clone-dependent, where UMB1 clone correlated best with $^{125}$I-[Tyr$^3$]-octreotide autoradiography compared to SS-80 or R2-88 clones (Körner et al. 2012).

### 2.4.2 EFFECTS OF TECHNIQAL ISSUES ON STAINING QUALITY

#### *2.4.2.1 Tissue fixation*

Tissue fixation aims to preserve the tissue morphology. The type of fixative and the quality of the fixation (under- versus overfixation) significantly impact the staining quality (Meyer and Hornickel 2010, Paavilainen et al. 2010).

Furthermore, pre-analytical factors affect the accuracy of the prognostic and predictive markers (Taylor and Levenson 2006, Engel and Moore 2011). For instance, Khoury et al. (2009) reported a weakened expression of estrogen and progesterone receptors with progressive ischemia (Khoury et al. 2009). The cell membrane receptor human epidermal growth factor receptor 2 (HER2) appeared vulnerable to underfixation leading to the weaker expression of the HER2 antigen on the cell membrane (Goldstein et al. 2003, Moatamed et al. 2011). SSTR2 is a prognostic marker in NENs (Brunner et al. 2017). When studying SSTR2, Körner et al. (2012) observed peripheral but not central IHC staining of UMB1, particularly in large NEN specimens (Körner et al. 2012), pointing towards the impact of poor fixation. Overfixation does not carry the same detrimental effect on antigenicity (Goldstein et al. 2003).

Fixation can be performed using different chemicals, whereby 10% buffered formalin represents the so-called universal fixative (Howat and Wilson 2014, Schacht and Kern 2015). The choice of fixative may influence the detection of antigens. As an example, Buonocore et al. (2019) tested the immunoreactivity of different Ki-67 clones using different fixatives. CytoLyt-fixed cell blocks exhibited lower PI values than parallel formalin-fixed cell blocks which lost up to 70% of the staining intensity and immunoreactivity with the MIB-1 clone (Buonocore et al. 2019).

#### *2.4.2.2 Antigen retrieval*

Antibody-antigen recognition depends on the compatibility of structures. Formaldehyde fixation masks the epitopes that an antibody recognizes (Fox et al. 1985, Matos et al. 2010). To recover the tissue antigenicity, tissue sections must be subjected to antigen retrieval (AR) (Shi et al. 2007, Schacht and Kern 2015), thereby increasing the sensitivity and intensity of IHC staining (Shi et al. 1991, Pileri et al. 1997). The selection of the optimal AR method is antibody-dependent (Pileri et al. 1997, Ramos-Vara and Beissenherz 2000). A comparison of different heat-induced epitope retrieval (HIER) techniques yielded an SSTR2 positivity in NENs, but the rate of false-negative staining increased under suboptimal AR, preferring high temperatures and a pH 9.0 buffer (Körner et al. 2012).

#### *2.4.2.3 Blocking of background staining*

Endogenous enzyme activity and unspecific binding of the primary antibody may cause background staining. If endogenous enzymes are present in cells and

tissues, they may react with label substrates used in IHC detection. Endogenous peroxidase activity appears in erythrocytes, monocytes, hepatocytes, and the kidney (Buchwalow and Böcker 2010). Also, nonspecific binding of Fc fragments of an antibody as well as noncovalent interactions may cause background staining. Phagocytes, lymphocytes, and follicular dendritic cells express the Fc receptor on their cell membranes, to which the Fc fragments of primary antibodies can bind (Jackson and Blythe 2008, Kim et al. 2016).

Nonspecific background staining can be blocked with blocking reagents. Endogenous peroxidase activity is frequently blocked with a 3% hydrogen peroxidase solution (Streefkerk 1972, Radulescu and Boenisch 2007). The insufficient quenching of endogenous peroxidase activity may associate with false-negative or false-positive IHC results (Radulescu and Boenisch 2007). For example, some antigens can be destroyed by high concentrations of hydrogen peroxidase (Kim et al. 2016). Most NENs are highly vascular tumors needing endogenous peroxidase blocking. The unspecific binding of Fc fragments is blocked with normal serum (Burry 2011). Protein blocks such as bovine serum albumin inhibit unspecific binding with the charged groups and epitope-like fragments (Burry 2011).

### 2.4.3 THE ROLE OF DETECTION METHODS

The selection of the detection system greatly impacts the technical details related to the IHC staining quality. Two principal detection methods are employed: direct and indirect (Carson and Cappellano 2015). In the direct method, the primary antibody is labeled with, for example, horseradish peroxidase (HRP) or alkaline phosphatase (AP) enzymes (Nakane and Pierce 1966). In the indirect method, a secondary linking antibody is tagged with a label (Schacht and Kern 2015, Kim et al. 2016), representing a present-day technique for visualization.

#### *2.4.3.1 Avidin-biotin detection*

The avidin-biotin method is an indirect technique, in which a biotin-labeled linking antibody binds to an unconjugated primary antibody followed by binding of an enzyme-labeled biotin-avidin complex (Hsu et al. 1981). The presence of endogenous biotin is a potential source of nonspecific staining (Bussolati and Leonardo 2008, Kim et al. 2016). For example, under proper detection conditions Iezzoni et al. (1999) discredited the claim for inhibin positivity in hepatocellular carcinomas (Iezzoni et al. 1999). Under AR conditions at a high temperature, paraffin sections may be exposed to biotin artifacts (Buchwalow and Böcker 2010).

#### *2.4.3.2 Polymer-conjugated detection*

The dextran monomer or polymer technology is biotin-free. Using Envision (Agilent) technology, a secondary linking antibody is conjugated to a labeled polymer chain consisting of dozens of HRP molecules (Sabattini et al. 1998, Kammerer et al. 2001). The OptiView™ (Roche) technology is a three-step detection method with a bridging technique using haptens (Jasani et al. 1981). The hapten-conjugated antibody linker is recognized by an enzyme-labeled tertiary antibody, named a multimer. Each multimer includes seven HRP molecules conjugated through multimer arms (http://reagent-catalog.roche.com). Using polymer-conjugated detection in a series of GEP–NENs, Schmid et al. (2012) found frequent SSTR1–2 (42% and 63%) and SSTR5 (65%) positivity, whereas SSTR3 and SSTR4 (6% and 32%) were less detectable (Schmid et al. 2012). Kulaksiz et al. (2002) detected higher levels of positivity with SSTR3 ranging from 71% to 79% compared to the 6% positivity reported by Schmid et al. (2012). Moreover, autoradiography studies by Reubi et al. (2001) indicated that GEP–NENs predominantly express SSTR1 and SSTR2 followed by SSTR5 (Reubi et al. 2001), in agreement with results reported by Schmid et al. (2012). The technical conditions in Kulaksiz et al.'s (2002) study may have contributed to the SSTR3 positivity they observed, although that study did not include biotin-rich tissue-derived NENs (Kulaksiz et al. 2002). Yet, NENs naturally vary in terms of SSTR expression (Hankus and Tomaszewska 2016).

## 2.5 ANTIBODY VALIDATION

Validation creates the baseline for the quality assessment of markers (Torlakovic et al. 2017). Prior knowledge (Reubi 2014) of expected staining patterns (nuclear, cytoplasmic or membranous) and the cellular location of the antigen assist in the assessment of validation steps (Gown 2016).

### 2.5.1 STEPS TO QUALITY ASSURANCE

Technical validation includes several variables. In a comparison of different AR methods, primarily comparing HIER buffers with pH 6 and pH 9, combined with using different antibody dilutions provides evidence for the best combination of the protocol settings (Howat et al. 2014). The serial dilution of a concentrated antibody will result in a strong specific labeling with minimal or no background staining (Hladik and White 2008). For example, a study by Copete et al. (2011) showed that half of the false-negative or false-positive stainings were

inappropriately calibrated (Copete et al. 2011). Other variables, such as antibody incubation times and temperatures, are also options to consider during validation (Howat et al. 2014). The expression levels of an antigen determine the choice of the detection method.

The appropriate protocol settings are determined by positive and negative tissue sections ensuring that low-expression tumors are not missed and false-positive results are minimized (Hewitt et al. 2014, Gown 2016). If possible, the positive tissue control should match the tissue under investigation (Burry 2011, Torlakovic et al. 2015), thus normal NE cells represent a proper positive control for the investigation of NEN.

### 2.5.2 THE VALUE OF CONTROLS

Controls are used to confirm the reliability of the staining result (Burry 2000). Controls include a) primary antibody controls showing the specific binding to the target antigen, and b) secondary reagent and label controls to confirm that the resulting color precipitate is from an antigen-primary antibody-complex, not from reaction products (Burry 2011).

#### *2.5.2.1 Primary antibody controls*

Primary antibody controls confirm that an antibody is binding to its correct antigen. A positive normal tissue component or cell known to express the antigen of interest serves as a good primary antibody control (Hewitt et al. 2014). This positive control can be found in the specimen (internal positive control) or can be expressed in a separate tissue (external positive control) (Hewitt et al. 2014, Torlakovic et al. 2015). A negative control is an internal or external tissue component assumed to be negative for the corresponding antigens, thus not expressing the molecule of interest (Hewitt et al. 2014, Torlakovic et al. 2014).

Different genetic approaches can confirm the specificity of the primary antibody. In knockout animals, the expression of a specific protein is blocked using gene manipulation, thus serving as the negative control (Burry 2011). Transfected HEK293 cell lines have been used to demonstrate the stable expression of a specific SSTR subtype (Fischer et al. 2008, Lupp et al. 2011, Lupp et al. 2012, Schmid et al. 2012). In addition Western blotting represents a typical method to determine the binding of the primary antibody to its target molecule by labelling the correct molecular weight target protein.

#### 2.5.2.2 *Secondary reagent control*

Controlling the detection reagents serves to confirm that the labelling seen after IHC detection is caused by reactions between antibody complexes rather than the unspecific binding of secondary reagents (Burry 2011, Hewitt et al. 2014). Nonspecific binding can result from charged groups in the cells and tissues or from the Fc fragment of an detection antibody (Buchwalow and Böcker 2010). This can be controlled by excluding the primary antibody.

## 2.6 DIGITAL PATHOLOGY

Digital pathology offers multiple advances including consultation, re-reviewing, education, image analysis, archiving, and quality assurance (Pantanowitz 2010, Griffin and Treanor 2017). The adaptation of digital pathology in routine practice is challenging not only given the technical investments, but also because of other costs (Griffin and Treanor 2017). Figure 12 summarizes the potential steps to digital pathology in the diagnostic laboratory workflow.

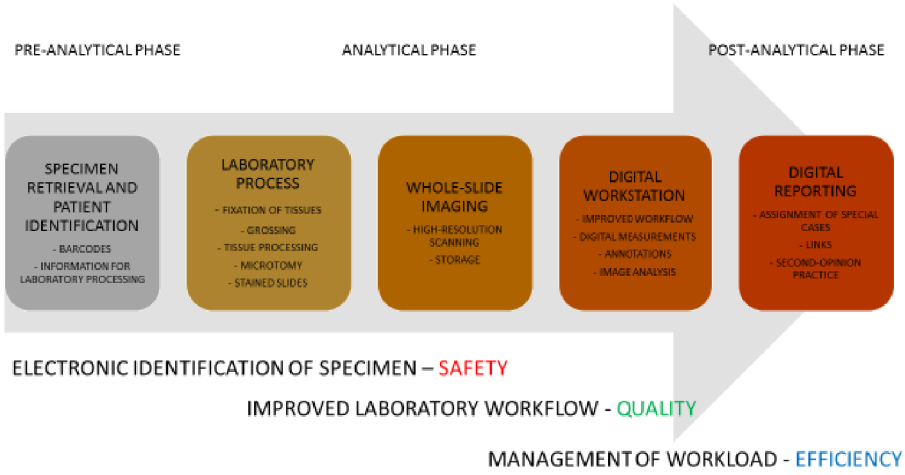


**Figure 12.** Phases of digital pathology in the laboratory workflow process. Modified from Griffin and Treanor (2017).

### 2.6.1 BASICS OF IMAGE ANALYSIS

"Image analysis" refers to quantitative analysis in an objective manner. It allows for the recording of diagnostic information from digitalized slides (whole-slide image (WSI) or digital pictures) in a precise and reproducible manner using analytical tools (Aeffner et al. 2019). Image analysis begins with the identification of the ROI. After defining the ROI, analytical algorithms are configured for the accurate segmentation (Aeffner et al. 2019) to classify cells, typically as either positive or negative based on the staining result (Bankhead et al. 2017, Lykkegaard Andersen et al. 2018). Using segmentation algorithms, different tissue compartments and cell structures are artificially separated. However, nontumor cells along with poor fixation and tissue processing may compromise segmentation (Kwon et al. 2019). In breast cancer studies, cytokeratin-based recognition of tumor cells has provided better recognition of tumor areas and assessment of Ki-67 (Roge et al. 2016, Koopman et al. 2018, Valkonen et al. 2020). In virtual double staining, parallel slides are digitally aligned and fused to one image, from which algorithms automatically detect ROIs and the segment antigen of interest (Roge et al. 2016, Koopman et al. 2018, Lykkegaard Andersen et al. 2018).

Algorithms typically employ fixed or adaptive thresholding. Normally, user-configurable parameters include the color and object size threshold (Zarella et al. 2019). Using graphical icons and tools, the user can interpret the image, guide the analytical process, and evaluate the result of the analysis (Tuominen et al. 2010, Aeffner et al. 2019). This fine adjustment is often included in order to improve accuracy via human interaction. In an analysis of Ki-67 in breast cancer, Kwon et al. (2019) identified discrepancies in the image analysis compared to the visual assessment when the final PI data from an image analysis was not confirmed by a pathologist (Kwon et al. 2019). Furthermore, a study of pancreatic NENs by Reid et al. (2015) highlighted the importance of optimizing image analysis algorithms given that the software was unable to distinguish Ki-67-positive tumor cells from nontumor cells without manual thresholding (Reid et al. 2015).

Digital imaging consists of four key steps: 1) scanning, 2) storing, 3) editing, and 4) viewing images (Pantanowitz 2010). WSI includes the digitalization of slides by scanning (Figure 13), during which the image is captured in a tile- or inline-scanning fashion to generate the final digital image (Zarella et al. 2019). A high-magnification lens together with a high-resolution camera yield good and reliable digital images, but with large file sizes (2 gigabytes). The JPEG, JPEG 2000 or LZW-tiff formats represent the most common packing strategies, although depending upon the compression algorithm, information may be lost during processing (Zarella et al. 2019).

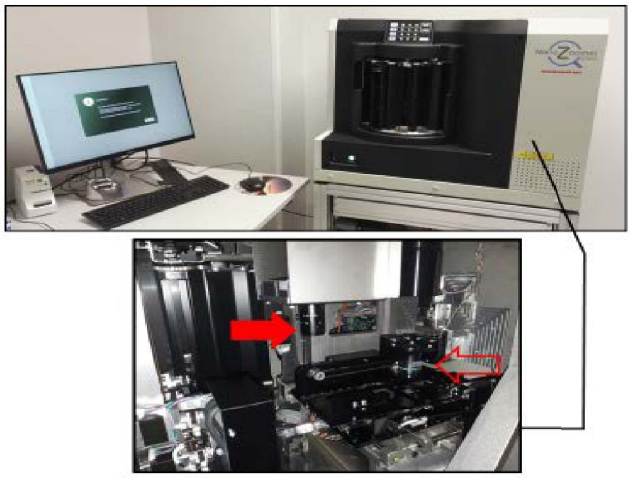

**Figure 13.** Whole-slide scanners are connected to computers with software that sends commands to the scanner. Inside the scanner are the slide stage, the objective lens (right arrow), and the digital camera (solid red arrow on the left).

The accuracy of digital images is appropriate for diagnostic purposes (Snead et al. 2016, Mukhopadhyay et al. 2018). Kaemmerer et al. (2014) compared the SSTR status among 25 NEN patients, comparing manual and digitalized slides in the evaluation of SSTRs, finding a comparable reliability (Kaemmerer et al. 2014). The key elements in high-quality image analysis include high-resolution images (meaning 0.25 µm/pixel equivalent to a 40x objective magnification), the selection of algorithms and ROIs, and the subjective expertise of the pathologist capable of correlating results with relevant clinical data ensuring an appropriate diagnostic interpretation (Griffin and Treanor 2017, Aeffner et al. 2019).

### *ImmunoRatio*

ImmunoRatio image analysis software, originally developed for the quantitative analysis of nuclear breast cancer markers, is based on the ImageJ platform (Tuominen et al. 2010). Analysis uses the digital images taken from the ROI and requires a light microscope with a digital camera. ImmunoRatio includes different algorithms that separate, filter, and combine the image information (Figure 14).

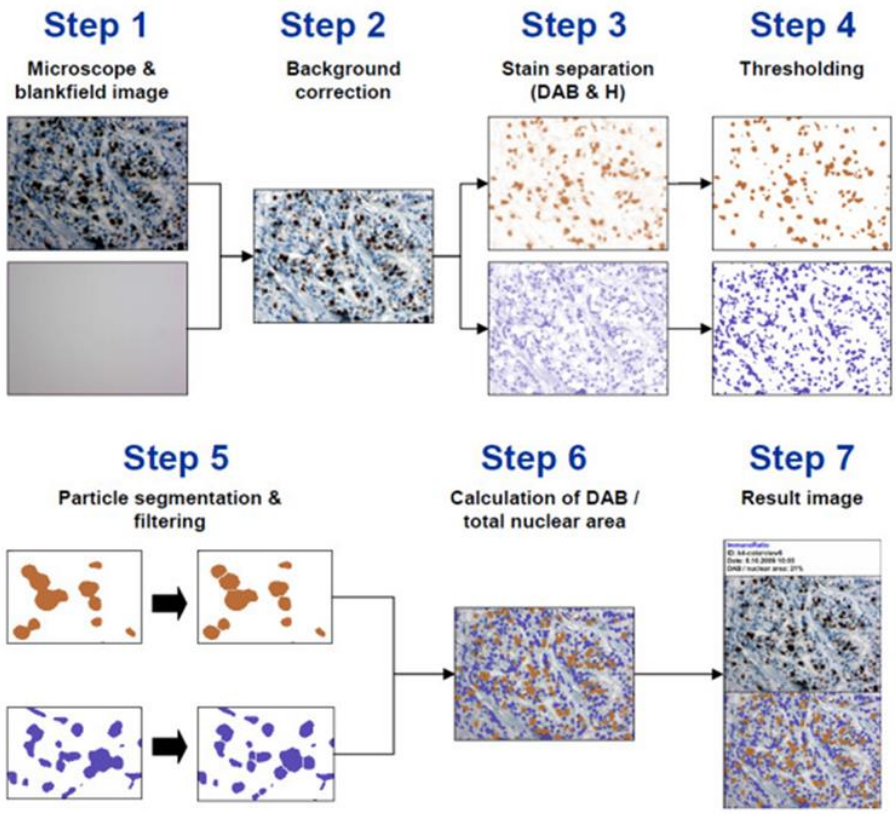


**Figure 14.** Process flowchart of the ImmunoRatio analysis algorithm. Image taken from Tuominen et al. (2010), reprinted in accordance with BioMed Central Ltd. Creative Commons Attribution License (CC BY 2.0).

ImmunoRatio's operational principle is based on the color deconvolution algorithm (Ruifrok and Johnston 2001), which differentiates staining components (DAB and hematoxylin) as separate images by analyzing the absorption spectra of the stains. During this process, the software calculates the intensity of the colors (red, green, and blue) per pixel, quantifying the optical density of a given stain. After separation, components are processed using a mean filter and the adaptive IsoData algorithm thresholding (Ridler and Calvard 1978) to minimize the possible background staining in the images. The binarized components are processed with a median filter to smooth the outline of the nuclei. By using the watershed algorithm (Beucher and Mayer 1993), the nuclei of both stain components are segmented, and then small particles and thin cells are removed. The PI in ImmunoRatio is provided by the percentage of the DAB-stained nuclear area (DAB component) out of the total (DAB and hematoxylin components)

nuclear area (Tuominen et al. 2010). At the end of image processing, the DAB and hematoxylin components are overlaid on the original image and the result is presented as a pseudo-colored image together with the original digital image (Figure 15) (Tuominen et al. 2010). While the DAB density cannot accurately reflect the abundance of the protein in the nuclei, ImmunoRatio's ability to discriminate between positively and negatively stained nuclei (van der Loos 2008) has proved useful in the assessment of breast cancer markers (Tuominen et al. 2010).

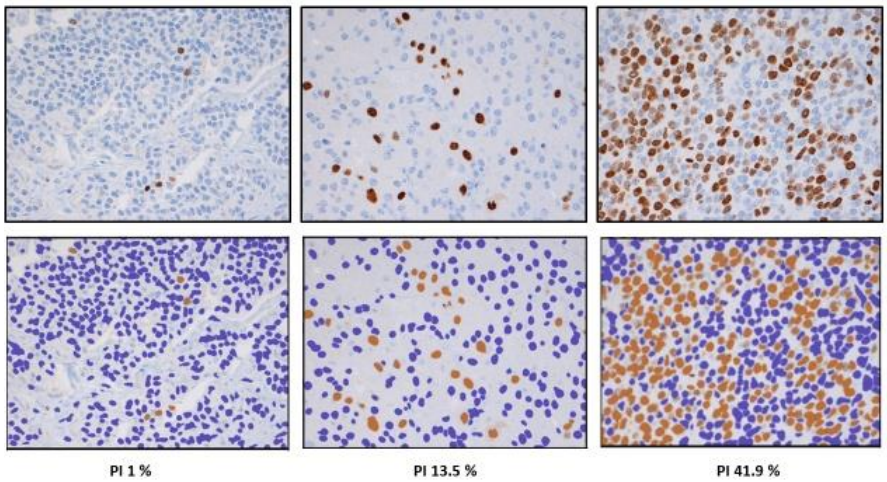


**Figure 15.** ImmunoRatio algorithms process digital images (top row) and display the result as a pseudo-colored image (bottom row) with the calculated proliferation index (PI).

### 2.6.2 QUANTITATIVE CALCULATION OF KI-67

The most common evaluation of Ki-67 is the semi-quantitative counting of PI, referred to as eyeballing. Conventional eyeballing is subjective to interobserver and interlaboratory variability (Mengel et al. 2002, Blank et al. 2015, Reid et al. 2015, Cottenden et al. 2018). For accurate assessment, digital pathology has been introduced to analyze the prognostic and predictive markers (Tuominen et al. 2010, Tuominen et al. 2012, Stalhammar et al. 2018, Wang et al. 2019).

Studies using digital image analysis have provided evidence of the accuracy and objectivity of the interpretation of Ki-67 (Tang et al. 2012, Volynskaya et al. 2019). A semi-automated analysis of Ki-67 by Basile et al. (2019) indicated that the calculation of Ki-67 from scanned slides using image analysis software tools proved more accurate than eyeballing (Basile et al. 2019). Reid et al.

(2015) compared different Ki-67 counting methods finding that the accuracy and reproducibility of the camera-captured/printed-image method was highest (81.7%) and the interobserver variability was lowest (43%). The newest classification of GEP–NENs prefers the camera-captured/printed-image method (Klöppel et al. 2017a, Klimstra et al. 2019).

### 2.6.3 ARTIFICIAL INTELLIGENCE AND DEEP LEARNING

Publicly or commercially available image analysis software programs are based on the differentiation of a stained target using a color deconvolution algorithm (Ruifrok and Johnston 2001) or require parallel virtually combined sections (Roge et al. 2016, Koopman et al. 2018, Lykkegaard Andersen et al. 2018) for accurate analysis. These actions require human supervision.

In recent years, artificial intelligence (AI) and deep learning methods have emerged as the primary approaches to medical analysis (Niazi et al. 2019). Broadly, AI refers to machine-based technology that performs specific activities as intelligently as "humans" (Aeffner et al. 2019). Deep learning is a specific field of AI, which is a subset of machine learning where deep learning utilizes artificial neural networks (ANNs) to make their own determination of the output (Khosravi et al. 2018). ANNs are a set of connected layers with defined pathways regarding how data are moved and distributed through a system (Aeffner et al. 2019). The output of ANNs results from many independent steps consisting of calculations, weighting, and assessing (Aeffner et al. 2019, Niazi et al. 2019).

As the utilization of WSI expands, a large volume of digital tissue data becomes more available for AI (Niazi et al. 2019). The emergence of graphic processing units during the millennium has further advanced AI (Aeffner et al. 2019). Machine learning and ANN methods have recently become popular in pathology as well. Pathological approaches include the identification of tumor cells, the tumor microenvironment, and histological features, as well as predicting clinical outcomes (Beck et al. 2011, Luo et al. 2017, Ström et al. 2020).

# 3 AIMS OF THE STUDY

This thesis aimed to identify novel IHC markers and the best interpretation processes for the diagnosis of NENs. In doing so, this thesis primarily focuses on the quality of techniques, their validation as well as the objective interpretation of staining results, which could provide the best results for diagnosing and managing NEN patients.

The detailed aims were:

1. To identify novel and specific neuroendocrine markers by studying NPSR1 and its ligand NSP expression in a large cohort of different types of NENs.

2. To identify novel and specific neuroendocrine markers by studying PCSK2 expression in a large cohort of different types of NENs.

3. To test different SSTR clones and define the appropriate IHC protocol for SSTR1–5 subtype detection for different NENs.

4. To define a reproducible Ki-67 scoring for grading NENs.

# 4 MATERIAL AND METHODS

## 4.1 TUMOR MATERIAL

The tumor material was collected from the archives of the Department of Pathology (HUSLAB) at Helsinki University Hospital, and comprised primary NENs from 12 different primary sites and nine metastatic tumors.

In studies I, II, and III, we used a multi-NET TMA including tumors from 1997 through 2010. Additional tumor cohorts consisting of PHEOs and PGLs (collected 1995–2004) and pulmonary carcinoid tumors (collected 1990–2013) were used in study II. Study IV comprised a total of 51 pancreatic and small intestine NETs collected from 2003 through 2009. Histopathological diagnoses were confirmed from HE-, CGA-, and SYP-stained slides by an endocrine pathologist. Table 8 summarizes the demographic chacteristics for the patients from whom tumor material was extracted.

**Table 8.** Tumor cohorts in studies I through IV.

| ORIGIN OF TUMORS | N | GENDER (M:F) | AGE (IN YEARS) | STUDY |
|---|---|---|---|---|
| MULTI-NET TMA | | | | |
| RECTUM | 6 | 1:4 | 43–75 | Studies I, II, and III |
| THYROID | 5 | 2:3 | 29–59 | |
| LUNG | 16 | 4:12 | 35–85 | |
| THYMUS | 1 | 0:1 | 43 | |
| APPENDIX | 8 | 3:5 | 17–77 | |
| SKIN | 4 | 3:1 | 68–91 | |
| SMALL INTESTINE | 6 | 4:2 | 53–75 | |
| PARATHYROID | 5 | 1:4 | 19–78 | |
| GASTRIC MUCOSA | 8 | 4:4 | 49–87 | |
| PANCREAS | 13 | 4:9 | 23–77 | |
| PHEOCHROMOCYTOMA | 5 | 3:2 | 36–67 | |
| PARAGANGLIOMA | 5 | 2:3 | 45–82 | |
| METASTASES | 9 | 5:4 | 43–74 | |
| Total | n = 91 | n = 36:54 | | |
| ADDITIONAL TMA-TUMOR MATERIAL | | | | |
| PHEOCHROMOCYTOMA | 32 | 14:18 | 17–69 | Studies II |
| PARAGANGLIOMA | 4 | 3:1 | 31–48 | |
| PULMONARY CARCINOIDS | 38 | 18:21 | 19–84 | |
| Total | n = 94 | | | |
| WHOLE-SLIDE TUMOR MATERIAL | | | | |
| SMALL INTESTINE | 20 | 8:12 | 30–78 | Studies II and IV |
| PANCREAS | 31 | 9:22 | 12–79 | Study IV |
| Total | n = 51 | | | |

## 4.2 TISSUE MICROARRAY

Representative tumor areas were annotated from HE slides to construct the multi-NET TMA (studies I, II, and III). Tumor tissue cores of 1-mm in diameter were taken using a semiautomated TMA instrument (Beecher Instruments, Silver Spring, MD, USA) from both the border and the middle area of each tumor. In total, six cores per tumor were extracted, comprising three parallel blocks with double punches. In study II, a pulmonary carcinoid-TMA block series was constructed with a TMA Grandmaster (3DHistech, Budapest, Hungary) covering 1-mm double punches from the outside, middle, and border of the tumor with a normal bronchus yielding seven punches per tumor sample.

## 4.3 IMMUNOHISTOCHEMISTRY

For IHC, 3-µm-thick tissue sections were cut onto TOMO® adhesion microscope slides (Matsunami, Bellingham, WA, USA). Deparaffinization was completed in xylene followed by a graded-alcohol series or in the staining instrument with the EZ Prep buffer (Ventana, Tucson, AZ, USA) depending upon the IHC protocol. Standard protocols for stainings were based on biotin-free polymer detection kits: Envision (Agilent, Santa Clara, CA, USA), UltraVIEW or OptiVIEW DAB (Ventana, Tucson, AZ, USA). Depending upon the staining instrument, the Autostainer 480 (LabVision Thermo Scientific, Cheshire, UK) or the BechMark XT (Ventana, Tucson, AZ, USA), endogenous peroxidase was blocked with the Dako REAL Peroxidase-Blocking Solution (Agilent, Santa Clara, CA, USA) for 5 min or with the Inhibitor dispenser (Ventana, Tucson, AZ, USA) as part of the kit for 4 min before primary antibody incubation. Table 9 presents the detailed data on the primary antibodies we used.

**Table 9.** Details of the primary antibodies.

| PRIMARY ANTIBODY | CATALOG NUMBER, SUPPLIER | CLONE | SPECIES | STUDY |
|---|---|---|---|---|
| Ki-67 | M7240, Agilent | MIB-1 | Mouse | I, II, and IV |
| NPSR1-A | Quattromed | CREQRSQDSRMTFRERTER* | Mouse | I |
| NPSR1-N | Quattromed | TEGSFDSSGTGQTLDSSPVA* | Mouse | I |
| NPS | Abcam | Polyclonal | Rabbit | I |
| SSTR1 | MCA5924, AbDSerotec | sstr1 | Mouse | III |
| | ab137083, Abcam | UMB7 | Rabbit | |
| SSTR2 | ab134152, Abcam | UMB1 | Rabbit | III |
| SSTR3 | MCA5921, Bio-RAD | sstr3 | Mouse | III |
| | 20696-1-AP, Proteintech Europe | Polyclonal | Rabbit | |
| | ab137026, Abcam | UMB5 | Rabbit | |
| SSTR4 | MCA5922, AbD Serotec | sstr4 | Mouse | II |
| SSTR5 | MCA5923, Bio-RAD | sstr5 | Mouse | III |
| | ab109495, Abcam | UMB4 | Rabbit | |
| PCSK2 | HPA048851, Sigma-Aldrich | Polyclonal | Rabbit | II |
| Chromogranin A | A0430, Agilent | Polyclonal | Rabbit | I, II, and III |
| Serotonin | M0758, Agilent | 5HT-H209 | Mouse | II |
| Synaptophysin | Novocastra | 27G12 | Mouse | I and II |

* Syntetic peptide

In the Autostainer, the secondary antibody polymer was incubated for 30 min, while the DAB substrate mix (Agilent, Santa Clara, CA, USA) was incubated for 10 min at room temperature. Washes were completed using 1XPBS with 0.5% Tween 20 (Acros, Geel, Antwerp, Belgium) following incubation. Using the BenchMark XT, we incubated the secondary antibody for 8 min in the UltraVIEW DAB protocol and 8 to 12 min in the OptiVIEW DAB including incubations of different linkers. The DAB chromogen with the substrate and copper was incubated for 8 and 4 minutes, respectively. Washes were completed using the Reaction Buffer (Ventana, Tucson, AZ, USA) according to the instrument's instructions. The slides were counterstained with Mayer's hematoxylin (Lillie's Modification; Agilent, Santa Clara, CA, USA) and mounted with the Eukitt® quick-hardening mounting medium (Sigma-Aldrich, Saint Louis, MO, USA).

### 4.3.1 SPECIFICITY STUDIES OF PRIMARY ANTIBODIES

#### *4.3.1.1 Neuropeptide S receptor 1*

The epitope specificity of NPSR1-A and NPSR1-N primary antibodies (study I) were analyzed using the recombinant NPSR1 protein. The recombinant protein fused with either red (NPSR1-A-pDsRed) or green (NPSR1-B-GFP) fluorescent protein was transfected with the COS-7 (African green monkey kidney fibroblast) cell line. This cell line was grown in Dulbecco's modified Eagle's medium containing (DMEM) GlutaMAX-I (Invitrogen), fetal bovine serum (FBS), and 100 U/ml penicillin together with 100 mg/ml streptomycin in a humid +37°C incubator. After 24 h of seeding, 4–5 x $10^4$ cells on 24-well plates were transfected with recombinant full-length NPSR1 constructs fused with either pDsRed or GFP fluorescent protein. Incubation followed fixation with 4% paraformaldehyde. The cell lines for the NPSR1-A antibody staining were permeabilized with 0.1% Triton X-100 in 1XPBS. The cells for NPSR1-N staining remained untreated. Primary antibodies were incubated for 1 h. Binding of the primary antibodies were visualized after washes with secondary antibodies labeled with either green (FITC) or red (TRITC) tags, respectively. Colocalization was examined using a conventional fluorescent microscope. A yellow color in the overlay images indicated the colocalization of protein and antibodies.

The epitope specificity of the NPSR1 antibodies was also analyzed with 10% SDS-PAGE and bacterial lysate immunoblots. NPSR1-A and NPSR1-N fragments expressed pGEX 4 T-3 glutathione-S-transferase (GST) and dihydrofolate reductase (DHFR). Monoclonal antibodies against C-terminus and N-terminus expressed a band of the correct molecular size.

#### *4.3.1.2 Proprotein convertase subtilisin/kexin type 2*

The specificity of the PCSK2 antibody (study II) was confirmed using Western blot analysis of fresh-frozen PHEOs stored at -70°C. The tissue was homogenized and lysed with an LSB buffer (Bio-Rad, Hercules, CA, USA) and titrated to volumes of 2 µl, 5 µl, and 10 µl. The tissue homogenate was subjected to 10% SDS-PAGE and immunoblotted onto the Immobilon-FL Transfer Membrane (Merck Millipore, Burlington, MA, USA). The blots were incubated overnight at +4°C with PCSK2 (Sigma-Aldrich, Saint Louis, MO, USA), diluted to 1:1000, followed by the Alexa Fluor 680-conjugated secondary goat anti-rabbit antibody (1:10 000), and enhanced with Odyssey (LI-COR Biosciences, Lincoln, NE, USA) for chemiluminescence detection. PCSK2 revealed a clear band migrating at an expected size of 70 565 Da.

**Table 10.** Scoring criteria.

| NPSR1-A, NPSR1-N & NPS STUDY I | PCSK2 & SSTRS STUDIES II, III | SSTRS STUDY III | Ki-67 STUDY IV |
|---|---|---|---|
| Cytoplasmic / Membranous | Cytoplasmic | Membranous | PI from "hot spots" |
| 0 = No staining | 0 = No staining | 0 = No staining | <2% (G1) |
| 1 = Mild | 1 = Mild | 1 = Weak (<10%) | 2–20% (G2) |
| 2 = Moderate | 2 = Moderate | 2 = Weak to moderate (≥10%) | >20% (G3) |
| 3 = Strong | 3 = Strong | 3 = Moderate to strong | |
| | | 4 = Strong, complete circumferential (>95%) | |

#### *4.3.1.3 Somatostatin receptors*

The validation of different SSTR clones (study III) was based on the assessment of the staining profile of normal NE cells in the small intestine and pancreas. Different pretreatment buffers (Tris-EDTA pH 9.0, citrate pH 6.0, CC1), antibody dilutions (1:50–1:7000), primary antibody incubation times (30–60 min), detection systems (Envision, UltraVIEW DAB, and OptiVIEW DAB), and staining platforms (LabVision and BenchMark XT) were tested. The criteria for acceptable staining results included the correct staining pattern and the cellular location in the positive control tissues according to the reviewed literature with no or minimal background staining.

### 4.3.2 SCORING

Two different researchers independently scored samples in each study, whereby we selected the highest consensus score for statistical analysis. We considered scores of 2 to 4 for a membranous pattern (study III) and intensity levels of 2 and 3 for cytoplasmic staining (study II, III) as appropriate. The serotonin staining (study II) was interpreted as positive or negative. Table 10 describes the scoring criteria.

Ki-67 (in study IV) was assessed conventionally according to the WHO 2010 guidelines using microscopic manual counting. Hot spots were chosen and at least 500 to 2000 cells were counted. The tumor material was reassessed independently by one person. The reassessed PI values and corresponding tumor grades were compared to the original values. Any variation in the conventional assessment practice between the two observers was evaluated blindly from a series of 20 tumors. The observers chose the hot spots independently.

### 4.3.3 IMMUNORATIO

The Ki-67 PI (studies I, II, and IV) was assessed using the image analysis software ImmunoRatio (jvsmicroscope.uta.fi/immunoratio/). Digital images were taken with a Nikon Eclipse 80i light microscope (40x objective) connected to a Digital Sight DS-5M (Nikon) digital camera and the NIS-Elements F 3.0 image capture software. In studies I and II, one digital image (JPEG format, resolution 1280 x 960 pixels) was captured from every tumor tissue core from the most proliferative area covering 50% of the core. In study IV, five different image fields were captured as digital images (JPEG format, resolution 1280 x 960 pixels) from the hot spots of each tumor covering a total of 2000 cells. A blank field image was included for each capture round to balance the uneven illuminations in the final digital images. Using ImmunoRatio's Advanced Mode setting, threshold values for studies I and II (hematoxylin -10 and DAB 10) and study IV (hematoxylin +10 and DAB -30) were adjusted without a correction equation. We used consistent settings in the image analysis after light exposure (manual exposure, 10 ms, gain 1) and the thresholds were considered adequate.

## 4.4 NEUROPEPTIDE S INDUCTION OF CANCER-RELATED PATHWAYS IN THE SH-SY5Y CELL LINE

We used the human neuroblastoma cell line (SH-SY5Y) to study the downstream targets of the NPS–NPSR1 signaling pathway (study I) using the HGUI133plus2 Array (Affymetrix). The SH-SY5Y cells were placed in the DMEM-GlutaMAX-I incubation medium with FBS, 100 U/ml penicillin, and 100 mg/ml streptomycin at +37°C in a humid incubator. Cells were transfected with NPSR1-A-GFP plasmid using the FuGENE reagent (Roche) and stable clones were selected with 500 µg/ml G418. The RNA was extracted using the RNeasy® Plus Mini Kit (Qiagen) and the cDNA was synthesized with TaqMan Reverse Transcription Reagents (Biosystems). Then, 100 nM NPS-treated cells were compared to untreated cells. We also compared the parental SH-SY5Y cells with and without NPS treatment. Upregulated genes for the transcripts of the MAPK pathway were studied using real-time quantitative PCR for time course and dose responsiveness.

## 4.5 STATISTICAL ANALYSIS

In studies I and IV, correlations between the marker expression and the Ki-67 PI and PI values across different assessment methods were analyzed using two-tailed tests and the Pearson's correlation ($r$). In study IV, the Cohen's kappa ($\kappa$) was calculated to evaluate the agreement of the tumor grade across different assessment conditions. In study II, the Fisher's exact test was used to study the correlations between the tumor origin and marker expression. We considered $p < 0.5$ (study I), $p < 0.001$ (study II), and $p < 0.01$ (study IV) as statistically significant. Statistical analyses were performed using IBM's SPSS version 17.0 (SPSS Inc., Chicago, IL, USA).

# 5 RESULTS

## 5.1 NEUROPEPTIDE S RECEPTOR 1 AND NEUROPEPTIDE S EXPRESSION IN NEUROENDOCRINE TUMORS (STUDY I)

In study I, NPSR1 and NPS were widely expressed in normal NE cells and NENs from various origins (Figure 16). Normal NE cells of the small intestine and islet cells of the pancreas expressed NPSR1. The majority of NENs expressed NPSR1 and NPS. That is, gastric, small intestine, appendicular, rectal, pancreatic, pulmonary, and thymic NENs as well as parathyroid adenomas and carcinomas, medullary carcinomas, and PGLs showed a strong reactivity to NPSR1-N, NPSR1-A, and NPS. All markers were negative or weakly positive in PHEOs. Colon adenocarcinomas were negative for NPSR1. Table 11 summarizes the NPSR1 staining in NENs.

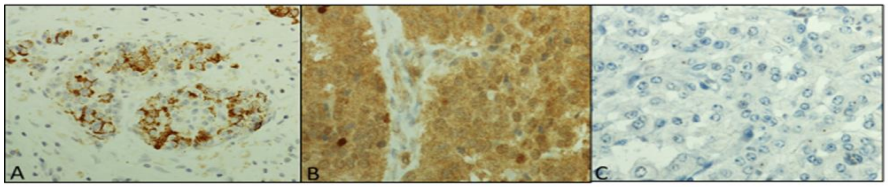


**Figure 16.** Pancreatic islets (A) expressed neuropeptide S receptor 1 (NPSR1). Most neuroendocrine neoplasias (NENs) were positive for NPSR1, including pancreatic NENs (B), although paragangliomas (C) were negative.

In metastatic NENs, the expressions of NPSR1-N and NPSR1-A were similar between primary tumors and metastatic tumors. G1 through G3 tumors of the pancreas and small intestine exhibited similar expression levels of NPSR in primary tumors and in corresponding metastases.

NPSR1 antibodies showed epitope specificity in the immunoblot and fluorescent studies. Immunoblotting with NPSR1 fragments in the bacteria lysate indicated that antibodies recognized the correct size epitopes. The colocalization of the expressed green fluorescent NPSR1 fusion protein with TRITC-labelled anti-NPSR1-N suggested that the full-length NPSR1 protein was recognized by the NPSR1-N antibody. FITC-labelled anti-NPSR1-A colocalized with the red fluorescent NPSR1 fusion protein exhibiting antibody binding to the full-length NPSR1 protein.

NPS-treated SH-SY5Y cells yielded an upregulation of 552 and downregulation of 184 transcripts with 1.25 and 0.75 cut-offs, respectively. The upregulated genes belonged primarily to the MAPK pathway, circadian activity, focal adhesion, transforming growth factor β, and cytokine–cytokine interactions. The expression of the MAPK pathway genes (GADD45A–MYC and NR4A1–NFKB1) peaked at 3 h and 6 h, respectively. NPS treatment of the parental SH-SY5Y induced minor changes in the gene expression due to endogenous NPSR1.

## 5.2 THE EXPRESSION OF PROPROTEIN CONVERTASE SUBTILISIN/KEXIN TYPE 2 (STUDY II)

In study II, we found PCSK2 expression (Table 11) mainly in midgut NENs (12/12), PHEOs (4/5), and PGLs (3/5), as well as in some typical and atypical pulmonary carcinoids (4/8). NENs from the thymus, gastric mucosa, pancreas, rectum, thyroid, and parathyroid were negative. Using an additional tumor cohort, PCSK2 was positive in 20/20 small intestine NENs, 13/19 typical and 9/19 atypical pulmonary carcinoids, 24/32 PFEOs, and 3/4 PGLs. The results across these two different staining rounds were similar.

The expression level of PCSK2 in metastatic NENs was comparable to the level found in the primary tumor. Pulmonary carcinoids (n = 5) and a small intestine NEN (n = 1) that were strongly PCSK2 positive exhibited a strong positivity in the corresponding metastatic tumors as well, whereas pulmonary carcinoids (n = 6) and pancreatic NENs (n = 4) that were PCSK2 negative exhibited negative staining in metastatic tumors. None of the pancreatic or gastric adenocarcinomas stained with PCSK2, but one-third of the colon adenocarcinomas were positive for PCKS2 (Figure 17).

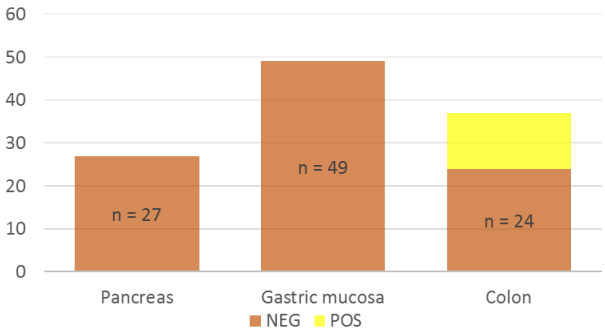


**Figure 17.** Proprotein convertase subtilisin/kexin type 2 positivity in adenocarcinomas of the pancreas, gastric mucosa, and colon.

The validity of the PCSK2 primary antibody was confirmed in normal NE cells (Figure 18). The NE cells of the small intestine and adrenal medulla were strongly positive for PCSK2. The gastric, bronchial, thyroid C cells, and pancreatic islet cells were positive, but at a lower intensity. The NE cells of the large intestine were negative. Table 11 summarizes the PCSK2 staining for different NENs.

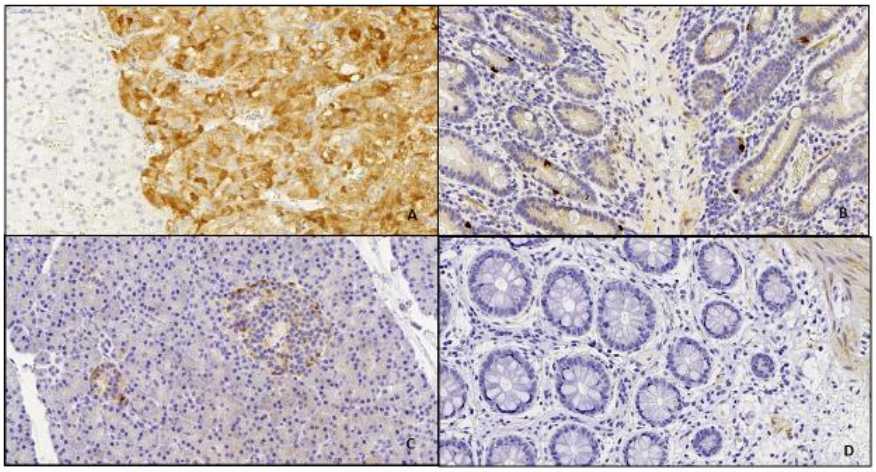


**Figure 18.** Proprotein convertase subtilisin/kexin type 2 expression in the normal A) adrenal medulla, B) small intestine, C) pancreas, and D) rectum. Objective: 40x.

**Table 11.** Immunohistochemical expression of neuropeptide S receptor 1 (NPSR1) and proprotein convertase subtilisin/kexin type 2 (PCSK2) in NENs of different origins.

| TUMOR LOCATION | NPSR1 | PCSK2 |
|---|---|---|
| LUNG | POS (+) | + |
| THYMUS | + | NEG (–) |
| GASTRIC MUCOSA | + | – |
| PANCREAS | + | – |
| APPENDIX | + | + |
| SMALL INTESTINE | + | + |
| RECTUM | + | – |
| THYROID | + | – |
| PARATHYROID | + | – |
| ADRENAL MEDULLA | – | + |
| PARAGANGLIA | + | + |
| SKIN | + | – |

## 5.3 DESCRIPTION OF SOMATOSTATIN RECEPTOR CLONES AND THEIR EXPRESSION IN DIFFERENT NEUROENDOCRINE TUMORS (STUDY III)

In study III, SSTR1 clones sstr1 and UMB7, SSTR2 clone UMB1, SSTR3 clone UMB5, SSTR4 clone sstr4, and SSTR5 clones sstr5 and UMB4 demonstrated the expected staining patterns (membranous and cytoplasmic) and tissue locations (small intestine NE cells and the islet of Langerhans) using standard protocol settings (Figure 19). However, the polyclonal SSTR3 primary antibody and clone sstr3 did not yield the appropriate staining pattern or localization in the positive and negative control tissues. The UMB clones (UMB7, UMB1, UMB5, and UMB4) showed clear membrane positivity and localization in the positive control tissues. The clones sstr1, sstr4, and sstr5 exhibited the expected staining in the correct cell types, but at a weaker intensity than the corresponding rabbit monoclonal. The polyclonal SSTR3 antibody and the clone sstr3 yielded an overall nonspecific staining in the control tissues. The UMB clones were considered preferable clones for the SSTR staining.

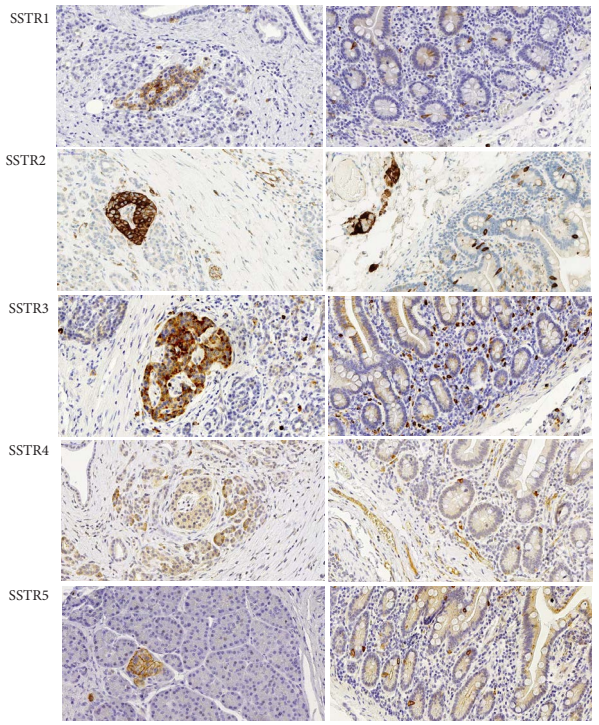


**Figure 19.** Somatostatin receptor (SSTR) clone validation for positive normal tissue controls, where the pancreas (left column) and the small intestine (right column) indicated the correct tissue localization of SSTRs in normal tissue.

Table 12 shows the overall SSTR positivity (including membranous and cytoplasmic positivity) in NENs using the UMB clones and sstr4.

**Table 12.** Immunohistochemical expression of somatostatin receptor (SSTR) subtypes in neuroendocrine neoplasms (NENs) of different origins. Results are shown as a percentage of overall positivity.

| NEN | SSTR1 (UMB7) % | | SSTR2 (UMB1) % | | SSTR3 (UMB5) % | | SSTR4 (sstr4) % | | SSTR5 (UMB4) % | |
|---|---|---|---|---|---|---|---|---|---|---|
| | Membrane | Cytoplasmic | Membrane | Cytoplasmic | Membrane | Cytoplasmic | Membrane | Cytoplasmic | Membrane | Cytoplasmic |
| Pulmonary NENs (n = 14) | 21.4 | 21.4 | 71.4 | 57.1 | 0 | 21.4 | 0 | 35.7 | 7.1 | 0 |
| Thymic NEN (n = 1) | 0 | 0 | 0 | 0 | 100 | 100 | 0 | 0 | 0 | 0 |
| Gastric mucosal NEN (n = 6) | 0 | 16.6 | 83.3 | 83.3 | 0 | 0 | 0 | 33.3 | 0 | 33.3 |
| Pancreatic NENs (n = 11) | 36.6 | 63.6 | 72.7 | 72.7 | 9 | 45.4 | 0 | 45.4 | 27.2 | 18.2 |
| Appendicular NENs (n = 5) | 0 | 20 | 100 | 100 | 0 | 40 | 0 | 100 | 20 | 20 |
| Small intestine NENs (n = 5) | 0 | 0 | 100 | 100 | 0 | 80 | 0 | 0 | 20 | 0 |
| Rectal NENs (n = 5) | 0 | 20 | 100 | 100 | 0 | 60 | 0 | 0 | 40 | 60 |
| Medullary carcinomas (n = 5) | 20 | 60 | 20 | 20 | 0 | 60 | 0 | 0 | 20 | 40 |
| Parathyroid adenomas and carcinomas (n = 5) | 0 | 0 | 0 | 0 | 0 | 0 | 0 | 20 | 0 | 0 |
| PHEOs (n = 5) | 0 | 0 | 60 | 40 | 20 | 100 | 0 | 0 | 0 | 20 |
| PGLs (n = 5) | 20 | 20 | 80 | 80 | 20 | 100 | 0 | 0 | 0 | 0 |
| Merkel cell carcinoma (n = 4) | 0 | 0 | 100 | 50 | 0 | 0 | 0 | 25 | 0 | 0 |

Figures 20 through 22 summarize the SSTR staining in different NENs, with the results shown as the highest percentage of membranous positivity. If membranous positivity was not detected, the corresponding percentage of cytoplasmic is shown in Figures 20, 21, and 22. In NENs, SSTR2 was the most commonly detected receptor followed by SSTR5, SSTR1, SSTR3, and SSTR4.

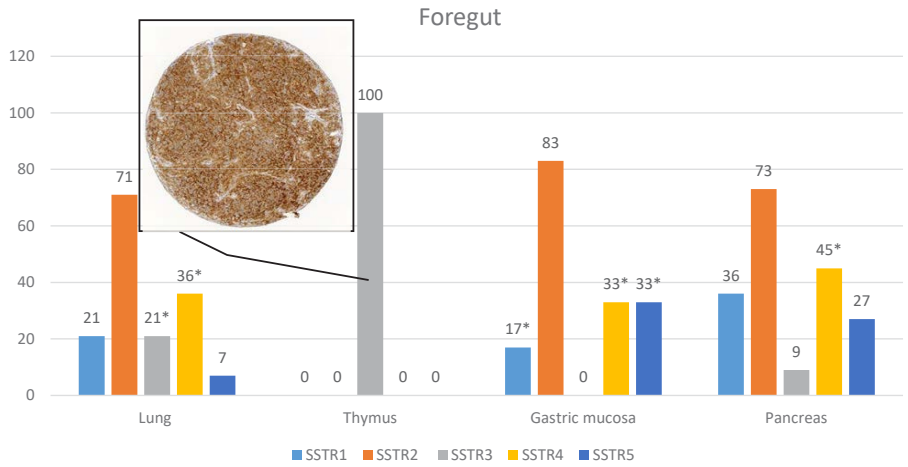


**Figure 20.** Percentage of highest somatostatin receptor (SSTR) positivity in foregut NENs. The insert shows an image of SSTR3 staining. *Indicates cytoplasmic positivity.

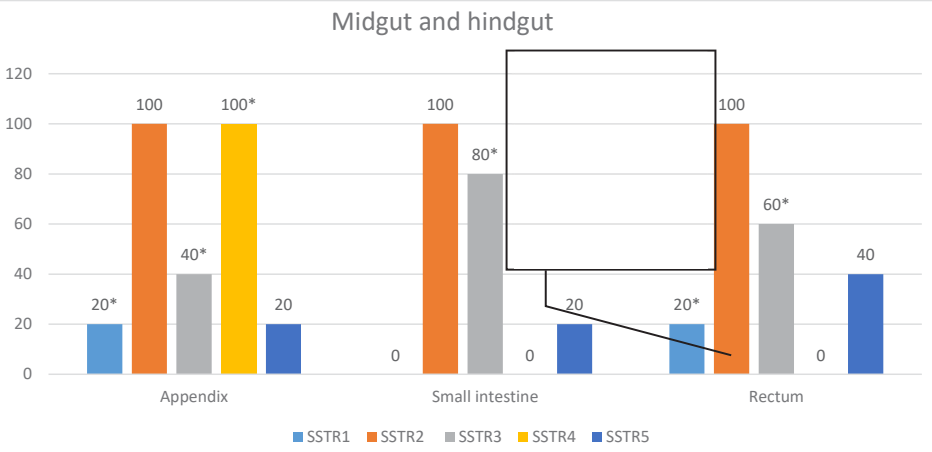


**Figure 21.** Percentage of the highest somatostatin receptor (SSTR) positivity in midgut and hindgut NENs. The insert shows an image of SSTR2 staining. *Indicates cytoplasmic positivity.

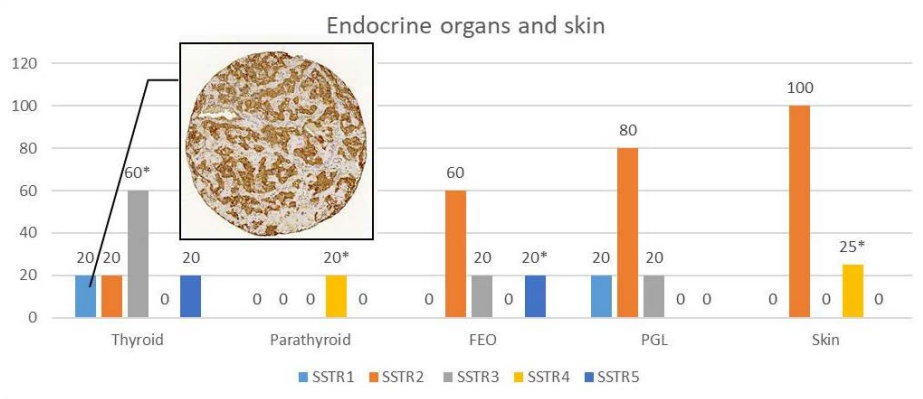


**Figure 22.** Percentage of the highest somatostatin receptor (SSTR) positivity in NENs from endocrine organs and skin. The insert shows an image of SSTR1 staining. *Indicates cytoplasmic positivity.

## 5.4 ASSESSMENT OF THE PROLIFERATION INDEX (STUDY IV)

In study IV, the conventional assessment of PI by eyeballing for the same tumor varied between the different pathologists, the PI values taken from the original pathology reports, and the reassessment by one observer. The PI values were significantly different yielding moderate coherence in the tumor grading ($\kappa = 0.373$; $p = 0.000$; Figure 23). When two observers blinded to one another assessed the same tumors (n = 20), the variation in PI was smaller compared to the differences detected in the re-evaluation of the original PI, demonstrating a good correlation between observers ($p < 0.001$) with a high agreement in grading ($\kappa = 0.662$; $p = 0.000$; data not shown).

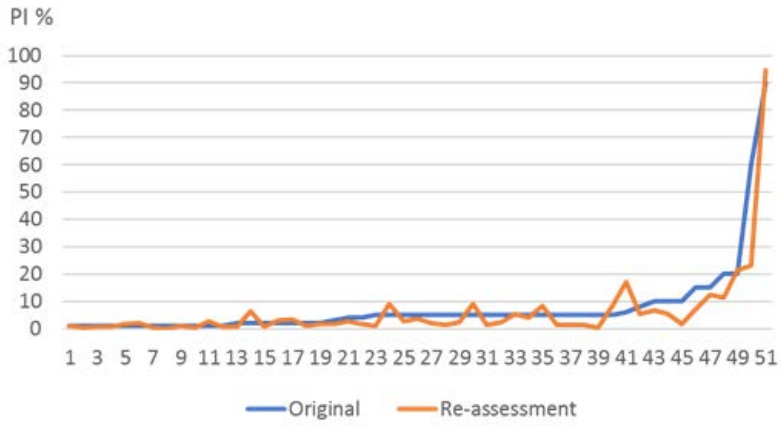


**Figure 23.** Variation of proliferation index (PI) between conventional assessments of Ki-67 in 51 neuroendocrine neoplasias. Original values are from pathology reports. The reassessment was completed by one observer.

The PI assessment using ImmunoRatio was highly reproducible in the three repeated assessments, with the standard PI values correlating (r = 0.985, r = 0.987, and r = 0.995; $p < 0.001$) and the coefficients of variation (CV = 2.08, 2.26, and 2.27) in repeated series (Figure 24). Tumor gradings using ImmunoRatio were also quite similar ($\kappa = 0.886$, $\kappa = 0.886$, and $\kappa = 1.000$; $p = 0.000$). The differences in grades were mainly between G1 and G2 rather than between G2 and G3 for all assessment methods. The ImmunoRatio PI values were close to those analyzed by a qualified observer in a conventional manner. Conventional and ImmunoRatio assessments (mean PI value of three independent assessment rounds) conducted by the same person were in good agreement (r = 0.969; $p < 0.001$; Figure 25).

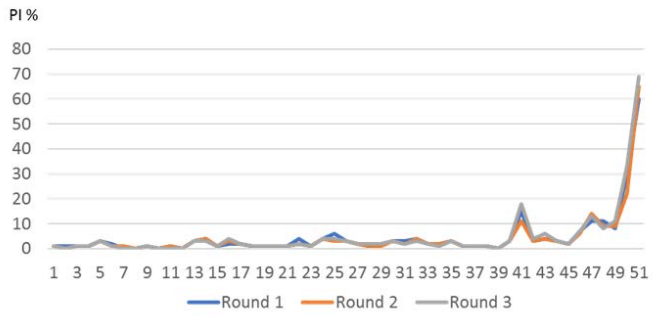


**Figure 24.** Reproducibility of the proliferation index (PI) in repeated assessment of Ki-67 in ImmunoRatio for 51 neuroendocrine neoplasias.

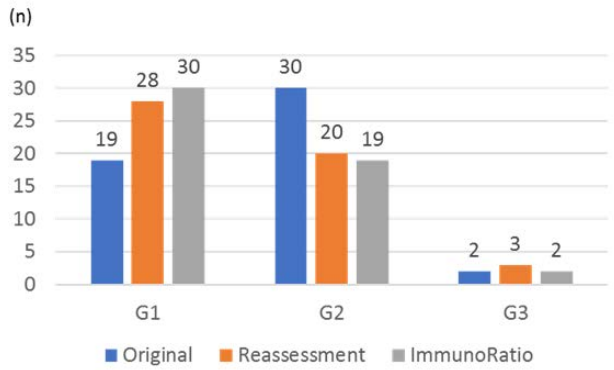


**Figure 25.** Grading across different assessments for 51 neuroendocrine tumors.

# 6 DISCUSSION

## 6.1 TISSUE MICROARRAY IN STUDY OF NEUROENDOCRINE NEOPLASIAS

***(Studies I–IV)***

Tumors of an NE origin appear in various organs due to the disseminated NE cell system (Rekhtman 2008), yet NENs are considered a rare tumor entity. The study of rare tumors is challenging. Constructing a TMA using technology, including automated tissue microarraying and digitalization, carries multiple advantages when studying these rare tumors and novel markers (Zlobec et al. 2014). Therefore, this thesis includes studies using TMA material constructed from a broad spectrum (n = 91) of well-documented NENs from 12 different primary tumor origins including metastatic pairs. Typically, NEN studies have included only a few NEN locations (Qian et al. 2016, Zhao et al. 2019) or a moderate number of tissue cores in a TMA (Schmid et al. 2012, Qian et al. 2016, Bellizzi 2020). Our study setting enabled the simultaneous and comparative analysis of NENs arising from different primary sites in order to examine their expression of potential biomarkers. Although TMAs are efficient for large-scale screening research, a problem persists in the representativeness of the antigen expression in TMA spots. In this NEN cohort, six to seven parallel tissue cores were analyzed from the same NEN to improve the representativeness of the samples (Elfving et al. 2019). In addition, interesting findings were re-evaluated with larger tumor cohorts.

## 6.2 VALIDATION OF IMMUNOHISTOCHEMICAL MARKERS

***(Studies I–III)***

In modern surgical pathology, the use of IHC remains crucial. IHC is used for tumor typing, and the classification of tumor subtypes and malignancies of an unknown primary origin (Conner and Hornick 2015), as well as demonstrating prognostic and predictive markers (Wolff et al. 2018). When new IHC markers are studied, the verification and validation of the primary antibodies and detection reagents used remain important (Matos et al. 2010). A lack of techniqal standardization represents an observable challenge in diagnosic pathology (Howat et al. 2014, Cheung et al. 2016).

Ideally, validation analyses should include tissue known to express the target antigen as well as tissue devoid of the antigen in question (Burry 2011, Torlakovic et al. 2014, Torlakovic et al. 2015). In our studies, we used normal tissues from the organs from whence the tumor cohort NENs originated. In study I, control specimens from the small intestine and pancreas showed NPSR1 receptor positivity in NE cells as previously stated (Sundman et al. 2010). Our results regarding NPSR1 expression confirm that receptors are also expressed in non-inflammed human NE tissues. In study II, PCSK2 positivity localized to the cytoplasm of NE cells similar to previous descriptions by Portela-Gomes et al. (2008) and Scopsi et al. (1995). This indicates that the polymer-based detection of the protein localizes the enzyme correctly according to its biological nature (Portela-Gomes et al. 2004). In the normal tissue material, consisting of the bronchus, gastric mucosa, pancreas, small intestine, colorectum, thyroid C cells, and adrenal medulla, the intensities of the PCSK2 expression varied between different NE cells. Perhaps the staining intensity of PCSK2 relates to the presence of the enzyme in these cells. As Portela-Gomes et al. (2008) showed, PCSK2 expression varies in the islet of Langerhans; PCSK2 is present in insulin cells, glucagon cells, and somatostatin cells, but absent in pancreatic polypeptide cells (Portela-Gomes et al. 2008).

### *Primary antibody validation of somatostatin receptor clones (Study III)*

NEN patients with proper SSTR expression profiles benefit from SSA therapy (Gatto et al. 2013, Pokuri et al. 2016) and radio-labeled SSA imaging (Pauwels et al. 2018, Vitale et al. 2018). The therapy of NEN patients using SSA relies on the membrane expression of SSTRs (Theodoropoulou and Stalla 2013, Kanakis et al. 2015). Many studies have found a correlation between IHC and autoradiography (Körner et al. 2005, Körner et al. 2012), scintigraphy (Diakatou et al. 2015), and PET/CT (Kaemmerer et al. 2011). The evaluation of SSTRs using IHC compares favorably to PET/CT (Miederer et al. 2009, Kaemmerer et al. 2011).

Study III aimed to validate the staining protocols for commercially available SSTR clones and to identify the most favorable protocol settings for each clone. SSTRs are transmembrane protein receptors pointing to a membranous staining pattern in IHC (Reubi 2014). Our validation of the SSTR primary antibodies indicated a specific and correct location in the small intestine NE cells, the islet of Langerhans, and the nerves, similar to findings from earlier studies (Reubi et al. 2001, Fischer et al. 2008, Lupp et al. 2011, Lupp et al. 2012, Lupp et al. 2013). SSTR antibodies showed both membranous and cytoplasmic staining as previously described (Reubi et al. 2001, Fischer et al. 2008, Lupp et al. 2011, Lupp

et al. 2012, Schmid et al. 2012, Lupp et al. 2013, Elston et al. 2015, Kaemmerer et al. 2015). However, the membranous staining pattern depended upon the clone used. We found that UMB clones were more likely to detect membrane positivity in SSTRs. Polyclonal antibodies were suboptimal due to the background staining. The differences between clones could be explained through antibody production methods. The monoclonal antibodies have a higher specificity because of the hybridoma production method (Spieker-Polet et al. 1995, Saper 2009, Buchwalow and Böcker 2010). Polyclonal antibodies, on the other hand, are produced by the immunization of the production animal (Saper 2009, Buchwalow and Böcker 2010). In addition, according to our study, mouse monoclonal antibodies showed membranous but less intense staining compared to rabbit monoclonal antibodies. Rabbit monoclonal antibodies have a demonstrably higher affinity than the mouse monoclonal (Huang et al. 2006, La Rosa et al. 2010, Weber et al. 2017), possibly explaining the visible correct but less intense membranous staining pattern for SSTRs.

SSTRs are internalized after the ligand binds to the receptor (Jacobs and Schulz 2008, Waser et al. 2009, Csaba et al. 2012). The cytoplasmic staining observed in SSTRs (Schmid et al. 2012, Elston et al. 2015, Kaemmerer et al. 2015) may result from the ligand-induced internalization of the receptors (Reubi et al. 2010). In addition, given the ability of antibodies to crossreact between different epitopes (Saper 2009), hypothetically different SSTR clones (Fischer et al. 2008, Righi et al. 2010, Lupp et al. 2011, Körner et al. 2012, Lupp et al. 2012, Schmid et al. 2012, Lupp et al. 2013) may react differently to internalized receptors or differentially recognize epitope-like structures in the cytoplasm, thereby explaining the cytoplasmic reactions of SSTR antibodies.

NENs originating from different organs feature varying SSTR subtype profiles. SSTR2 is the most universally expressed subtype, followed by SSTR5, SSTR1, SSTR3, and SSTR4 (Reubi et al. 2001, Hankus and Tomaszewska 2016) as demonstrated in our work as well. The evidence for IHC's suitability to evaluate the SSTR profile in NENs (Körner et al. 2005, Miederer et al. 2009, Kaemmerer et al. 2011, Körner et al. 2012, Diakatou et al. 2015) underscores the need for the verification and validation of the SSTR primary antibodies (Matos et al. 2010, Howat et al. 2014, Cheung et al. 2016). Thus, the IHC analysis of SSTRs to predict patients' suitability for SSA therapy is possible, however, only if the technical requirements for IHC are prioritized (Torlakovic et al. 2017).

## 6.3. NEUROPEPTIDE S RECEPTOR 1 AND NEUROPEPTIDE S IN NEUROENDOCRINE NEOPLASIAS (STUDY I)

Not all NETs express conventional NE markers, despite the histopathology presenting NE-type features (Gut et al. 2016, Perren et al. 2017). The differential diagnosis of NEN may be difficult, particularly for poorly differentiated NECs, small biopsies, or cytological samples (Schmitt et al. 2016, Fujino et al. 2017). In this thesis, we aimed to identify NE-specific markers. Previously, the G-protein coupled receptor NPSR1 was found to express in the NE cells of the GI tract (Sundman et al. 2010). In study I, the majority of NENs widely expressed NPSR1 and its ligand NPS, with only PHEOs emerging as an exception. Both the N-terminal and C-terminal antibodies of NPSR1 yield the same staining result. Furthermore, the staining of the receptor and ligand NPS recognized the same NENs. This observation supports Sundman et al. (2010), who showed that the NPS expression pattern mirrored NPSR1. According to our tumor cohort, widely expressed NPSR1 or NPS could serve as a general NE marker, excluding tumors with a PHEO origin.

Earlier studies found that NPS stimulated the growth of Colo205 human colon cancer cells (Reinscheid et al. 2005). In our work, we sought to study the role of NPS in tumorogenesis. NPSR1-transfected SH-SY5Y neuroblastoma cells were stimulated with NPS, revealing the expression of many genes in different signaling pathways, especillay genes of the MAPK pathway. We detected an abundant IHC expression of NPSR1 in most NENs, except in PHEOs. Thus, the potential activation of intracellular signaling pathways may be relevant to malignant behavior in NENs. PHEOs are potentially malignant tumors and histological indicators of their metastatic behavior remain limited (Tischler et al. 2017). The lack of NPSR1 expression in PHEOs may be partly related to the benign behavior of these tumors, since they may not link to NPS stimulation with gene activation, which is relevant to tumorgenesis.

## 6.4 PROPROTEIN CONVERTASE SUBTILISIN/KEXIN TYPE 2 EXPRESSION INDICATES A NEUROENDOCRINE TUMOR ORIGIN (STUDY II)

Tumor markers and organ-specific markers represent transcription factors (Goto et al. 1992, Koo et al. 2012, Li et al. 2015, Schmitt et al. 2016, Zhao et al. 2019), naturally occurring proteins (Perren et al. 2017), or structural components (Gerdes et al. 1991) of a given cell type. PCSK2 is part of the NE secretory granules (Portela-Gomes et al. 2004, Seidah et al. 2011). A few earlier studies

have speculated the role of PCSK2 as a marker for NENs (Scopsi et al. 1995, Kajiwara et al. 1999, Kimura et al. 2000, Tomita 2001). In our NEN material, we found a strong cytoplasmic PCSK2 positivity in midgut NENs, PHEOs, and PGLs as well as in half of the typical and atypical pulmonary carcinoids. NENs from other organs such as the thymus, gastric mucosa, pancreas, and colorectum did not express PCSK2. These findings agreed with previous studies (Scopsi et al. 1995, Kajiwara et al. 1999, Kimura et al. 2000, Tomita 2001). According to our results, however, thyroid medullary carcinomas were PCSK2 negative unlike previous reports, although the expression in parathyroid adenomas and carcinomas was comparable (Scopsi et al. 1995, Kajiwara et al. 1999).

Technical factors may explain these differences in the staining results. The antigen morphology changes during tissue fixation (Hladik and White 2008, Buchwalow and Böcker 2010, Meyer and Hornickel 2010). Part of the tumor material used in Scopsi's (1995) study was fixed in a Bouin fixative carrying both coagulating and cross-linking effects on proteins (Grizzle et al. 2008), unlike our formalin-fixed tumor material. The streptavidin-biotin technique (Hsu et al. 1981) was widely used before the introduction of polymer techniques (Kammerer et al. 2001). Diverging from Scopsi et al. (1995) and Kajiwara et al. (1999), we employed a polymer-based detection system (Sabattini et al. 1998), eliminating the characteristic problems of biotin (Buchwalow and Böcker 2010). Finally, all PCKS2 studies including ours used a polyclonal antibody. Repeated production of a polyclonal primary antibody against the same antigen will provide unique combinations of antibody clones in the serum, leading to an antibody content that may differ (Saper 2009), albeit polyclonal antibodies are good in detecting a low expression level or heterogeneous antigens (Acharya et al. 2017).

The primary tumor location of the NEN influences patient management (Alexandraki et al. 2017, Chan et al. 2017). Tissue-specific markers for the detection of NENs of an unknown origin remain valuable (Schmitt et al. 2016). PCSK2 is an endogenous proteolytic enzyme of NE cells, activating and cleaving prohormones arising in a number of biologically active peptides (Doblinger et al. 2003, Portela-Gomes et al. 2004, Portela-Gomes et al. 2008). We found that the primary tumor exhibited similar PCSK2 staining profiles as the corresponding metastatic tumor. Thus, PCSK2 positivity indicates a NEN tumor arising in the small intestine, appendix, lungs, or adrenal medulla, and paraganglions. Furthermore, the expression of PCSK2 did not associate with the NEN grade. Other studies have identified similar correlations between Ki-67 and PCSK2 (Iino et al. 2010). These may stem from the stability of PCSK2 as an antigen sustaining its expression in tumor differentiation. Yet, PCKS2 is an integral part of dense-core granules (Portela-Gomes et al. 2004). Because the staining

intensity of CGA depends on the amount of granules in the tumor cells (Gut et al. 2016), PCSK2 expression may vary also depending upon the number of granules.

## 6.5 ASSESSMENT OF THE PROLIFERATION INDEX (STUDY IV)

In the most recent WHO guidelines for endocrine organs published in 2017 and digestive system tumors released in 2019, Ki-67 is used as the key determinant for NEN grading (Klöppel et al. 2017b, Klimstra et al. 2019). NENs are divided into two groups according to their morphology: 1) well-differentiated NENs, grades G1 through G3 depending on their Ki-67 PI and/or the number of mitosis; and 2) poorly differentiated NENs, namely, NECs, which are high grade by definition (Cavalcanti et al. 2016). A well-known challenge in Ki-67-based PI assessment is the subjective interpretation that causes inter- and intraobserver variation (Klimstra et al. 2010). We also illustrated the pitfalls of the conventional assessment of proliferation via eyeballing. Variations in conventional PI assessment can be explained in several ways. The most important factors consist of the experience and competence of the pathologist, the choice of hot spots, and the quality of IHC along with the interpretation of the staining outcome.

The assessment of Ki-67 should be based on a more accurate and reliable method than subjective visual estimation (Reid et al. 2015). Different image analysis software (Roge et al. 2016, Bankhead et al. 2017, Koopman et al. 2018, Acs et al. 2019) and supervised machine learning (Luo et al. 2017, Valkonen et al. 2020) can assist in quantitative pathology (Niazi et al. 2019). Digitalized slides together with image analysis are suitable for diagnostics (Snead et al. 2016, Mukhopadhyay et al. 2018). To demonstrate this, we used a cohort of GEP–NETs and online image analysis software, ImmunoRatio. ImmunoRatio and eyeballing assessments of PIs yielded comparable PI values, supporting the suitability of image analysis for clinical use. The strengths of such image analysis tools include their user-friendliness, speed, and objectivity (Aeffner et al. 2019). In repeated rounds of assessment, ImmunoRatio yielded comparable grades. The low PI values determined between G1 and G2 were the most prone to errors. If correctly used, image analysis is better than conventional human assessment for determining the proliferation activity of NETs.

## 6.6 STRENGHT AND LIMITATIONS OF THE STUDY

In this thesis, we constructed a broad-spectrum TMA platform of well-characterized NE tumors including NENs from 12 different primary locations with various grades together with primary tumor–metastases pairs. During a metastatic event, tumor cell populations may differ from those of the primary tumor. Having tumor material from both the primary and metastatic tumor cell populations makes it possible to study both the differences and similarities between these populations. Using NENs from different anatomical sites and grades provided a solid overview of the expression of markers and their possible expression patterns among NENs.

The proper validation of the markers studied given current knowledge renders the assessment of expression profiles more reproducible. Combining these technical aspects to image analysis and their standardization increases the objectivity and reproducibility of NEN diagnostics.

Given these strengths, this study also carries limitations, including the use of TMAs compared to whole slides, which possibly excluded some tumor areas. However, using many parallel multiple tissue cores from the same tumor area limits the sampling error. In addition, the low number of G3 tumors may have biased the grade variation analysis. However, recognizing the rarity and infrequent operations involving NEC tumors, the option to use these tumors for research remains limited. The availability of the offered antibody clones of SSTR4 was restricted, whereby only one clone coud be tested. Similarly, the imaging and SSA therapy data were not available for a comparison of SSTR IHC expression profiles. Finally, variation in the preclinical handling of the tumor material, including its sampling and processing, cannot be completely avoided.

# 7 FUTURE PROSPECTS

As our understanding of the nature of NENs expands, ideally future studies should further investigate the role of NPSR1 and its ligand in NENs. NPSR1 expression may indicate metastatic potential. NPS can influence tumor cell growth through the phosphorylation of the MAPK kinase pathways (Reinscheid et al. 2005). This association should be studied using a larger tumor material that includes more metastatic and nonmetastatic NENs. The role of NPS should also be examined more deeply to understand the mechanism behind the stimulation of tumor cell growth.

In addition, the predictive role of the SSTR profile and Ki-67 requires further study. Image analysis and digital pathology offer the needed objectivity and accuracy for assessing these important prognostic and predictive markers. In addition, the prerequisite development of image analysis will change the pathology laboratory workflow towards digitalization. Virtual double staining of prognostic and predictive markers using common NE markers could improve the specificity and reproducibility of NEN diagnostics in future. Utilizing Al and ANNs could also provide the needed accurary in classifying and categorizing this heterogenous tumor group.

# 8 CONCLUSIONS

To conclude, NPSR1 and PCSK2 can be used as a part of the NE antibody panel. Different antibody clones should be tested in a standardized setting in order to obtain a validated clone optimal for diagnostic purposes. The accuracy of grading NENs can be further improved by using image analysis tools.

The specific conclusions are:

1. The majority of NENs express NPSR1 and its ligand NSP, while the PHEO expression level is low. Thus, a strong expression of NPSR1 points towards an NE nature of a tumor.

2. The strong PCSK2 expression in midgut NENs, lung carcinoids, PHEOs, and PGLs allows for the use of this marker, directing pathologists towards the location of unknown primary tumors.

3. NENs with different tumor locations exhibited distinctive SSTR profiles, and UMB clones indicating that validated staining protocols should be used.

4. The conventional assessment of the PI in NENs is subject to inter- and intraobserver variation. Image analysis provides a more objective and reproducible NEN grading.

# ACKNOWLEDGEMENTS

This thesis was carried out within the Department of Pathology at the University of Helsinki and at Helsinki University Hospital. I wish to thank all of the professors in the Pathology Department, specifically Professors Tom Böhling and Olli Carpén, for providing excellent facilities in which to conduct research throughout my PhD project. This thesis was supported by grants from the Helsinki University Hospital Research Fund and the Finnish Cancer Foundation.

I also extend my warm thanks to the former Head of HUSLAB Pathology, Professor Heikki Helin, for opening the doors of pathology to me, to Docent Kaisa Salmenkivi and present Head of Pathology, Docent Päivi Heikkilä, for the continually supportive attitude towards research.

I am immensely grateful for my supervisors Professor Johanna Arola and Professor Caj Haglund. Johanna, I admire your extensive knowledge in the field of neuroendocrine pathology. Thank you for all of your help during these years — I am beyond grateful for each moment of assistance! Caj, I am grateful to you for your encouraging support and positive mental attitude. I respect the enormous enthusiastic commitment to research by my supervisors, and I consider it a privilege to have been a part of this research group.

I warmly thank the reviewers, Docent Anita Naukkarinen and Docent Teemu Tolonen, for their dedication and for their thorough review of my thesis as well as for their invaluable comments.

I would like to extend my deepest gratitude to all of the co-authors on my publications, especially Professor Jorma Isola and Vilppu Tuominen, PhD, Ville Pulkkinen, PhD, and Professor Juha Kere for their insightful and necessary collaborations. I extend a special thanks to Helena Leijon, PhD, for her kindness and support in scoring and for her knowledge in the field of clinical pathology. I express my deep appreciation to Tiina Vesterinen, PhD, Docent Jaana Hagström, Mirkka Pennanen MD, and Professor Leif Andersson for their fruitful collaborations. In addition, laboratory technicians including the lovely Eija Heiliö, Päivi Peltomäki, Tiiu Arumäe, and scientist Petri Lankila, deserve my warm thanks for their high-quality laboratory work and assistance. I also thank Päivi Mulari-Matikainen for her kind assistance.

I thank all of the friendly personnel from the Department of Pathology in Helsinki and Kuopio University Hospital for their help and supportive attitude throughout this journey. My fellow workers Yinka, Reija, and Anna in Helsinki, I thank you all — I have been delighted to work with you.

My dear colleague and good friend Mia, I want you to know that I truly value the time and adventures that we have had together.

I also express my deepest gratitude to my family. Thank you, Mom and Dad, for your support during this academic project. I thank my sister for her help and encouragement throughout this thesis project. I also send a special thanks to my parents-in-law.

To the boys in my life – without you I would be rootless. 

Helsinki, July 2020

*Satu Maria Remes*

# REFERENCES

**Abe H., Takase Y., Sadashima E., Fukumitsu, C., Murata K., Ito, T., Kawahara A., Naito Y. and Akiba J.** (2019). Insulinoma-associated protein 1 is a novel diagnostic marker of small cell lung cancer in bronchial brushing and cell block cytology from pleural effusions: validity and reliability with cutoff value. *Cancer Cytopathol* **127**, 598-605.

**Acharya P., Quinlan A. and Neumeister V.** (2017). The ABCs of finding a good antibody: How to find a good antibody, validate it, and publish meaningful data. *F1000Research* **6**, 851.

**Acs B., Pelekanou V., Bai Y., Martinez-Morilla S., Toki M., Leung S. C. Y., Nielsen T. O. and Rimm D. L.** (2019). Ki67 reproducibility using digital image analysis: an inter-platform and inter-operator study. *Laboratory investigation, a journal of technical methods and pathology* **99**, 107-117.

**Aeffner F., Zarella M. D., Buchbinder N., Bui M. M., Goodman M. R., Hartman D. J., Lujan G. M., Molani M. A., Parwani A. V., Lillard K., Turner O. C., Vemuri V. N. P., Yuil-Valdes A. G. and Bowman D.** (2019). Introduction to Digital Image Analysis in Whole-slide Imaging: A White Paper from the Digital Pathology Association. *Journal of pathology informatics* **10**, 9.

**Agaimy A., Erlenbach-Wunsch K., Konukiewitz B., Schmitt A. M., Rieker R. J., Vieth M., Kiesewetter F., Hartmann A., Zamboni G., Perren A. and Kloppel G.** (2013). ISL1 expression is not restricted to pancreatic well-differentiated neuroendocrine neoplasms, but is also commonly found in well and poorly differentiated neuroendocrine neoplasms of extrapancreatic origin. *Modern pathology: an official journal of the United States and Canadian Academy of Pathology, Inc* **26**, 995-1003.

**Agoff S. N., Lamps L. W., Philip A. T., Amin M. B., Schmidt R. A., True L. D. and Folpe A. L.** (2000). Thyroid transcription factor-1 is expressed in extrapulmonary small cell carcinomas but not in other extrapulmonary neuroendocrine tumors. *Modern pathology: an official journal of the United States and Canadian Academy of Pathology, Inc* **13**, 238-242.

**Alexandraki K., Angelousi A., Boutzios G., Kyriakopoulos G., Rontogianni D. and Kaltsas G.** (2017). Management of neuroendocrine tumors of unknown primary. *Reviews in endocrine & metabolic disorders* **18**, 423-431.

**Aluri V. and Dillon J. S.** (2017). Biochemical Testing in Neuroendocrine Tumors. *Endocrinology and metabolism clinics of North America* **46**, 669-677.

**Andrew A., Kramer B. and Rawdon B. B.** (1998). The origin of gut and pancreatic neuroendocrine (APUD) cells--the last word? *The Journal of pathology* **186**, 117-118.

**Bankhead P., Loughrey M. B., Fernandez J. A., Dombrowski Y., McArt D. G., Dunne P. D., McQuaid S., Gray R. T., Murray L. J., Coleman H. G., James J. A., Salto-Tellez M. and Hamilton P. W.** (2017). QuPath: Open source software for digital pathology image analysis. *Scientific reports* **7**, 16878-017-17204-5.

**Basile M. L., Kuga F. S. and Bernardi F.** (2019). Comparation of the quantification of the proliferative index KI67 between eyeball and semi-automated digital analysis in gastro-intestinal neuroendrocrine tumors. *Surgical and Experimental Pathology* **2:21**.

**Battifora H.** (1986). The multitumor (sausage) tissue block: novel method for immunohistochemical antibody testing. *Laboratory investigation, a journal of technical methods and pathology* **55**, 244-248.

**Beck A. H., Sangoi A. R., Leung S., Marinelli R. J., Nielsen T. O., van de Vijver M. J., West R. B., van de Rijn M. and Koller D.** (2011). Systematic analysis of breast cancer morphology uncovers stromal features associated with survival. *Science translational medicine* **3**, 108ra113.

**Beljan Perak R., Durdov M. G., Capkun V., Ivcevic V., Pavlovic A., Soljic V. and Peric M.** (2012). IMP3 can predict aggressive behaviour of lung adenocarcinoma. *Diagnostic pathology* **7**, 165-1596-7-165.

**Bellizzi A. M.** (2020). SATB2 in neuroendocrine neoplasms: strong expression is restricted to well-differentiated tumours of lower gastrointestinal tract origin and is most frequent in Merkel cell carcinoma among poorly differentiated carcinomas. *Histopathology* **76**, 251-264.

**Bellizzi A. M.** (2013). Assigning site of origin in metastatic neuroendocrine neoplasms: a clinically significant application of diagnostic immunohistochemistry. *Advances in Anatomic Pathology* **20**, 285-314

**Beucher S. and Meyer F.** (1993). The morphological approach to segmentation: The watershed transformation. *Mathematical Morphology in Image Processing* **12**, 433-481.

**Binderup T., Knigge U., Loft A., Federspiel B. and Kjaer A.** (2010). 18F-fluorodeoxyglucose positron emission tomography predicts survival of patients with neuroendocrine tumors. *Clinical cancer research: an official journal of the American Association for Cancer Research* **16**, 978-985.

**Blank A., Wehweck L., Marinoni I., Boos L. A., Bergmann F., Schmitt A. M. and Perren A.** (2015). Interlaboratory variability of MIB1 staining in well-differentiated pancreatic neuroendocrine tumors. *Virchows Archiv: an international journal of pathology* **467**, 543-550.

**Brenner R., Metens T., Bali M., Demetter P. and Matos C.** (2012). Pancreatic neuroendocrine tumor: added value of fusion of T2-weighted imaging and high b-value diffusion-weighted imaging for tumor detection. *European Journal of Radiology* **81**, e746-9.

**Brierley J. D., Gospodarowicz M. K. and Wittenkind C.** (2017). *TNM Classification of Malignant Tumours*. John Wiley & Son, Ltd, Oxford, UK.

**Brown D. C. and Gatter K. C.** (1990). Monoclonal antibody Ki-67: its use in histopathology. *Histopathology* **17**, 489-503.

**Brunner P., Jorg A. C., Glatz K., Bubendorf L., Radojewski P., Umlauft M., Marincek N., Spanjol P. M., Krause T., Dumont R. A., Maecke H. R., Muller-Brand J., Briel M., Schmitt A., Perren A. and Walter M. A.** (2017). The prognostic and predictive value of sstr2-immunohistochemistry and sstr2-targeted imaging in neuroendocrine tumors. *European journal of nuclear medicine and molecular imaging* **44**, 468-475.

**Buchwalow I. B. and Böcker W.** (2010). *Immunohistochemistry: Basics and Methods*. Springer, Heidelberg, German.

**Buonocore D. J., Konno F., Jungbluth A. A., Frosina D., Fayad M., Edelweiss M., Lin O. and Rekhtman N.** (2019). CytoLyt fixation significantly inhibits MIB1 immunoreactivity whereas alternative Ki-67 clone 30-9 is not susceptible to the inhibition: Critical diagnostic implications. *Cancer cytopathology* **127**, 643-649.

**Burry R. W.** (2011). Controls for immunocytochemistry: an update. *The journal of histochemistry and cytochemistry: official journal of the Histochemistry Society* **59**, 6-12.

**Burry R. W.** (2000). Specificity controls for immunocytochemical methods. *The journal of histochemistry and cytochemistry: official journal of the Histochemistry Society* **48**, 163-166.

**Busam K. J., Walsh N. and Wood B. A.** (2018). Merkel cell carcinoma. In *WHO Classification of Skin Tumours*. (eds. Elder D. E., Massi D., Scolyer R. A. and Willemze R.), pp. 48-50. International Agency for Research on Cancer (IARC), Lyon, France.

**Bussolati G. and Leonardo E.** (2008). Technical pitfalls potentially affecting diagnoses in immunohistochemistry. *Journal of clinical pathology* **61**, 1184-1192.

**Capella C., Heitz P. U., Hofler H., Solcia E. and Klöppel G.** (1995). Revised classification of neuroendocrine tumours of the lung, pancreas and gut. *Virchows Archiv: an international journal of pathology* **425**, 547-560.

**Carson F. L. and Cappellano C. H.** (2015). Immunohistochemistry. In *Histotechnology. A self Instructional Text, 4th Edition* (eds. Carson F. L. and Cappellano C. H.), pp. 263-292. American Society for Clinical Pathology (ASCP), USA.

**Cavalcanti M. S., Gonen M. and Klimstra D. S.** (2016). The ENETS/WHO grading system for neuroendocrine neoplasms of the gastroenteropancreatic system: a review of the current state, limitations and proposals for modifications. *International journal of endocrine oncology* **3**, 203-219.

**Chan D. L., Clarke S. J., Diakos C. I., Roach P. J., Bailey D. L., Singh S. and Pavlakis N.** (2017). Prognostic and predictive biomarkers in neuroendocrine tumours. *Critical reviews in oncology/hematology* **113**, 268-282.

**Cheung C. C., D'Arrigo C., Dietel M., Francis G. D., Fulton R., Gilks C. B., Hall J. A., Hornick J. L., Ibrahim M., Marchetti A., Miller K., van Krieken J. H., Nielsen S., Swanson P. E., Taylor C. R., Vyberg M., Zhou X., Torlakovic E. E. and From the International Society for Immunohistochemistry and Molecular Morphology (ISIMM) and International Quality Network for Pathology (IQN Path).** (2016). Evolution of Quality Assurance for Clinical Immunohistochemistry in the Era of Precision Medicine: Part 4: Tissue Tools for Quality Assurance in Immunohistochemistry. *Applied immunohistochemistry & molecular morphology* ***00****, 000-000.*

**Comperat E., Zhang F., Perrotin C., Molina T., Magdeleinat P., Marmey B., Regnard J. F., Audouin J. and Camilleri-Broet S.** (2005). Variable sensitivity and specificity of TTF-1 antibodies in lung metastatic adenocarcinoma of colorectal origin. *Modern pathology: an official journal of the United States and Canadian Academy of Pathology, Inc* **18**, 1371-1376.

**Conner J. R. and Hornick J. L.** (2015). Metastatic carcinoma of unknown primary: diagnostic approach using immunohistochemistry. *Advances in Anatomic Pathology* **22**, 149-167.

**Copete M., Garratt J., Gilks B., Pilavdzic D., Berendt R., Bigras G., Mitchell S., Lining L. A., Cheung C. and Torlakovic E. E.** (2011). Inappropriate calibration and optimisation of pan-keratin (pan-CK) and low molecular weight keratin (LMWCK) immunohistochemistry tests: Canadian Immunohistochemistry Quality Control (CIQC) experience. *Journal of clinical pathology* **64**, 220-225.

**Cottenden J., Filter E. R., Cottreau J., Moore D., Bullock M., Huang W. Y. and Arnason T.** (2018). Validation of a Cytotechnologist Manual Counting Service for the Ki67 Index in Neuroendocrine Tumors of the Pancreas and Gastrointestinal Tract. *Archives of Pathology & Laboratory Medicine* **142**, 402-407.

**Crona J. and Skogseid B.** (2016). GEP- NETS UPDATE: Genetics of neuroendocrine tumors. *European journal of endocrinology* **174**, R275-90.

**Csaba Z., Peineau S. and Dournaud P.** (2012). Molecular mechanisms of somatostatin receptor trafficking. *Journal of Molecular Endocrinology* **48**, R1-12

**D'Amato M, Bruce S, Bresso F, Zucchelli M, Ezer S, Pulkkinen V, Lindgren C, Astegiano M, Rizzetto M, Gionchetti P, Riegler G, Sostegni R, Daperno M, D'Alfonso S, Momigliano-Richiardi P, Torkvist L, Puolakkainen P, Lappalainen M, Paavola-Sakki P, Halme L, Farkkila M, Turunen U, Kontula K, Lofberg R, Pettersson S, Kere J.** (2007). Neuropeptide s receptor 1 gene polymorphism is associated with susceptibility to inflammatory bowel disease**.** *Gastroenterology* **133**, 808–817.

**Dasari A., Shen C., Halperin D., Zhao B., Zhou S., Xu Y., Shih T. and Yao J. C.** (2017). Trends in the Incidence, Prevalence, and Survival Outcomes in Patients With Neuroendocrine Tumors in the United States. *JAMA oncology* **3**, 1335-1342.

**de Herder W. W.** (2007). Biochemistry of neuroendocrine tumours. *Best practice & research.Clinical endocrinology & metabolism* **21**, 33-41.

**Delellis R. A., Al Ghuzlan A., Albores Saavedra J., Baloch Z. W., Basolo F., Elisei R., Kaserer K., LiVolsi V., Matias-Guiu X., Mete O., Moley J. F., Nikiforov Y. E., Nose V. and Pinto A. E.** (2017). Medullary thyroid carcinoma. In *WHO Classification of Tumours of Endocrine Organs*. (eds. Lloyd R. V., Osamura R. Y., Klöppel G. and Rosai J.), pp. 108-113. International Agency for Research on Cancer, Lyon, France.

**Diakatou E., Alexandraki K. I., Tsolakis A. V., Kontogeorgos G., Chatzellis E., Leonti A. and Kaltsas G. A.** (2015). Somatostatin and dopamine receptor expression in neuroendocrine neoplasms: correlation of immunohistochemical findings with somatostatin receptor scintigraphy visual scores. *Clinical endocrinology* **83**, 420-428.

**Doblinger A., Becker A., Seidah N. G. and Laslop A.** (2003). Proteolytic processing of chromogranin A by the prohormone convertase PC2. *Regulatory peptides* **111**, 111-116.

**Duran-Prado M., Gahete M. D., Martinez-Fuentes A. J., Luque R. M., Quintero A., Webb S. M., Benito-Lopez P., Leal A., Schulz S., Gracia-Navarro F., Malagon M. M. and Castano J. P.** (2009). Identification and characterization of two novel truncated but functional isoforms of the somatostatin receptor subtype 5 differentially present in pituitary tumors. *The Journal of clinical endocrinology and metabolism* **94**, 2634-2643.

**E.Brambilla.** (2015). Neuroendocrine tumours. In *WHO classification of Tumours of the Lung, Pleura, Thymus and Heart* (eds. Travis W. D., Brambilla E., Burke A. P., Marx A. and Nicholson A. G.), pp. 63-77. International Agency for Research on Cancer (IARC), Lyon, France.

**Elfving H., Mattsson J. S. M., Lindskog C., Backman M., Menzel U. and Micke P.** (2019). Programmed Cell Death Ligand 1 Immunohistochemistry: A Concordance Study Between Surgical Specimen, Biopsy, and Tissue Microarray. *Clinical lung cancer* **20**, 258-262.e1.

**Elias D., Lefevre J. H., Duvillard P., Goere D., Dromain C., Dumont F. and Baudin E.** (2010). Hepatic metastases from neuroendocrine tumors with a "thin slice" pathological examination: they are many more than you think.. *Annals of Surgery* **251**, 307-310.

**Elston M. S., Meyer-Rochow G. Y., Conaglen H. M., Clarkson A., Clifton-Bligh R. J., Conaglen J. V. and Gill A. J.** (2015). Increased SSTR2A and SSTR3 expression in succinate dehydrogenase-deficient pheochromocytomas and paragangliomas. *Human pathology* **46**, 390-396.

**Engel K. B. and Moore H. M.** (2011). Effects of preanalytical variables on the detection of proteins by immunohistochemistry in formalin-fixed, paraffin-embedded tissue. *Archives of Pathology & Laboratory Medicine* **135**, 537-543.

**Er L-M., LI Y., Wu M-L., Zao Q., Tan B-B., Wang X-L. and Wang S-J**. (2017). Expression of IMP3 as a marker for predicting poor outcome in gastroenteropancreatic neuroendocrine neoplasms. *Oncology Letters* **13**, 2391-2396.

**Eriksson B., Annibale B., Bajetta E., Mitry E., Pavel M., Platania M., Salazar R., Plockinger U., Mallorca Consensus Conference participants and European Neuroendocrine Tumor Society.** (2009). ENETS Consensus Guidelines for the Standards of Care in Neuroendocrine Tumors: chemotherapy in patients with neuroendocrine tumors. *Neuroendocrinology* **90**, 214-219.

**Fischer T., Doll C., Jacobs S., Kolodziej A., Stumm R. and Schulz S.** (2008). Reassessment of sst2 somatostatin receptor expression in human normal and neoplastic tissues using the novel rabbit monoclonal antibody UMB-1. *The Journal of clinical endocrinology and metabolism* **93**, 4519-4524.

**Fonatsch C., Duchrow M., Rieder H., Schluter C. and Gerdes J.** (1991). Assignment of the human Ki-67 gene (MK167) to 10q25-qter. *Genomics* **11**, 476-477.

**Fox C. H., Johnson F. B., Whiting J. and Roller P. P.** (1985). Formaldehyde fixation. *The journal of histochemistry and cytochemistry: official journal of the Histochemistry Society* **33**, 845-853.

**Frilling A., Akerstrom G., Falconi M., Pavel M., Ramos J., Kidd M. and Modlin I. M.** (2012). Neuroendocrine tumor disease: an evolving landscape. *Endocrine-related cancer* **19**, R163-85.

**Fujino K., Yasufuku K., Kudoh S., Motooka Y., Sato Y., Wakimoto J., Kubota I., Suzuki M. and Ito S.** (2017). INSM1 is the best marker for the diagnosis of neuroendocrine tumors: comparison with CGA,SYP and CD56. **Int J Clin Exp Pathol 10(5)**, 5393-5405.

**Galloway M. and Sim R.** (2007). TTF-1 staining in glioblastoma multiforme. *Virchows Archiv: an international journal of pathology* **451**, 109-111.

**Gabriel M., Decristoforo C., Kendler D., Dobrozemsky G., Heute D., Uprimny C., Kovacs P., Von Guggenberg E., Bale R. and Virgolini I. J.** (2007). 68Ga-DOTA-Tyr3-octreotide PET in neuroendocrine tumors: comparison with somatostatin receptor scintigraphy and CT. *Journal of nuclear medicine: official publication, Society of Nuclear Medicine* **48**, 508-518.

**Garcia-Carbonero R., Rinke A., Valle J. W., Fazio N., Caplin M., Gorbounova V., O Connor J., Eriksson B., Sorbye H., Kulke M., Chen J., Falkerby J., Costa F., de Herder W., Lombard-Bohas C., Pavel M. and Antibes Consensus Conference participants.** (2017). ENETS Consensus Guidelines for the Standards of Care in Neuroendocrine Neoplasms. Systemic Therapy 2: Chemotherapy. *Neuroendocrinology* **105**, 281-294.

**Gatto F., Feelders R. A., van der Pas R., Kros J. M., Waaijers M., Sprij-Mooij D., Neggers S. J., van der Lelij A. J., Minuto F., Lamberts S. W., de Herder W. W., Ferone D. and Hofland L. J.** (2013). Immunoreactivity score using an anti-sst2A receptor monoclonal antibody strongly predicts the biochemical response to adjuvant treatment with somatostatin analogs in acromegaly. *The Journal of clinical endocrinology and metabolism* **98**, E66-71.

**George J., Walter V., Peifer M., Alexandrov L. B., Seidel D., Leenders F., Maas L., Muller C., Dahmen I., Delhomme T. M., Ardin M., Leblay N., Byrnes G., Sun R., De Reynies A., McLeer-Florin A., Bosco G., Malchers F., Menon R., Altmuller J., Becker C., Nurnberg P., Achter V., Lang U., Schneider P. M., Bogus M., Soloway M. G., Wilkerson M. D., Cun Y., McKay J. D., Moro-Sibilot D., Brambilla C. G., Lantuejoul S., Lemaitre N., Soltermann A., Weder W., Tischler V., Brustugun O. T., Lund-Iversen M., Helland A., Solberg S., Ansen S., Wright G., Solomon B., Roz L., Pastorino U., Petersen I., Clement J. H., Sanger J., Wolf J., Vingron M., Zander T., Perner S., Travis W. D., Haas S. A., Olivier M., Foll M., Buttner R., Hayes D. N., Brambilla E., Fernandez-Cuesta L. and Thomas R. K.** (2018). Integrative genomic profiling of large-cell neuroendocrine carcinomas reveals distinct subtypes of high-grade neuroendocrine lung tumors. *Nature communications* **9**, 1048-018-03099-x.

**Gerdes J., Li L., Schlueter C., Duchrow M., Wohlenberg C., Gerlach C., Stahmer I., Kloth S., Brandt E. and Flad H. D.** (1991). Immunobiochemical and molecular biologic characterization of the cell proliferation-associated nuclear antigen that is defined by monoclonal antibody Ki-67. *The American journal of pathology* **138**, 867-873.

**Gerdes J., Lemke H., Baisch H., Wacker H. H., Schwab U. and Stein H.** (1984). Cell cycle analysis of a cell proliferation-associated human nuclear antigen defined by the monoclonal antibody Ki-67. *Journal of immunology (Baltimore, Md.: 1950)* **133**, 1710-1715.

**Gerdes J., Schwab U., Lemke H. and Stein H.** (1983). Production of a mouse monoclonal antibody reactive with a human nuclear antigen associated with cell proliferation. *International journal of cancer.Journal international du cancer* **31**, 13-20.

**Gierl M. S., Karoulias N., Wende H., Strehle M. and Birchmeier C.** (2006). The zinc-finger factor Insm1 (IA-1) is essential for the development of pancreatic beta cells and intestinal endocrine cells. *Genes & development* **20**, 2465-2478.

**Goldstein N. S., Ferkowicz M., Odish E., Mani A. and Hastah F.** (2003). Minimum formalin fixation time for consistent estrogen receptor immunohistochemical staining of invasive breast carcinoma. *American Journal of Clinical Pathology* **120**, 86-92.

**Goto Y., De Silva M. G., Toscani A., Prabhakar B. S., Notkins A. L. and Lan M. S.** (1992). A novel human insulinoma-associated cDNA, IA-1, encodes a protein with "zinc-finger" DNA-binding motifs. *The Journal of biological chemistry* **267**, 15252-15257.

**Gown A. M.** (2016). Diagnostic Immunohistochemistry: What Can Go Wrong and How to Prevent It. *Archives of Pathology & Laboratory Medicine* **140**, 893-898.

**Graham R. P., Shrestha B., Caron B. L., Smyrk T. C., Grogg K. L., Lloyd R. V. and Zhang L.** (2013). Islet-1 is a sensitive but not entirely specific marker for pancreatic neuroendocrine neoplasms and their metastases. *The American Journal of Surgical Pathology* **37**, 399-405.

**Griffin J. and Treanor D.** (2017). Digital pathology in clinical use: where are we now and what is holding us back? *Histopathology* **70**, 134-145.

**Grizzle W. E., Fredenburgh J. L. and Myers R. B.** (2008). Fixation of Tissues. In *Theory and Practice of Histological Techniques* (eds. Bancroft J. D. and Gamble. M.), pp. 53-74. Churchill Livingstone Elsevier, Philadelphia, USA.

**Gut P., Czarnywojtek A., Fischbach J., Baczyk M., Ziemnicka K., Wrotkowska E., Gryczynska M. and Ruchala M.** (2016). Chromogranin A - unspecific neuroendocrine marker. Clinical utility and potential diagnostic pitfalls. *Archives of medical science: AMS* **12**, 1-9.

**Hankus J. and Tomaszewska R.** (2016). Neuroendocrine neoplasms and somatostatin receptor subtypes expression. *Nuclear medicine review. Central & Eastern Europe* **19**, 111-117.

**Haynes C. M., Sangoi A. R. and Pai R. K.** (2011). PAX8 is expressed in pancreatic well-differentiated neuroendocrine tumors and in extrapancreatic poorly differentiated neuroendocrine carcinomas in fine-needle aspiration biopsy specimens. *Cancer cytopathology* **119**, 193-201.

**Hermans B. C. M., Derks J. L., Thunnissen E., van Suylen R. J., den Bakker M. A., Groen H. J. M., Smit E. F., Damhuis R. A., van den Broek E. C., PALGA-group, Ruland A., Speel E. J. M. and Dingemans A. M. C.** (2019). DLL3 expression in large cell neuroendocrine carcinoma (LCNEC) and association with molecular subtypes and neuroendocrine profile. *Lung cancer (Amsterdam, Netherlands)* **138**, 102-108.

**Hewitt S. M., Baskin D. G., Frevert C. W., Stahl W. L. and Rosa-Molinar E.** (2014). Controls for immunohistochemistry: the Histochemical Society's standards of practice for validation of immunohistochemical assays. *The journal of histochemistry and cytochemistry: official journal of the Histochemistry Society* **62**, 693-697.

**Hicks R. J., Kwekkeboom D. J., Krenning E., Bodei L., Grozinsky-Glasberg S., Arnold R., Borbath I., Cwikla J., Toumpanakis C., Kaltsas G., Davies P., Horsch D., Tiensuu Janson E., Ramage J. and Antibes Consensus Conference participants.** (2017). ENETS Consensus Guidelines for the Standards of Care in Neuroendocrine Neoplasias: Peptide Receptor Radionuclide Therapy with Radiolabeled Somatostatin Analogues. *Neuroendocrinology* **105**, 295-309.

**Hladik C. L. and White C. L.** (2008). Immunohistochemistry Quality Control. In *Theory and Practice of Histological Techniques* (eds. Bancroft J. D. and Gamble.M.), pp. 473-491. Churchill Livingstone Elsevier, Philadelphia, USA.

**Hofland J., Zandee W. T. and de Herder W. W.** (2018). Role of biomarker tests for diagnosis of neuroendocrine tumours. *Nature reviews. Endocrinology* **14**, 656-669.

**Howat W. J., Lewis A., Jones P., Kampf C., Ponten F., van der Loos C. M., Gray N., Womack C. and Warford A.** (2014). Antibody validation of immunohistochemistry for biomarker discovery: recommendations of a consortium of academic and pharmaceutical based histopathology researchers. *Methods (San Diego, Calif.)* **70**, 34-38.

**Howat W. J. and Wilson B. A.** (2014). Tissue fixation and the effect of molecular fixatives on downstream staining procedures. *Methods (San Diego, Calif.)* **70**, 12-19.

**Hsu S. M., Raine L. and Fanger H.** (1981). Use of avidin-biotin-peroxidase complex (ABC) in immunoperoxidase techniques: a comparison between ABC and unlabeled antibody (PAP) procedures. *The journal of histochemistry and cytochemistry: official journal of the Histochemistry Society* **29**, 577-580.

**Huang Z., Zhu W., Meng Y. and Xia H.** (2006). Development of new rabbit monoclonal antibody to progesterone receptor (Clone SP2): no heat pretreatment but effective for paraffin section immunohistochemistry. *Applied immunohistochemistry & molecular morphology: AIMM* **14**, 229-233.

**Ibrahim M., Dodson A., Barnett S., Fish D., Jasani B. and Miller K.** (2008). Potential for false-positive staining with a rabbit monoclonal antibody to progesterone receptor (SP2): findings of the UK National External Quality Assessment Scheme for Immunocytochemistry and FISH highlight the need for correct validation of antibodies on introduction to the laboratory. *American Journal of Clinical Pathology* **129**, 398-409.

**Iezzoni J. C., Mills S. E., Pelkey T. J. and Stoler M. H.** (1999). Inhibin is not an immunohistochemical marker for hepatocellular carcinoma. An example of the potential pitfall in diagnostic immunohistochemistry caused by endogenous biotin. *American Journal of Clinical Pathology* **111**, 229-234.

**Iino K., Oki Y., Yamashita M., Matsushita F., Hayashi C., Yogo K., Nishizawa S., Yamada S., Maekawa M., Sasano H. and Nakamura H.** (2010). Possible relevance between prohormone convertase 2 expression and tumor growth in human adrenocorticotropin-producing pituitary adenoma. *The Journal of clinical endocrinology and metabolism* **95**, 4003-4011.

**Isola J., Helin H. and Kallioniemi O. P.** (1990). Immunoelectron-microscopic localization of a proliferation-associated antigen Ki-67 in MCF-7 cells. *The Histochemical journal* **22**, 498-506.

**Jacobs S. and Schulz S.** (2008). Intracellular trafficking of somatostatin receptors. *Molecular and cellular endocrinology* **286**, 58-62.

**Jackson P. and Blythe D.** (2008). Immunohistochemical Tehniques. In *Theory and Practice of Histological Techniques* (eds. Bancroft J. D. and Gamble.M), pp. 433-472. Churchill Livingstone Elsevier, Philadelphia, USA.

**James R. and Kazenwadel J.** (1991). Homeobox gene expression in the intestinal epithelium of adult mice. *The Journal of biological chemistry* **266**, 3246-3251.

**Jasani B., Thomas D. W. and Williams E. D.** (1981). Use of monoclonal antihapten antibodies for immunolocalisation of tissue antigens. *Journal of clinical pathology* **34**, 1000-1002.

**Johnbeck C. B., Knigge U., Langer S. W., Loft A., Berthelsen A. K., Federspiel B., Binderup T. and Kjaer A.** (2016). Prognostic Value of 18F-FLT PET in Patients with Neuroendocrine Neoplasms: A Prospective Head-to-Head Comparison with 18F-FDG PET and Ki-67 in 100 Patients. *Journal of nuclear medicine: official publication, Society of Nuclear Medicine* **57**, 1851-1857.

**Kaemmerer D., Athelogou M., Lupp A., Lenhardt I., Schulz S., Luisa P., Hommann M., Prasad V., Binnig G. and Baum R. P.** (2014). Somatostatin receptor immunohistochemistry in neuroendocrine tumors: comparison between manual and automated evaluation. *International journal of clinical and experimental pathology* **7**, 4971-4980.

**Kaemmerer D., Peter L., Lupp A., Schulz S., Sanger J., Prasad V., Kulkarni H., Haugvik S. P., Hommann M. and Baum R. P.** (2011). Molecular imaging with (6)(8)Ga-SSTR PET/CT and correlation to immunohistochemistry of somatostatin receptors in neuroendocrine tumours. *European journal of nuclear medicine and molecular imaging* **38**, 1659-1668.

**Kaemmerer D., Specht E., Sanger J., Wirtz R. M., Sayeg M., Schulz S. and Lupp A.** (2015). Somatostatin receptors in bronchopulmonary neuroendocrine neoplasms: new diagnostic, prognostic, and therapeutic markers. *The Journal of clinical endocrinology and metabolism* **100**, 831-840.

**Kajiwara H., Itoh Y., Itoh J., Yasuda M. and Osamura R. Y.** (1999). Immunohistochemical expressions of prohormone convertase (PC)1/3 and PC2 in carcinoids of various organs. *The Tokai journal of experimental and clinical medicine* **24**, 13-20.

**Kammerer U., Kapp M., Gassel A. M., Richter T., Tank C., Dietl J. and Ruck P.** (2001). A new rapid immunohistochemical staining technique using the EnVision antibody complex. *The journal of histochemistry and cytochemistry: official journal of the Histochemistry Society* **49**, 623-630.

**Katoh R., Miyagi E., Nakamura N., Li X., Suzuki K., Kakudo K., Kobayashi M. and Kawaoi A.** (2000). Expression of thyroid transcription factor-1 (TTF-1) in human C cells and medullary thyroid carcinomas. *Human pathology* **31**, 386-393.

**Khosravi P., Kazemi E., Imielinski M., Elemento O. and Hajirasouliha I.** (2018). Deep Convolutional Neural Networks Enable Discrimination of Heterogeneous Digital Pathology Images. *EBioMedicine* **27**, 317-328.

**Khoury T., Sait S., Hwang H., Chandrasekhar R., Wilding G., Tan D. and Kulkarni S.** (2009). Delay to formalin fixation effect on breast biomarkers. *Modern pathology: an official journal of the United States and Canadian Academy of Pathology, Inc* **22**, 1457-1467.

**Kim S. W., Roh J. and Park C. S.** (2016). Immunohistochemistry for Pathologists: Protocols, Pitfalls, and Tips. *Journal of pathology and translational medicine* **50**, 411-418.

**Kimura N., Pilichowska M., Okamoto H., Kimura I. and Aunis D.** (2000). Immunohistochemical expression of chromogranins A and B, prohormone convertases 2 and 3, and amidating enzyme in carcinoid tumors and pancreatic endocrine tumors. *Modern pathology: an official journal of the United States and Canadian Academy of Pathology, Inc* **13**, 140-146.

**Klimstra D. S., Klöppel G., La Rosa S. and Rindi G.** (2019). Classification of neuroendocrine neoplasms of the digestive system. In *WHO Classification of Tumours. Digestive System Tumours*. (eds. Carneiro F., Chan J. K. C., Cheung N. A., et al), pp. 16-22. International Agency for Research on Cancer (IARC), Lyon, France.

**Klimstra D. S., Modlin I. R., Adsay N. V., Chetty R., Deshpande V., Gonen M., Jensen R. T., Kidd M., Kulke M. H., Lloyd R. V., Moran C., Moss S. F., Oberg K., O'Toole D., Rindi G., Robert M. E., Suster S., Tang L. H., Tzen C. Y., Washington M. K., Wiedenmann B. and Yao J.** (2010). Pathology reporting of neuroendocrine tumors: application of the Delphic consensus process to the development of a minimum pathology data set. *The American Journal of Surgical Pathology* **34**, 300-313.

**Klöppel G., Couvelard A., Hruban R. H., Klimstra D. S., Komminoth P., Osamura R. Y., Perren A. and Rindi G.** (2017a). Introduction. In *WHO Classification of Tumours of Endocrine Organs* (eds. Lloyd R. V., Osamura R. Y., Klöppel G. and Rosai J.), pp. 211-214. International Agency for Research on Cancer (IARC), Lyon, France.

**Klöppel G.** (2007). Tumour biology and histopathology of neuroendocrine tumours. *Best practice & research.Clinical endocrinology & metabolism* **21**, 15-31.

**Klöppel G., Couvelard A., Hruban R. H., Klimstra D. S., Komminoth P., Osamura R. Y., Perren A. and Rindi G.** (2017b). Neoplasms of the neuroendocrine pancreas. In *WHO Classification of Tumours of Endocrine Organs* (eds. Lloyd R. V., Osamura R. Y., Klöppel G. and Rosai J.), pp. 210-239. International Agency for Research on Cancer (IARC), Lyon, France.

**Klöppel G., Couvelard A., Perren A., Komminoth P., McNicol A. M., Nilsson O., Scarpa A., Scoazec J. Y., Wiedenmann B., Papotti M., Rindi G., Plockinger U., Mallorca Consensus Conference participants and European Neuroendocrine Tumor Society.** (2009). ENETS Consensus Guidelines for the Standards of Care in Neuroendocrine Tumors: towards a standardized approach to the diagnosis of gastroenteropancreatic neuroendocrine tumors and their prognostic stratification. *Neuroendocrinology* **90**, 162-166.

**Klöppel G. and Lloyd R. V.** (2017). Inherited tumours syndromes. In *WHO Classification of Tumours of Endocrine Organs*. (eds. Lloyd R. V., Osamura R. Y., Klöppel G. and Rosai J.), pp. 242-283. International Agency for Research on Cancer (IARC), France, Lyon.

**Kohler G. and Milstein C.** (1975). Continuous cultures of fused cells secreting antibody of predefined specificity. *Nature* **256**, 495-497.

**Kononen J., Bubendorf L., Kallioniemi A., Barlund M., Schraml P., Leighton S., Torhorst J., Mihatsch M. J., Sauter G. and Kallioniemi O. P.** (1998). Tissue microarrays for high-throughput molecular profiling of tumor specimens. *Nature medicine* **4**, 844-847.

**Koo J., Mertens R. B., Mirocha J. M., Wang H. L. and Dhall D.** (2012). Value of Islet 1 and PAX8 in identifying metastatic neuroendocrine tumors of pancreatic origin. *Modern pathology: an official journal of the United States and Canadian Academy of Pathology, Inc* **25**, 893-901.

**Koo J., Zhou X., Moschiano E., De Peralta-Venturina M., Mertens R. B. and Dhall D.** (2013). The immunohistochemical expression of islet 1 and PAX8 by rectal neuroendocrine tumors should be taken into account in the differential diagnosis of metastatic neuroendocrine tumors of unknown primary origin. *Endocrine pathology* **24**, 184-190.

**Koopman T., Buikema H. J., Hollema H., de Bock G. H. and van der Vegt B.** (2018). Digital image analysis of Ki67 proliferation index in breast cancer using virtual dual staining on whole tissue sections: clinical validation and inter-platform agreement. *Breast cancer research and treatment* **169**, 33-42.

**Kulaksiz H., Eissele R., Rossler D., Schulz S., Hollt V., Cetin Y. and Arnold R.** (2002). Identification of somatostatin receptor subtypes 1, 2A, 3, and 5 in neuroendocrine tumours with subtype specific antibodies. *Gut* **50**, 52-60.

**Kulke M. H., Siu L. L., Tepper J. E., Fisher G., Jaffe D., Haller D. G., Ellis L. M., Benedetti J. K., Bergsland E. K., Hobday T. J., Van Cutsem E., Pingpank J., Oberg K., Cohen S. J., Posner M. C. and Yao J. C.** (2011). Future directions in the treatment of neuroendocrine tumors: consensus report of the National Cancer Institute Neuroendocrine Tumor clinical trials planning meeting. *Journal of clinical oncology: official journal of the American Society of Clinical Oncology* **29**, 934-943.

**Kwon A. Y., Park H. Y., Hyeon J., Nam S. J., Kim S. W., Lee J. E., Yu J. H., Lee S. K., Cho S. Y. and Cho E. Y.** (2019). Practical approaches to automated digital image analysis of Ki-67 labeling index in 997 breast carcinomas and causes of discordance with visual assessment. *PloS one* **14**, e0212309.

**Körner M., Eltschinger V., Waser B., Schonbrunn A. and Reubi J. C.** (2005). Value of immunohistochemistry for somatostatin receptor subtype sst2A in cancer tissues: lessons from the comparison of anti-sst2A antibodies with somatostatin receptor autoradiography. *The American Journal of Surgical Pathology* **29**, 1642-1651.

**Körner M., Waser B., Schonbrunn A., Perren A. and Reubi J. C.** (2012). Somatostatin receptor subtype 2A immunohistochemistry using a new monoclonal antibody selects tumors suitable for in vivo somatostatin receptor targeting. *The American Journal of Surgical Pathology* **36**, 242-252.

**Lang D., Powell S. K., Plummer R. S., Young K. P. and Ruggeri B. A.** (2007). PAX genes: roles in development, pathophysiology, and cancer. *Biochemical pharmacology* **73**, 1-14.

**La Rosa S., Chiaravalli A. M., Placidi C., Papanikolaou N., Cerati M. and Capella C.** (2010). TTF1 expression in normal lung neuroendocrine cells and related tumors: immunohistochemical study comparing two different monoclonal antibodies. *Virchows Archiv: an international journal of pathology* **457**, 497-507.

**Lazzaro D., Price M., de Felice M. and Di Lauro R.** (1991). The transcription factor TTF-1 is expressed at the onset of thyroid and lung morphogenesis and in restricted regions of the foetal brain. *Development (Cambridge, England)* **113**, 1093-1104.

**Leijon H., Remes S., Hagstrom J., Louhimo J., Maenpaa H., Schalin-Jantti C., Miettinen M., Haglund C. and Arola J.** (2019). Variable somatostatin receptor subtype expression in 151 primary pheochromocytomas and paragangliomas. *Human pathology* **86**, 66-75.

**Leoncini E., Boffetta P., Shafir M., Aleksovska K., Boccia S. and Rindi G.** (2017). Increased incidence trend of low-grade and high-grade neuroendocrine neoplasms. *Endocrine* **58**, 368-379.

**Li Q. L., Naqvi S., Shen X., Liu Y. J., Lindberg I. and Friedman T. C.** (2003). Prohormone convertase 2 enzymatic activity and its regulation in neuro-endocrine cells and tissues. *Regulatory peptides* **110**, 197-205.

**Li Z., Yuan J., Wei L., Zhou L., Mei K., Yue J., Gao H., Zhang M., Jia L., Kang Q., Huang X. and Cao D.** (2015). SATB2 is a sensitive marker for lower gastrointestinal well-differentiated neuroendocrine tumors. *International journal of clinical and experimental pathology* **8**, 7072-7082.

**Lin X., Saad R. S., Luckasevic T. M., Silverman J. F. and Liu Y.** (2007). Diagnostic value of CDX-2 and TTF-1 expressions in separating metastatic neuroendocrine neoplasms of unknown origin. *Applied immunohistochemistry & molecular morphology: AIMM* **15**, 407-414.

**Lipman N. S., Jackson L. R., Trudel L. J. and Weis-Garcia F.** (2005). Monoclonal versus polyclonal antibodies: distinguishing characteristics, applications, and information resources. *ILAR journal* **46**, 258-268.

**Lopez F., Belloc F., Lacombe F., Dumain P., Reiffers J., Bernard P. and Boisseau M. R.** (1991). Modalities of synthesis of Ki67 antigen during the stimulation of lymphocytes. *Cytometry* **12**, 42-49.

**Lorenzo P. I., Jimenez Moreno C. M., Delgado I., Cobo-Vuilleumier N., Meier R., Gomez-Izquierdo L., Berney T., Garcia-Carbonero R., Rojas A. and Gauthier B. R.** (2011). Immunohistochemical assessment of Pax8 expression during pancreatic islet development and in human neuroendocrine tumors. *Histochemistry and cell biology* **136**, 595-607.

**Luo X., Zang X., Yang L., Huang J., Liang F., Rodriguez-Canales J., Wistuba I. I., Gazdar A., Xie Y. and Xiao G.** (2017). Comprehensive Computational Pathological Image Analysis Predicts Lung Cancer Prognosis. *Journal of thoracic oncology: official publication of the International Association for the Study of Lung Cancer* **12**, 501-509.

**Lupp A., Hunder A., Petrich A., Nagel F., Doll C. and Schulz S.** (2011). Reassessment of sst(5) somatostatin receptor expression in normal and neoplastic human tissues using the novel rabbit monoclonal antibody UMB-4. *Neuroendocrinology* **94**, 255-264.

**Lupp A., Nagel F., Doll C., Rocken C., Evert M., Mawrin C., Saeger W. and Schulz S.** (2012). Reassessment of sst3 somatostatin receptor expression in human normal and neoplastic tissues using the novel rabbit monoclonal antibody UMB-5. *Neuroendocrinology* **96**, 301-310.

**Lupp A., Nagel F. and Schulz S.** (2013). Reevaluation of sst(1) somatostatin receptor expression in human normal and neoplastic tissues using the novel rabbit monoclonal antibody UMB-7. *Regulatory peptides* **183**, 1-6.

**Lykkegaard Andersen N., Brugmann A., Lelkaitis G., Nielsen S., Friis Lippert M. and Vyberg M.** (2018). Virtual Double Staining: A Digital Approach to Immunohistochemical Quantification of Estrogen Receptor Protein in Breast Carcinoma Specimens. *Applied immunohistochemistry & molecular morphology: AIMM* **26**, 620-626.

**Majala S., Seppanen H., Kemppainen J., Sundstrom J., Schalin-Jantti C., Gullichsen R., Schildt J., Mustonen H., Vesterinen T., Arola J. and Kauhanen S.** (2019). Prediction of the aggressiveness of non-functional pancreatic neuroendocrine tumors based on the dual-tracer PET/CT. *EJNMMI research* **9**, 116-019-0585-7.

**Margulies D. H.** (2005). Monoclonal antibodies: producing magic bullets by somatic cell hybridization. *Journal of immunology (Baltimore, Md.: 1950)* **174**, 2451-2452.

**Matos L. L., Trufelli D. C., de Matos M. G. and da Silva Pinhal M. A.** (2010). Immunohistochemistry as an important tool in biomarkers detection and clinical practice. *Biomarker insights* **5**, 9-20.

**Matoso A., Singh K., Jacob R., Greaves W. O., Tavares R., Noble L., Resnick M. B., Delellis R. A. and Wang L. J.** (2010). Comparison of thyroid transcription factor-1 expression by 2 monoclonal antibodies in pulmonary and nonpulmonary primary tumors. *Applied immunohistochemistry & molecular morphology: AIMM* **18**, 142-149.

**Maxwell J. E. and Howe J. R.** (2015). Imaging in neuroendocrine tumors: an update for the clinician. *International journal of endocrine oncology* **2**, 159-168.

**Mayerhoefer M. E., Ba-Ssalamah A., Weber M., Mitterhauser M., Eidherr H., Wadsak W., Raderer M., Trattnig S., Herneth A. and Karanikas G.** (2013). Gadoxetate-enhanced versus diffusion-weighted MRI for fused Ga-68-DOTANOC PET/MRI in patients with neuroendocrine tumours of the upper abdomen. *European radiology* **23**, 1978-1985.

**McCall C. M., Shi C., Cornish T. C., Klimstra D. S., Tang L. H., Basturk O., Mun L. J., Ellison T. A., Wolfgang C. L., Choti M. A., Schulick R. D., Edil B. H. and Hruban R. H.** (2013). Grading of well-differentiated pancreatic neuroendocrine tumors is improved by the inclusion of both Ki67 proliferative index and mitotic rate. *The American Journal of Surgical Pathology* **37**, 1671-1677.

**Mengel M., von Wasielewski R., Wiese B., Rudiger T., Muller-Hermelink H. K. and Kreipe H.** (2002). Inter-laboratory and inter-observer reproducibility of immunohistochemical assessment of the Ki-67 labelling index in a large multi-centre trial. *The Journal of pathology* **198**, 292-299.

**Meyer W. and Hornickel I. N.** (2010). Tissue fixation-the most underestimated methodical feature of immunohistochemistry. 953959.

**Miederer M., Seidl S., Buck A., Scheidhauer K., Wester H. J., Schwaiger M. and Perren A.** (2009). Correlation of immunohistopathological expression of somatostatin receptor 2 with standardised uptake values in 68Ga-DOTATOC PET/CT. *European journal of nuclear medicine and molecular imaging* **36**, 48-52.

**Mirvis E., Mandair D., Garcia-Hernandez J., Mohmaduvesh M., Toumpanakis C. and Caplin M.** (2014). Role of interferon-alpha in patients with neuroendocrine tumors: a retrospective study. *Anticancer Research* **34**, 6601-6607.

**Moatamed N. A., Nanjangud G., Pucci R., Lowe A., Shintaku I. P., Shapourifar-Tehrani S., Rao N., Lu D. Y. and Apple S. K.** (2011). Effect of ischemic time, fixation time, and fixative type on HER2/neu immunohistochemical and fluorescence in situ hybridization results in breast cancer. *American Journal of Clinical Pathology* **136**, 754-761.

**Montuenga L. M., Guembe L., Burrell M. A., Bodegas M. E., Calvo A., Sola J. J., Sesma P. and Villaro A. C.** (2003). The diffuse endocrine system: from embryogenesis to carcinogenesis. *Progress in histochemistry and cytochemistry* **38**, 155-272.

**Moskaluk C. A., Zhang H., Powell S. M., Cerilli L. A., Hampton G. M. and Frierson H. F.,Jr.** (2003). Cdx2 protein expression in normal and malignant human tissues: an immunohistochemical survey using tissue microarrays. *Modern pathology: an official journal of the United States and Canadian Academy of Pathology, Inc* **16**, 913-919.

**Mukhopadhyay S., Feldman M. D., Abels E., Ashfaq R., Beltaifa S., Cacciabeve N. G., Cathro H. P., Cheng L., Cooper K., Dickey G. E., Gill R. M., Heaton R. P.,Jr, Kerstens R., Lindberg G. M., Malhotra R. K., Mandell J. W., Manlucu E. D., Mills A. M., Mills S. E., Moskaluk C. A., Nelis M., Patil D. T., Przybycin C. G., Reynolds J. P., Rubin B. P., Saboorian M. H., Salicru M., Samols M. A., Sturgis C. D., Turner K. O., Wick M. R., Yoon J. Y., Zhao P. and Taylor C. R.** (2018). Whole Slide Imaging Versus Microscopy for Primary Diagnosis in Surgical Pathology: A Multicenter Blinded Randomized Noninferiority Study of 1992 Cases (Pivotal Study). *The American Journal of Surgical Pathology* **42**, 39-52.

**Mulligan L. M., Kwok J. B., Healey C. S., Elsdon M. J., Eng C., Gardner E., Love D. R., Mole S. E., Moore J. K. and Papi L.** (1993). Germ-line mutations of the RET proto-oncogene in multiple endocrine neoplasias type 2A. *Nature* **363**, 458-460.

**Nakane P. K. and Pierce G. B. Jr.** (1966). Enzyme-labeled antibodies: preparation and application for the localization of antigens. *The journal of histochemistry and cytochemistry: official journal of the Histochemistry Society* **14**, 929-931.

**Niazi M. K. K., Parwani A. V. and Gurcan M. N.** (2019). Digital pathology and artificial intelligence. *The Lancet.Oncology* **20**, e253-e261.

**Nordstrom-O'Brien M., van der Luijt R. B., van Rooijen E., van den Ouweland A. M., Majoor-Krakauer D. F., Lolkema M. P., van Brussel A., Voest E. E. and Giles R. H.** (2010). Genetic analysis of von Hippel-Lindau disease. *Human mutation* **31**, 521-537.

**Oberg K., Couvelard A., Delle Fave G., Gross D., Grossman A., Jensen R. T., Pape U. F., Perren A., Rindi G., Ruszniewski P., Scoazec J. Y., Welin S., Wiedenmann B., Ferone D. and Antibes Consensus Conference participants.** (2017). ENETS Consensus Guidelines for Standard of Care in Neuroendocrine Tumours: Biochemical Markers. *Neuroendocrinology* **105**, 201-211.

**Okada K., Fujiwara Y., Nakamura Y., Takiguchi S., Nakajima K., Miyata H., Yamasaki M., Kurokawa Y., Takahashi T., Mori M. and Doki Y.** (2012). Oncofetal protein, IMP-3, a potential marker for prediction of postoperative peritoneal dissemination in gastric adenocarcinoma. *Journal of surgical oncology* **105**, 780-785.

**Olsen I. H., Langer S. W., Federspiel B. H., Oxbol J., Loft A., Berthelsen A. K., Mortensen J., Oturai P., Knigge U. and Kjaer A.** (2016). (68)Ga-DOTATOC PET and gene expression profile in patients with neuroendocrine carcinomas: strong correlation between PET tracer uptake and gene expression of somatostatin receptor subtype 2. *American journal of nuclear medicine and molecular imaging* **6**, 59-72.

**Ordonez N. G.** (2000). Value of thyroid transcription factor-1 immunostaining in distinguishing small cell lung carcinomas from other small cell carcinomas. *The American Journal of Surgical Pathology* **24**, 1217-1223.

**Oronsky B., Ma P. C., Morgensztern D. and Carter C. A.** (2017). Nothing But NET: A Review of Neuroendocrine Tumors and Carcinomas. *Neoplasias (New York, N.Y.)* **19**, 991-1002.

**Paavilainen L., Edvinsson A., Asplund A., Hober S., Kampf C., Ponten F. and Wester K.** (2010). The impact of tissue fixatives on morphology and antibody-based protein profiling in tissues and cells. *The journal of histochemistry and cytochemistry: official journal of the Histochemistry Society* **58**, 237-246.

**Packeisen J., Korsching E., Herbst H., Boecker W. and Buerger H.** (2003). Demystified...tissue microarray technology. *Molecular pathology: MP* **56**, 198-204.

**Pantanowitz L.** (2010). Digital images and the future of digital pathology. *Journal of pathology informatics* **1**, 10.4103/2153-3539.68332.

**Patel Y. C., Greenwood M., Kent G., Panetta R. and Srikant C. B.** (1993). Multiple gene transcripts of the somatostatin receptor SSTR2: tissue selective distribution and cAMP regulation. *Biochemical and biophysical research communications* **192**, 288-294.

**Pauwels E., Cleeren F., Bormans G. and Deroose C. M.** (2018). Somatostatin receptor PET ligands - the next generation for clinical practice. *American journal of nuclear medicine and molecular imaging* **8**, 311-331.

**Pavel M. and de Herder W. W.** (2017). ENETS Consensus Guidelines for the Standard of Care in Neuroendocrine Tumors. *Neuroendocrinology* **105**, 193-195.

**Perren A., Couvelard A., Scoazec J. Y., Costa F., Borbath I., Delle Fave G., Gorbounova V., Gross D., Grossma A., Jense R. T., Kulke M., Oeberg K., Rindi G., Sorbye H., Welin S. and Antibes Consensus Conference participants.** (2017). ENETS Consensus Guidelines for the Standards of Care in Neuroendocrine Tumors: Pathology: Diagnosis and Prognostic Stratification. *Neuroendocrinology* **105**, 196-200.

**Pileri SA, Roncador G, Ceccarelli C, Piccioli M, Briskomatis A, Sabattini E, Ascani S, Santini D, Piccaluga PP, Leone O, Damiani S, Ercolessi C, Sandri F, Pieri F, Leoncini L and Falini B.** (1997). Antigen Retrieval techniques in immunohistochemistry: comparison of different methods. *Journal of Pathology* **183**, 116-123.

**Pokuri V. K., Fong M. K. and Iyer R.** (2016). Octreotide and Lanreotide in Gastroenteropancreatic Neuroendocrine Tumors. *Current oncology reports* **18**, 7-015-0492-7.

**Portela-Gomes G. M., Grimelius L. and Stridsberg M.** (2008). Prohormone convertases 1/3, 2, furin and protein 7B2 (Secretogranin V) in endocrine cells of the human pancreas. *Regulatory peptides* **146**, 117-124.

**Portela-Gomes G. M., Hacker G. W. and Weitgasser R.** (2004). Neuroendocrine cell markers for pancreatic islets and tumors. *Applied immunohistochemistry & molecular morphology: AIMM* **12**, 183-192.

**Pusceddu S., De Braud F., Lo Russo G., Concas L., Femia D., Vernieri C., Indini A., Formisano B. and Buzzoni R.** (2016). How do the results of the RADIANT trials impact on the management of NET patients? A systematic review of published studies. *Oncotarget* **7**, 44841-44847.

**Qian Z. R., Li T., Ter-Minassian M., Yang J., Chan J. A., Brais L. K., Masugi Y., Thiaglingam A., Brooks N., Nishihara R., Bonnemarie M., Masuda A., Inamura K., Kim S. A., Mima K., Sukawa Y., Dou R., Lin X., Christiani D. C., Schmidlin F., Fuchs C. S., Mahmood U., Ogino S. and Kulke M. H.** (2016). Association Between Somatostatin Receptor Expression and Clinical Outcomes in Neuroendocrine Tumors. *Pancreas* **45**, 1386-1393.

**Radulescu R. T. and Boenisch T.** (2007). Blocking endogenous peroxidases: a cautionary note for immunohistochemistry. *Journal of Cellular and Molecular Medicine* **11**, 1419-4934.2007.00185.x. Epub 2007 Dec 5.

**Ramos-Vara J. A. and Beissenherz M. E.** (2000). Optimization of immunohistochemical methods using two different antigen retrieval methods on formalin-fixed paraffin-embedded tissues: experience with 63 markers. *Journal of veterinary diagnostic investigation: official publication of the American Association of Veterinary Laboratory Diagnosticians, Inc* **12**, 307-311.

**Ramya S Vokuda, Surendra Kumar Verma, Bheemanathi Hanuman Srinivas.** (2018). Tissue Microarray Technology-A Brief Review. **7**, PR01-PR04.

**Raymond E., Dahan L., Raoul J. L., Bang Y. J., Borbath I., Lombard-Bohas C., Valle J., Metrakos P., Smith D., Vinik A., Chen J. S., Horsch D., Hammel P., Wiedenmann B., Van Cutsem E., Patyna S., Lu D. R., Blanckmeister C., Chao R. and Ruszniewski P.** (2011). Sunitinib malate for the treatment of pancreatic neuroendocrine tumors. *The New England journal of medicine* **364**, 501-513.

**Reid M. D., Bagci P., Ohike N., Saka B., Erbarut Seven I., Dursun N., Balci S., Gucer H., Jang K. T., Tajiri T., Basturk O., Kong S. Y., Goodman M., Akkas G. and Adsay V.** (2015). Calculation of the Ki67 index in pancreatic neuroendocrine tumors: a comparative analysis of four counting methodologies. *Modern pathology: an official journal of the United States and Canadian Academy of Pathology, Inc* **28**, 686-694.

**Reinscheid R. K., Xu Y. L., Okamura N., Zeng J., Chung S., Pai R., Wang Z. and Civelli O.** (2005). Pharmacological characterization of human and murine neuropeptide s receptor variants. *The Journal of pharmacology and experimental therapeutics* **315**, 1338-1345.

**Rekhtman N.** (2008). Neuroendocrine Neoplasms. In *The Practice of Surgical Pathology: A Beginner's Guide to the Diagnostic Process* (ed. Molavi D. W.), pp. 279-285. Springer International Publishing.

**Reubi J. C.** (2014). Strict rules are needed for validation of G-protein-coupled receptor immunohistochemical studies in human tissues. *Endocrine* **47**, 659-661.

**Reubi J. C., Waser B., Cescato R., Gloor B., Stettler C. and Christ E.** (2010). Internalized somatostatin receptor subtype 2 in neuroendocrine tumors of octreotide-treated patients. *The Journal of clinical endocrinology and metabolism*.**95**, 2343-50.

**Reubi J. C., Waser B., Schaer J. C. and Laissue J. A.** (2001). Somatostatin receptor sst1-sst5 expression in normal and neoplastic human tissues using receptor autoradiography with subtype-selective ligands. *European journal of nuclear medicine* **28**, 836-846.

**Ridler T.W. and Calvard S.** (1978). Picture thresholding using an iterative selection method. *IEEE Trans System Man and Cybernetics* **8**, 630-632.

**Righi L., Volante M., Tavaglione V., Bille A., Daniele L., Angusti T., Inzani F., Pelosi G., Rindi G. and Papotti M.** (2010). Somatostatin receptor tissue distribution in lung neuroendocrine tumours: a clinicopathologic and immunohistochemical study of 218 'clinically aggressive' cases. *Annals of oncology: official journal of the European Society for Medical Oncology* **21**, 548-555.

**Rindi G., Klimstra D. S., Abedi-Ardekani B., Asa S. L., Bosman F. T., Brambilla E., Busam K. J., de Krijger R. R., Dietel M., El-Naggar A. K., Fernandez-Cuesta L., Klöppel G., McCluggage W. G., Moch H., Ohgaki H., Rakha E. A., Reed N. S., Rous B. A., Sasano H., Scarpa A., Scoazec J. Y., Travis W. D., Tallini G., Trouillas J., van Krieken J. H. and Cree I. A.** (2018). A common classification framework for neuroendocrine neoplasms: an International Agency for Research on Cancer (IARC) and World Health Organization (WHO) expert consensus proposal. *Modern pathology: an official journal of the United States and Canadian Academy of Pathology, Inc* **31**, 1770-1786.

**Rindi G., Klöppel G., Alhman H., Caplin M., Couvelard A., de Herder W. W., Erikssson B., Falchetti A., Falconi M., Komminoth P., Korner M., Lopes J. M., McNicol A. M., Nilsson O., Perren A., Scarpa A., Scoazec J. Y., Wiedenmann B., and all other Frascati Consensus Conference participants and European Neuroendocrine Tumor Society (ENETS).** (2006). TNM staging of foregut (neuro)endocrine tumors: a consensus proposal including a grading system. *Virchows Archiv: an international journal of pathology* **449**, 395-401.

**Rindi G., Klöppel G., Couvelard A., Komminoth P., Korner M., Lopes J. M., McNicol A. M., Nilsson O., Perren A., Scarpa A., Scoazec J. Y. and Wiedenmann B.** (2007). TNM staging of midgut and hindgut (neuro) endocrine tumors: a consensus proposal including a grading system. *Virchows Archiv: an international journal of pathology* **451**, 757-762.

**Rinke A., Muller H. H., Schade-Brittinger C., Klose K. J., Barth P., Wied M., Mayer C., Aminossadati B., Pape U. F., Blaker M., Harder J., Arnold C., Gress T., Arnold R. and PROMID Study Group.** (2009). Placebo-controlled, double-blind, prospective, randomized study on the effect of octreotide LAR in the control of tumor growth in patients with metastatic neuroendocrine midgut tumors: a report from the PROMID Study Group. *Journal of clinical oncology: official journal of the American Society of Clinical Oncology* **27**, 4656-4663.

**Roge R., Nielsen S., Riber-Hansen R. and Vyberg M.** (2019). Impact of Primary Antibody Clone, Format, and Stainer Platform on Ki67 Proliferation Indices in Breast Carcinomas. *Applied immunohistochemistry & molecular morphology: AIMM* **27**, 732-739.

**Roge R., Riber-Hansen R., Nielsen S. and Vyberg M.** (2016). Proliferation assessment in breast carcinomas using digital image analysis based on virtual Ki67/cytokeratin double staining. *Breast cancer research and treatment* **158**, 11-19.

**Rosai J.** (2011). The origin of neuroendocrine tumors and the neural crest saga. *Modern pathology : an official journal of the United States and Canadian Academy of Pathology, Inc* **24 Suppl 2**, S53-7.

**Ruf J., Schiefer J., Furth C., Kosiek O., Kropf S., Heuck F., Denecke T., Pavel M., Pascher A., Wiedenmann B. and Amthauer H.** (2011). 68Ga-DOTATOC PET/CT of neuroendocrine tumors: spotlight on the CT phases of a triple-phase protocol. *Journal of nuclear medicine: official publication, Society of Nuclear Medicine* **52**, 697-704.

**Ruifrok A. C. and Johnston D. A.** (2001). Quantification of histochemical staining by color deconvolution. *Analytical and Quantitative Cytology and Histology / the International Academy of Cytology [and] American Society of Cytology* **23**, 291-299.

**Sabattini E., Bisgaard K., Ascani S., Poggi S., Piccioli M., Ceccarelli C., Pieri F., Fraternali-Orcioni G. and Pileri S. A.** (1998). The EnVision++ system: a new immunohistochemical method for diagnostics and research. Critical comparison with the APAAP, ChemMate, CSA, LABC, and SABC techniques. *Journal of clinical pathology* **51**, 506-511.

**Sander M., Neubuser A., Kalamaras J., Ee H. C., Martin G. R. and German M. S.** (1997). Genetic analysis reveals that PAX6 is required for normal transcription of pancreatic hormone genes and islet development. *Genes & development* **11**, 1662-1673.

**Sangoi A. R., Ohgami R. S., Pai R. K., Beck A. H., McKenney J. K. and Pai R. K.** (2011). PAX8 expression reliably distinguishes pancreatic well-differentiated neuroendocrine tumors from ileal and pulmonary well-differentiated neuroendocrine tumors and pancreatic acinar cell carcinoma. *Modern pathology: an official journal of the United States and Canadian Academy of Pathology, Inc* **24**, 412-424.

**Saper C. B.** (2009). A guide to the perplexed on the specificity of antibodies. *The journal of histochemistry and cytochemistry: official journal of the Histochemistry Society* **57**, 1-5.

**Schacht V. and Kern J. S.** (2015). Basics of immunohistochemistry. *The Journal of investigative dermatology* **135**, 1-4.

**Schally A. V., Huang W. Y., Chang R. C., Arimura A., Redding T. W., Millar R. P., Hunkapiller M. W. and Hood L. E.** (1980). Isolation and structure of pro-somatostatin: a putative somatostatin precursor from pig hypothalamus. *Proceedings of the National Academy of Sciences of the United States of America* **77**, 4489-4493.

**Schmid H. A., Lambertini C., van Vugt H. H., Barzaghi-Rinaudo P., Schafer J., Hillenbrand R., Sailer A. W., Kaufmann M. and Nuciforo P.** (2012). Monoclonal antibodies against the human somatostatin receptor subtypes 1-5: development and immunohistochemical application in neuroendocrine tumors. *Neuroendocrinology* **95**, 232-247.

**Schmitt A. M., Blank A., Marinoni I., Komminoth P. and Perren A.** (2016). Histopathology of NET: Current concepts and new developments. *Best practice & research.Clinical endocrinology & metabolism* **30**, 33-43.

**Schmid-Tannwald C., Schmid-Tannwald C. M., Morelli J. N., Neumann R., Haug A. R., Jansen N., Nikolaou K., Schramm N., Reiser M. F. and Rist C.** (2013). Comparison of abdominal MRI with diffusion-weighted imaging to 68Ga-DOTATATE PET/CT in detection of neuroendocrine tumors of the pancreas. *European journal of nuclear medicine and molecular imaging* **40**, 897-907.

**Schott M., Klöppel G., Raffel A., Saleh A., Knoefel W. T. and Scherbaum W. A.** (2011). Neuroendocrine neoplasms of the gastrointestinal tract. *Deutsches Arzteblatt international* **108**, 305-312.

**Scopsi L., Gullo M., Rilke F., Martin S. and Steiner D. F.** (1995). Proprotein convertases (PC1/PC3 and PC2) in normal and neoplastic human tissues: their use as markers of neuroendocrine differentiation. *The Journal of clinical endocrinology and metabolism* **80**, 294-301.

**Seidah N. G. and Prat A.** (2012). The biology and therapeutic targeting of the proprotein convertases. *Nature reviews.Drug discovery* **11**, 367-383.

**Seidah N. G.** (2011). The proprotein convertases, 20 years later. *Methods in molecular biology (Clifton, N.J.)* **768**, 23-57.

**Shi S. R., Key M. E. and Kalra K. L.** (1991). Antigen retrieval in formalin-fixed, paraffin-embedded tissues: an enhancement method for immunohistochemical staining based on microwave oven heating of tissue sections. *The journal of histochemistry and cytochemistry: official journal of the Histochemistry Society* **39**, 741-748.

**Shi S. R., Liu C. and Taylor C. R.** (2007). Standardization of immunohistochemistry for formalin-fixed, paraffin-embedded tissue sections based on the antigen-retrieval technique: from experiments to hypothesis. *The journal of histochemistry and cytochemistry: official journal of the Histochemistry Society* **55**, 105-109.

**Snead D. R., Tsang Y. W., Meskiri A., Kimani P. K., Crossman R., Rajpoot N. M., Blessing E., Chen K., Gopalakrishnan K., Matthews P., Momtahan N., Read-Jones S., Sah S., Simmons E., Sinha B., Suortamo S., Yeo Y., El Daly H. and Cree I. A.** (2016). Validation of digital pathology imaging for primary histopathological diagnosis. *Histopathology* **68**, 1063-1072.

**Solcia E., Klöppel G., Sobin L. H., Williams E. D. and World Health Organization.** (2000). *Histological typing of endocrine tumours*. 2nd Edn. Springer, Berlin, New York.

**Spieker-Polet H., Sethupathi P., Yam P. C. and Knight K. L.** (1995). Rabbit monoclonal antibodies: generating a fusion partner to produce rabbit-rabbit hybridomas. *Proceedings of the National Academy of Sciences of the United States of America* **92**, 9348-9352.

**Stalhammar G., Robertson S., Wedlund L., Lippert M., Rantalainen M., Bergh J. and Hartman J.** (2018). Digital image analysis of Ki67 in hot spots is superior to both manual Ki67 and mitotic counts in breast cancer. *Histopathology* **72**, 974-989.

**Storvall S., Leijon H., Ryhanen E., Louhimo J., Haglund C., Schalin-Jantti C. and Arola J.** (2019). Somatostatin receptor expression in parathyroid neoplasms. *Endocrine connections* **8**, 1213-1223.

**Streefkerk J. G.** (1972). Inhibition of erythrocyte pseudoperoxidase activity by treatment with hydrogen peroxide following methanol. *The journal of histochemistry and cytochemistry: official journal of the Histochemistry Society* **20**, 829-831.

**Strosberg J., El-Haddad G., Wolin E., Hendifar A., Yao J., Chasen B., Mittra E., Kunz P. L., Kulke M. H., Jacene H., Bushnell D., O'Dorisio T. M., Baum R. P., Kulkarni H. R., Caplin M., Lebtahi R., Hobday T., Delpassand E., Van Cutsem E., Benson A., Srirajaskanthan R., Pavel M., Mora J., Berlin J., Grande E., Reed N., Seregni E., Oberg K., Lopera Sierra M., Santoro P., Thevenet T., Erion J. L., Ruszniewski P., Kwekkeboom D., Krenning E. and NETTER-1 Trial Investigators.** (2017). Phase 3 Trial of (177)Lu-Dotatate for Midgut Neuroendocrine Tumors. *The New England journal of medicine* **376**, 125-135.

**Ströbel P. S., Marx A., Chan J. K. C., Marom E. M., Matsuno Y., Nicholson A. G. and Travis W. D.** (2015). Thymic neuroendocrine tumours. In *WHO Classification of Tumours of the Lung, Pleura, Thymus and Heart* (eds. Travis W. D., Brambilla E., Burke A. P., Marx A. and Nicholson A. G.), pp. 234-242. International Agency for Research on Cancer (IARC), Lyon, France.

**Ström P., Kartasalo K., Olsson H., Solorzano L., Delahunt B., Berney D.M., Bostwick D.G., Evans A.J., Grignon D.J., Humphrey P.A., Iczkowski K.A., Kench J.G., Kristiansen G., van der Kwast T.H., Leite K.R.M., McKenney J.K., Oxley J., Pan C-C., Samaratunga H., Srigley J.R., Takahashi H., Tsuzuki T., Varma M., Zhou M., Lindberg J., Lindskog C., Ruusuvuori P., Wählby C., Grönberg H., Rantalainen M., Lars Egevad L. and Eklund M.** (2020). Artificial intelligence for diagnosis and grading of prostate cancer in biopsies: a population-based, diagnostic study. *Lancet Oncol,* **21**, 222–32.

**Sundin A., Arnold R., Baudin E., Cwikla J. B., Eriksson B., Fanti S., Fazio N., Giammarile F., Hicks R. J., Kjaer A., Krenning E., Kwekkeboom D., Lombard-Bohas C., O'Connor J. M., O'Toole D., Rockall A., Wiedenmann B., Valle J. W., Vullierme M. P. and Antibes Consensus Conference participants.** (2017). ENETS Consensus Guidelines for the Standards of Care in Neuroendocrine Tumors: Radiological, Nuclear Medicine & Hybrid Imaging. *Neuroendocrinology* **105**, 212-244.

**Sundman L., Saarialho-Kere U., Vendelin J., Lindfors K., Assadi G., Kaukinen K., Westerholm-Ormio M., Savilahti E., Maki M., Alenius H., D'Amato M., Pulkkinen V., Kere J. and Saavalainen P.** (2010). Neuropeptide S receptor 1 expression in the intestine and skin-putative role in peptide hormone secretion. *Neurogastroenterology and motility: the official journal of the European Gastrointestinal Motility Society* **22**, 79-87, e30.

**Tacha D., Qi W., Zhou D., Bremer R. and Cheng L.** (2013). PAX8 mouse monoclonal antibody [BC12] recognizes a restricted epitope and is highly sensitive in renal cell and ovarian cancers but does not cross-react with b cells and tumors of pancreatic origin. *Applied immunohistochemistry & molecular morphology: AIMM* **21**, 59-63.

**Tang L. H., Gonen M., Hedvat C., Modlin I. M. and Klimstra D. S.** (2012). Objective quantification of the Ki67 proliferative index in neuroendocrine tumors of the gastroenteropancreatic system: a comparison of digital image analysis with manual methods. *The American Journal of Surgical Pathology* **36**, 1761-1770.

**Taylor C. R. and Levenson R. M.** (2006). Quantification of immunohistochemistry-issues concerning methods, utility and semiquantitative assessment II. *Histopathology* **49**, 411-424.

**Theodoropoulou M. and Stalla G. K.** (2013). Somatostatin receptors: from signaling to clinical practice. *Frontiers in neuroendocrinology* **34**, 228-252.

**Tischler A. S., de Krijger R. R., Gill A., Kawashima A., Kimura N., Komminoth P., Papathomas T. G., Thompson L. D. R., Tissier F., Williams M. D. and Young W. F.** (2017). Tumours of the adrenal medulla and extra-adrenal paraganglia. In *WHO Classification of Tumours of Endocrine Organs* (eds. Lloyd R. V., Osamura R. Y., Klöppel G. and Rosai J.), pp. 180-207. International Agency for Research on Cancer (IARC), Lyon, France.

**Tomita T.** (2001). Immunocytochemical localization of prohormone convertase 1/3 and 2 in gastrointestinal carcinoids. *Endocrine pathology* **12**, 137-145.

**Torlakovic E. E., Cheung C. C., D'Arrigo C., Dietel M., Francis G. D., Gilks C. B., Hall J. A., Hornick J. L., Ibrahim M., Marchetti A., Miller K., van Krieken J. H., Nielsen S., Swanson P. E., Vyberg M., Zhou X., Taylor C. R. and From the International Society for Immunohistochemistry and Molecular Morphology (ISIMM) and**

**International Quality Network for Pathology (IQN Path).** (2017). Evolution of Quality Assurance for Clinical Immunohistochemistry in the Era of Precision Medicine. Part 3: Technical Validation of Immunohistochemistry (IHC) Assays in Clinical IHC Laboratories. *Applied immunohistochemistry & molecular morphology: AIMM* **25**, 151-159.

**Torlakovic E. E., Francis G., Garratt J., Gilks B., Hyjek E., Ibrahim M., Miller R., Nielsen S., Petcu E. B., Swanson P. E., Taylor C. R., Vyberg M. and International Ad Hoc Expert Panel.** (2014). Standardization of negative controls in diagnostic immunohistochemistry: recommendations from the international ad hoc expert panel. *Applied immunohistochemistry & molecular morphology: AIMM* **22**, 241-252.

**Torlakovic E. E., Nielsen S., Francis G., Garratt J., Gilks B., Goldsmith J. D., Hornick J. L., Hyjek E., Ibrahim M., Miller K., Petcu E., Swanson P. E., Zhou X., Taylor C. R. and Vyberg M.** (2015). Standardization of positive controls in diagnostic immunohistochemistry: recommendations from the International Ad Hoc Expert Committee. *Applied immunohistochemistry & molecular morphology: AIMM* **23**, 1-18.

**Tuominen V. J., Ruotoistenmaki S., Viitanen A., Jumppanen M. and Isola J.** (2010). ImmunoRatio: a publicly available web application for quantitative image analysis of estrogen receptor (ER), progesterone receptor (PR), and Ki-67. *Breast cancer research: BCR* **12**, R56.

**Tuominen V. J., Tolonen T. T. and Isola J.** (2012). ImmunoMembrane: a publicly available web application for digital image analysis of HER2 immunohistochemistry. *Histopathology* **60**, 758-767.

**Valkonen M., Isola J., Isola J., Ylinen O., Muhonen V., Saxlin A., Tolonen T., Nykter M. and Ruusuvuori P.** (2020). Cytokeratin-supervised deep learning for automatic recognition of epithelial cells in breast cancers stained for ER, PR, and Ki-67. *IEEE Transactions on Medical Imaging* ***39****, 534-542*.

**van der Loos C. M.** (2008). Multiple immunoenzyme staining: methods and visualizations for the observation with spectral imaging. *The journal of histochemistry and cytochemistry: official journal of the Histochemistry Society* **56**, 313-328.

**van Dierendonck J. H., Keijzer R., van de Velde C. J. and Cornelisse C. J.** (1989). Nuclear distribution of the Ki-67 antigen during the cell cycle: comparison with growth fraction in human breast cancer cells. *Cancer research* **49**, 2999-3006.

**van Velthuysen M. L., Groen E. J., Sanders J., Prins F. A., van der Noort V. and Korse C. M.** (2014). Reliability of proliferation assessment by Ki-67 expression in neuroendocrine neoplasms: eyeballing or image analysis? *Neuroendocrinology* **100**, 288-292.

**Veit-Haibach P., Schiesser M., Soyka J., Strobel K., Schaefer N. G., Hesselmann R., Clavien P. A. and Hany T. F.** (2011). Clinical value of a combined multi-phase contrast enhanced DOPA-PET/CT in neuroendocrine tumours with emphasis on the diagnostic CT component. *European radiology* **21**, 256-264.

**Vendelin J, Pulkkinen V, Rehn M, Pirskanen A, Raisanen-Sokolowski A, Laitinen A, Laitinen LA, Kere J, Laitinen T.** (2005). Characterization of GPRA, a novel G protein-coupled receptor related to asthma. *Am J Respir Cell Mol Biol.* **33**, 262-270.

**Verheijen R., Kuijpers H. J., van Driel R., Beck J. L., van Dierendonck J. H., Brakenhoff G. J. and Ramaekers F. C.** (1989). Ki-67 detects a nuclear matrix-associated proliferation-related antigen. II. Localization in mitotic cells and association with chromosomes. *Journal of cell science* **92 (Pt 4)**, 531-540.

**Vesterinen T., Leijon H., Mustonen H., Remes S., Knuuttila A., Salmenkivi K., Vainio P., Arola J. and Haglund C.** (2019). Somatostatin Receptor Expression Is Associated With Metastasis and Patient Outcome in Pulmonary Carcinoid Tumors. *The Journal of clinical endocrinology and metabolism* **104**, 2083-2093.

**Vinayek R., Capurso G. and Larghi A.** (2014). Grading of EUS-FNA cytologic specimens from patients with pancreatic neuroendocrine neoplasms: it is time move to tissue core biopsy? *Gland surgery* **3**, 222-225.

**Vitale G., Dicitore A., Sciammarella C., Di Molfetta S., Rubino M., Faggiano A. and Colao A.** (2018). Pasireotide in the treatment of neuroendocrine tumors: a review of the literature. *Endocrine-related cancer* **25**, R351-R364.

**Volynskaya Z., Mete O., Pakbaz S., Al-Ghamdi D. and Asa S. L.** (2019). Ki67 Quantitative Interpretation: Insights using Image Analysis. *Journal of pathology informatics* **10**, 8.

**Wang H. Y., Li Z. W., Sun W., Yang X., Zhou L. X., Huang X. Z., Jia L. and Lin D. M.** (2019). Automated quantification of Ki-67 index associates with pathologic grade of pulmonary neuroendocrine tumors. *Chinese medical journal* **132**, 551-561.

**Wang W. and Epstein J. I.** (2008). Small cell carcinoma of the prostate. A morphologic and immunohistochemical study of 95 cases. *The American Journal of Surgical Pathology* **32**, 65-71.

**Warth A., Fink L., Fisseler-Eckhoff A., Jonigk D., Keller M., Ott G., Rieker R. J., Sinn P., Soder S., Soltermann A., Willenbrock K., Weichert W. and Pulmonary Pathology Working Group of the German Society of Pathology.** (2013). Interobserver agreement of proliferation index (Ki-67) outperforms mitotic count in pulmonary carcinoids. *Virchows Archiv: an international journal of pathology* **462**, 507-513.

**Waser B., Tamma M. L., Cescato R., Maecke H. R. and Reubi J. C.** (2009). Highly efficient in vivo agonist-induced internalization of sst2 receptors in somatostatin target tissues. *Journal of nuclear medicine: official publication, Society of Nuclear Medicine* **50**, 936-941.

**Washington M. K.** (2019). Introduction to tumours of the digestive system. In *WHO Classification of Tumours. Digestive System Tumours*. (eds. Carneiro F., Chan J. K. C., Cheung N. A., et al), pp. 14-22. International Agency for Research on Cancer, IARC, Lyon, France.

**Weber J., Peng H. and Rader C.** (2017). From rabbit antibody repertoires to rabbit monoclonal antibodies. *Experimental & molecular medicine* **49**, e305.

**Wermer P.** (1954). Genetic aspects of adenomatosis of endocrine glands. *The American Journal of Medicine* **16**, 363-371.

**Werner R. A., Weich A., Kircher M., Solnes L. B., Javadi M. S., Higuchi T., Buck A. K., Pomper M. G., Rowe S. P. and Lapa C.** (2018). The theranostic promise for Neuroendocrine Tumors in the late 2010s - Where do we stand, where do we go? *Theranostics,* **8**, 6088-6100.

**Williams E. D. and Sandler M.** (1963). The classification of carcinoid tumours. *Lancet* **1**, 238-239.

**Williams E. D., Sobin L. H., Siebenmann R. E. and World Health Organization.** (1980). *Histological typing of endocrine tumours*. World Health Organization, Geneva.

**Wolff A. C., Hammond M. E. H., Allison K. H., Harvey B. E., Mangu P. B., Bartlett J. M. S., Bilous M., Ellis I. O., Fitzgibbons P., Hanna W., Jenkins R. B., Press M. F., Spears P. A., Vance G. H., Viale G., McShane L. M. and Dowsett M.** (2018). Human Epidermal Growth Factor Receptor 2 Testing in Breast Cancer: American Society of Clinical Oncology/ College of American Pathologists Clinical Practice Guideline Focused Update. *Journal of clinical oncology: official journal of the American Society of Clinical Oncology* **36**, 2105-2122.

**Zandee W. T. and de Herder W. W.** (2018). The Evolution of Neuroendocrine Tumor Treatment Reflected by ENETS Guidelines. *Neuroendocrinology* **106**, 357-365.

**Zarella M. D., Bowman D., Aeffner F., Farahani N., Xthona A., Absar S. F., Parwani A., Bui M. and Hartman D. J.** (2019). A Practical Guide to Whole Slide Imaging: A White Paper From the Digital Pathology Association. *Archives of Pathology & Laboratory Medicine* **143**, 222-234.

**Zimmermann N., Lazar-Karsten P., Keck T., Billmann F., Schmid S., Brabant G. and Thorns C.** (2016). Expression Pattern of CDX2, Estrogen and Progesterone Receptors in Primary Gastroenteropancreatic Neuroendocrine Tumors and Metastases. *Anticancer Research* **36**, 921-924.

**Zhao L. H., Chen C., Mao C. Y., Xiao H., Fu P., Xiao H. L. and Wang G.** (2019). Value of SATB2, ISL1, and TTF1 to differentiate rectal from other gastrointestinal and lung well-differentiated neuroendocrine tumors. *Pathology, research and practice* **215**, 152448.

**Zlobec I., Suter G., Perren A. and Lugli A.** (2014). A next-generation tissue microarray (ngTMA) protocol for biomarker studies. **91**, e51893.

**Zlobec I., Koelzer V. H., Dawson H., Perren A. and Lugli A.** (2013). Next-generation tissue microarray (ngTMA) increases the quality of biomarker studies: an example using CD3, CD8, and CD45RO in the tumor microenvironment of six different solid tumor types. 11, 104.

jvsmicroscope.uta.fi/immunoratio/

http://reagent-catalog.roche.com